

V; the sampling volume (m³)

The list of TSP concentrations is shown in Table 4-37. Flow (1) Flow (2) represent air sampling volume obtained by Equation (4-20) and (4-24).

Table 4-37 TSP concentration measured by Low volume sampler

Survey	Monitoring Station	(unit $\mu\text{g}/\text{m}^3$) (FLOW1)					Survey	Monitoring Station	(unit $\mu\text{g}/\text{m}^3$) (FLOW2)				
		MS 1	MS 2	MS 3	MS 4	MS 5			MS 1	MS 2	MS 3	MS 4	MS 5
No 1 (First Survey) 1/17 ~ 1/30	Quartz	52.9	52.1	82.6	67.5	50.6	No 1 (First Survey) 1/17 ~ 1/30	Quartz	62.8	59.4	86.9	73.6	55.5
	Polyfione	61.5	53.0	78.7	63.1	57.5		Polyfione	66.1	58.2	84.3	66.9	62.1
No 2 1/30 ~ 2/14	Quartz	46.0	36.3	61.3	47.2	30.1	No 2 1/30 ~ 2/14	Quartz	50.1	41.0	64.5	51.7	32.9
	Polyfione	48.8	38.9	60.7	44.2	35.0		Polyfione	52.8	41.5	66.8	47.2	38.4
No 3 2/14 ~ 2/29	Quartz	51.6	52.7	75.3	69.3	47.0	No 3 2/14 ~ 2/29	Quartz	55.8	59.6	79.4	75.5	51.6
	Polyfione	52.4	49.8	70.8	66.6	53.8		Polyfione	55.9	51.9	71.5	69.8	58.6
No 4 2/29 ~ 3/10	Quartz	39.7	42.8	64.2	53.7	40.9	No 4 2/29 ~ 3/10	Quartz	43.0	48.7	68.6	59.3	45.1
	Polyfione	41.8	42.9	65.6	49.5	45.1		Polyfione	45.6	45.3	72.0	53.3	49.2
No 5 (Second Survey) 3/11 ~ 3/24	Quartz	33.1	33.8	46.0	34.5	25.4	No 5 (Second Survey) 3/11 ~ 3/24	Quartz	34.4	38.1	48.8	38.2	28.0
	Polyfione	33.6	36.4	51.4	36.3	27.2		Polyfione	36.8	40.1	59.6	36.9	29.6
No 6 4/1 ~ 4/29	Quartz	42.3	36.5	45.4	48.4	31.9	No 6 4/1 ~ 4/29	Quartz	43.9	39.7	46.0	52.6	33.6
	Polyfione	42.3	39.3	49.9	46.4	34.3		Polyfione	43.6	41.5	52.6	47.8	36.3
No 7 5/2 ~ 5/16	Quartz	23.2	21.8	46.1	46.7	19.6	No 7 5/2 ~ 5/16	Quartz	24.1	23.7	46.7	50.9	20.5
	Polyfione	21.7	25.1	49.0	40.9	23.9		Polyfione	22.2	26.4	51.1	41.2	25.6
No 8 5/16 ~ 5/31	Quartz	45.3	31.5	41.2	42.5	25.2	No 8 5/16 ~ 5/31	Quartz	46.5	34.1	41.7	45.8	26.5
	Polyfione	47.9	32.9	45.3	41.2	25.4		Polyfione	48.7	34.2	47.1	41.8	26.2
No 9 5/31 ~ 6/15	Quartz	47.4	29.8	35.3	33.1	17.2	No 9 5/31 ~ 6/15	Quartz	49.3	31.9	35.7	36.0	19.5
	Polyfione	55.7	29.6	41.4	37.7	20.2		Polyfione	57.4	30.7	42.5	38.3	21.6
No 10 6/15 ~ 7/1	Quartz	52.4	32.2	38.6	36.7	26.4	No 10 6/15 ~ 7/1	Quartz	53.6	34.8	39.0	39.9	27.5
	Polyfione	62.9	33.7	47.5	42.3	28.3		Polyfione	63.3	34.8	49.0	43.3	28.8
No 11 7/1 ~ 7/12	Quartz	47.1	53.0	34.1	45.4	31.2	No 11 7/1 ~ 7/12	Quartz	48.2	35.7	34.3	47.3	32.5
	Polyfione	54.8	33.0	39.4	45.4	28.5		Polyfione	56.1	34.2	40.9	45.9	29.3
No 12 (Third Survey) 7/13 ~ 7/26	Quartz	38.9	28.8	37.9	41.3	25.8	No 12 (Third Survey) 7/13 ~ 7/26	Quartz	40.0	31.2	38.4	43.3	27.0
	Polyfione	41.3	28.3	39.8	39.6	26.0		Polyfione	42.7	29.6	41.6	40.7	26.7
No 13 7/26 ~ 8/15	Quartz	50.7	35.2	42.7	39.4	22.5	No 13 7/26 ~ 8/15	Quartz	52.4	38.1	43.2	41.2	23.7
	Polyfione	53.9	36.2	47.4	41.0	26.2		Polyfione	54.4	37.9	49.4	42.0	27.0
No 14 8/15 ~ 8/31	Quartz	26.8	23.6	54.1	44.9	25.8	No 14 8/15 ~ 8/31	Quartz	27.9	25.5	54.8	47.0	27.3
	Polyfione	30.1	28.0	51.2	40.9	38.6		Polyfione	30.9	29.4	54.0	42.6	39.9
No 15 8/31 ~ 9/16	Quartz	40.1	28.3	47.3	49.6	31.7	No 15 8/31 ~ 9/16	Quartz	41.5	33.2	47.6	51.8	33.2
	Polyfione	43.0	30.2	49.7	46.8	44.1		Polyfione	43.8	34.2	51.6	48.4	45.4
No 16 9/16 ~ 9/30	Quartz	39.3	33.9	49.8	58.6	24.7	No 16 9/16 ~ 9/30	Quartz	40.8	43.1	50.6	61.5	32.0
	Polyfione	38.3	39.2	51.9	56.3	33.5		Polyfione	39.0	40.8	54.0	57.5	42.8
No 17 9/30 ~ 10/17	Quartz	73.0	40.3	39.3	49.2	33.1	No 17 9/30 ~ 10/17	Quartz	75.5	43.7	40.0	51.7	34.6
	Polyfione	77.8	39.5	49.1	53.8	38.5		Polyfione	80.2	41.6	51.2	55.3	39.6
No 18 10/17 ~ 10/31	Quartz	60.8	50.6	68.2	80.4	31.3	No 18 10/17 ~ 10/31	Quartz	63.2	54.8	68.6	83.4	32.9
	Polyfione	65.3	66.1	76.5	85.5	39.4		Polyfione	66.9	66.6	79.8	87.8	40.5
No 19 10/31 ~ 11/16	Quartz	73.3	90.5	81.4	130.0	77.4	No 19 10/31 ~ 11/16	Quartz	76.3	97.1	84.8	136.6	82.0
	Polyfione	85.0	87.6	85.5	149.4	86.2		Polyfione	85.7	91.8	86.4	153.9	89.8
No 20 11/16 ~ 11/30	Quartz	84.3	104.8	115.6	114.1	92.1	No 20 11/16 ~ 11/30	Quartz	87.7	114.3	118.3	120.6	97.6
	Polyfione	84.8	100.6	107.9	118.4	104.2		Polyfione	88.1	106.2	112.1	121.9	107.6
No 21 11/30 ~ 12/16	Quartz	53.5	65.3	66.9	92.9	52.9	No 21 11/30 ~ 12/16	Quartz	56.1	71.6	68.1	98.0	55.8
	Polyfione	62.2	64.0	66.6	106.7	69.7		Polyfione	63.7	66.6	69.6	107.5	72.1
No 22 12/16 ~ 1/3	Quartz	79.3	78.8	92.8	94.4	89.2	No 22 12/16 ~ 1/3	Quartz	83.1	87.6	95.2	99.9	98.5
	Polyfione	86.6	83.4	94.8	104.1	96.5		Polyfione	88.4	86.5	98.6	105.7	105.3

4.2 Meteorological observations

4.2.1 Monitoring of wind direction and wind velocity

The meteorological conditions of the survey area are thought very important for estimation of the smoke diffusion behaviors. Among many of them, the wind pattern is one most influential in the calculation of atmospheric concentration of pollutants.

In this study, two variables, wind direction and its velocity were thought important and thus were monitored at three stations by using the instruments of continuous and automatic moving type. To maintain the desirable condition of such instruments, weekly inspection and scheduled maintenance by once every three months were done throughout the whole one year survey period.

(1) Monitoring of wind direction, its velocity and turbulency

The instruments to be used for monitoring both wind direction and velocity have long been a target of developments simply because they are such fundamental ones among meteorological variables. Today the following three types are commonly in use.

- ① Anemometer with a cup-type wind velocity meter and an arrow-type direction monitor combined
- ② Propeller type anemometer
- ③ Supersonic anemometer

Among these three types, one most commonly employed for monitoring atmospheric pollutants is one of the type ① which is improved in its windmill blade and in tail fin such that measurement can cover a low velocity range. The type is sometimes called the windmill type anemometer and detects the wind velocity in term of output of a DC generator which is directly connected to the propeller facing the wind. On the other hand, the wind direction is measured by the instrument because it constitutes itself an arrow-type direction monitor. The type ③ is a newly developed one, very sensitive which utilizes a phenomenon that the propagation speed of an ultrasonic wave differs between down- and up-stream side of the wind and has no moving part in it. Thus the meter is featured by a wind measurement at near-zero velocity, a good response, and a good performance for air turbulency monitoring. The type ① is today no longer popular.

(2) Anemometer employed in this survey

The two dimensional ultrasonic anemometer was used in the monitoring stations MS2 through MS5 and one of three dimensional type in MS1 for monitoring of wind velocity, direction and turbulency. As stated, those ultrasonic types utilizes a principle that the sound propagates differently depending upon the relative position of the meter and wind blowing direction.

When two heads, one for ultrasonic pulse transmission and the other for receiving, are positioned at a distance facing each other as shown in Figure 4- 27, and the pulse signal is sent from one to the other alternately at a fixed time interval, there are two pulse propagation times to be recorded, t_1 and t_2 . The relationship among t_1 , t_2 and wind velocity is then expressed by the following equation.

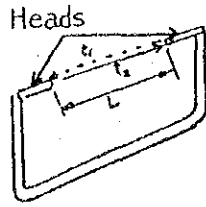


Figure 4-27 Propagation of pulse signal

$$\left. \begin{aligned} t_1 &= L / (C + V_x) \\ t_2 &= L / (C - V_x) \end{aligned} \right\} \dots\dots\dots (4-26)$$

where

- V_x ; Wind velocity vector in the direction of the ultrasonic propagation
- C ; Sound velocity in the air
- L ; the distance between heads (span)

The equation (4-26) is then converted into Equation (4-27) which gives the wind velocity vector as a function of t_1 , t_2 and L .

$$\left. \begin{aligned} L/t_1 - V_x &= L/t_2 + V_x \\ 2V_x &= (t_2L - t_1L)/t_1 \cdot t_2 \\ V_x &= (L/2) ((t_2 - t_1)/t_1 \cdot t_2) \end{aligned} \right\} \dots\dots\dots (4-27)$$

To measure V_y vector, a wind velocity in the Y direction, the same head arrangement is required in the direction at right angle against those stated above.

Now combining V_x and V_y , the wind velocity will be calculated by the Equation (4-28).

$$\left. \begin{aligned} V &= (V_x^2 + V_y^2)^{1/2} \\ \theta &= \tan^{-1} (V_x/V_y) \end{aligned} \right\} \dots\dots\dots (4-28)$$

As for three dimensional ultrasonic anemometer, W directional vector is added to V_x and V_y vectors. Thus probe heads are arranged in the W direction as well. The instrument can monitor not only horizontal vectors of blowing wind but its vertical vector.

The type of two dimensional anemometer used in this survey is one made by Koshin Denki Kogyo Co., Ltd. and the three dimensional one is manufactured by Kaijo Denki Co., Ltd. model S-2003, specifications of which are listed in Table 4-38. This instrument is such that it detects not only wind velocity vectors in three directions, X, Y, W but gives the standard deviations of them σ_x , σ_y and σ_w .

Table 4-38 (1) Specifications of the three dimensional ultrasonic anemometer

Description	Specifications
(Processing mode)	
Mean value of horizontal wind velocity (U)	Active low pass filter vector averaging
Mean value of horizontal wind direction (Θ)	Active low pass filter vector averaging
Mean value of vertical wind velocity (W)	Active low pass filter
Standard deviation of σ_u horizontal wind velocity	Square feedback rms detection
Standard deviation of σ_θ horizontal wind direction	Are sine processing of turbulent intensity
Standard deviation of σ_w vertical wind velocity	Square feedback rms detection
(Recording range)	
Mean value of horizontal wind velocity (U)	0-30 m/sec, or 0-60 m/sec
Mean value of horizontal wind direction (Θ)	0-540°
Mean value of vertical wind direction (W)	0-plus/minus 10 m/sec, 0-plus/minus 20 m/s
Standard deviation of horizontal wind velocity (σ_u)	0-15 m/sec, or 0-30 m/sec
Standard deviation of horizontal wind direction (σ_θ)	0-60°
Standard deviation of vertical wind velocity	0-5 m/sec or 0-10 m/sec
Wind velocity measuring mode	Ultrasonic pulse transmission (time sharing of transmission/receiving)
Recorder	Electric
Chart	Folding type, 250 mm width
Chart consumption	One month/chart based on 30 mm/hr
Power supply	50 Hz/60 Hz, approx. 100VA AC 100V (115, 220 V OK) plus/minus 10%
Service temp. range	Probe and junction box -10°C - +50°C

Table 4-38 (2) Two dimensional ultrasonic anemometer specifications

(1) System measurement operation	1-head time division transmitting/receiving switching system Frequency differential system through pulse propagation time
(2) Measuring range wind velocity wind direction	0-20 m/sec 540°/360° automatic shifting
(3) Accuracy wind velocity wind direction	within plus/minus 5% within plus/minus 5° (at wind speed of 0.8 m/sec)
(4) Resolution	plus/minus 1/10 %
(5) Measuring cycle	38 cycles/sec
(6) Response	voltage output=0.05 sec

(3) Measurement and calibration

If the instrument is properly installed, the need for frequent additional calibrations does not arise. In this survey, calibration was performed by transmitting a standard signal (in term of voltage) to the meter. The detail of operation procedures and calibration is as described in brochures.

(4) Inspection

Major inspection points associated with the meteorological observations are the confirmation of whether or not the supporting pole being kept vertical, if data recorders are properly run and time correction. Those jobs were done by ONHB staff once every week. In addition, calibration by feeding a standard signal into the meter and probe/recorder position check (at N point) were practiced once every three months by Japanese and ONEB staffs.

(5) Measurement

The summary of measurements made by each station (MS1, MS2, MS5) is shown in Table 4-39. When those effective measuring hours being reviewed, all of monitoring stations satisfy the minimum required for an effective monitoring station in Japan. Also noted is a comparatively lower availability of MS1, being about 85%. This is mainly because of downtime for one month period caused by lightning.

Table 4-39 Effective measuring hours for wind velocity, direction and air turbulency

Variables	Station	Effective hours	Availability (%)
Wind direction	MS1	7,530	85.7
	MS2	8,629	98.2
	MS5	8,569	97.6
Wind velocity	MS1	7,524	85.7
	MS2	8,629	98.2
	MS5	8,488	96.6
Vertical wind vel.	MS1	7,540	85.8
Std. dev. wind vel.	MS1	7,542	85.9
Std. dev. wind dir.	MS1	7,542	85.9
Std. dev. vertical wind vel.	MS1	7,527	85.7

Total hours for the period of Jan. 17, 1988 through Jan. 16, 1989 is 8,784 hrs.

An example of hourly recorded data is shown in Table 4-40 and all others and discussion are to be referred to Appendix and Chapter III respectively.

4.2.2 Measurement of solar radiation and net radiation

In order to forecast the pollution status of any specified area, the diffusion coefficient in turbulent state to be applied to such area is thought utmost important and must be properly evaluated. In other words, calculation of pollutant concentrations in the down-stream side of wind requires a means to quantify the spread of smoke and the degree of air stability associated with that. The atmospheric stability is defined in term of the vertical distribution of air temperature but the monitoring of such distribution up to 1,000 m high level for a long period on continuous base is thought practically prohibitive. Furthermore, the spread of smoke will be influenced not only by the vertical temperature profile but by such factors as wind velocity, solar radiation, etc. Accordingly, Pasquill developed a method to classify the degree of atmospheric stability into groups A through F depending upon such factors as wind velocity, solar radiation, cloud volume (or radiation balance) and has been employed by the Meteorological Department of English Government.

In compliance with this method, measured at 7 (seven) stations were solar radiation, net radiation of the survey area and wind velocities, which are then converted into hourly values to show atmospheric stability. Monitoring continued from January 17, 1988 until January 16, 1989 for one year period by automatic and continuous instruments, which were subject to both weekly inspections and scheduled maintenance once every three months.

(1) Methods to measure solar radiation and net radiation balance

The major part of radiation energy from the sun is in the wave range of under 4 micron meter and the instrument to be used measure such solar radiation is usually called pyrheliometer or pyranometer. The former is designed to measure the energy of solar radiation directly reaching the ground through atmosphere, and avoids the indirect radiation by scattering and reflection from the ground. The instrument is also equipped with a tracer for sun movement. The pyranometer is designed to monitor total solar radiation, both direct and indirect, whereas the diffuse radiation meter is designed to measure the radiation by scattering excluding the direct solar radiation. Accordingly the pyranometer is usually used for the purpose of evaluating air stability. Some of typical examples in this group are those developed by Robitzsch, Moll and Eppley, all of which are based on the principle to detect a temperature difference between white and black plates that absorb the solar radiation by means of bimetal or thermocouple.

The use of bimetal and thermocouple gives readings in terms of a mechanical displacement and an electromotive force respectively. As for the net radiation meter, it measures the difference between upward radiation from the ground and downward radiation from the sky.

(2) Instruments used to measure solar radiation and net radiation balance

1) Solar radiation meter

The type of radiation meter applied for this survey is a pyranometer of Eppley type widely in use in Japan that was made by EKO Instruments Trading Co., Ltd. type MS-42. Specifications of the instrument are shown in Table 4-41 and its probing head in Figure 4-28.

Table 4-41 Specifications of pyranometer used in this study

(a) Sensitivity	:	abt. $5\text{mV/cal.cm}^{-2}\cdot\text{mm}^{-1}$ 7mV/kW m^{-2}
(b) Internal resistance	:	abt. 500Ω
(c) Responce speed	:	abt. 3.8 sec. (63.2%)
(d) Coefficient of Temp.	:	abt. $-0.1\%/^{\circ}\text{C}$
(e) Cosine eorro	:	abt. 2% (angle 45° against sensing plate)
(f) Aziumth error	:	No
(g) Weight	:	2 Kg
(h) Length of lead wire	:	10 m (additional lead cable shall be prepared by user)

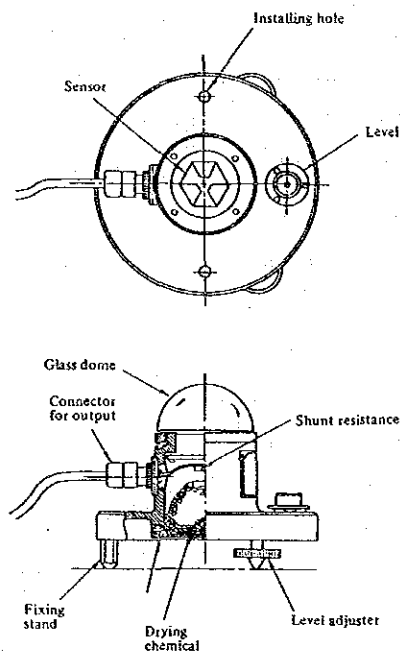


Figure 4-28 Probing part of the pyranometer

As seen in Figure 4-28, white and black plates are arranged radially about the center and the intensity of solar radiation is measured in term of a temperature difference between them. The probing head is made of 39 copper/ constantan thermocouples and white plates of barium sulphate highly reflective and moisture resistant and black plates coated by Parsons Opticals Black. In order to avoid the influences of a sudden temperature change and wind, the upper part of probing head is covered by a transparent glass made dome and is maintained as sealed. The silicagel was put inside the dome cover to avoid the blur of the dome glass.

The radiation measured is converted into both instantaneous value ($\text{cal}\cdot\text{cm}^{-2}\cdot\text{min}^{-1}$) and one hour cumulative value ($\text{cal}\cdot\text{cm}^{-2}\cdot\text{hr}^{-1}$) and then recorded.

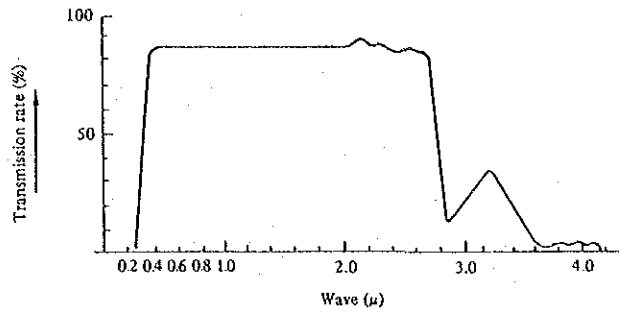


Figure 4-29 Transmission characteristics of dome glass of the pyranometer

2) Net radiation meter

A net radiation meter manufactured by EKO Instruments Trading Co., Ltd. type CN-11 was applied for this survey since it enable the observer to monitor radiation energy in the wide range of from short to long wave length. Specifications of the instrument are listed in Table 4-42 and its external appearance is shown in Figure 4-30.

Table 4-42 Specifications of the net radiation meter used

1)	1-1	Sensitivity	: 35mV/kW.m ⁻² 25mV/cal.cm ⁻² .min ⁻¹
	1-2	Internal resistance	: about 90Ω
	1-3	Response speed	: about 20 sec.
	1-4	Temperature range	: -15° to 40°C
	1-5	Accuracy	: ±5%
	1-6	Wave length region	: 0.3 - 30μm or more
	1-7	Size of sensing plate	: 38 x 38 (mm)
	1-8	Painting of sensing plate:	Parson Optical Black
	1-9	Polyethylene dome	: Special polyethylene dome
		As to its transmissivity	see attached Fig. 7
2)		Main body	
	2-1	Size	: 640 ^L x 220 ^W x 220 ^H (mm)
	2-2	Weight	: about 7.6 kg
	2-3	Power source	: AC 100V/220V ±10% 50/60Hz
	2-4	Power consumption:	about 55W
	2-5	Fuse	: 2A
	2-6	Coating	: Manssel N-6

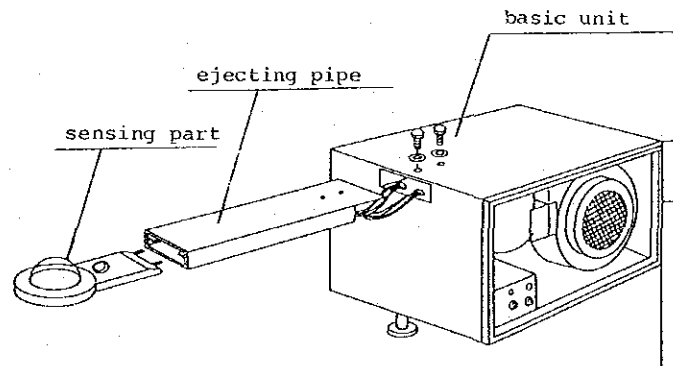


Figure 4-30 The external appearance of net radiation meter

The probing part of the instrument (as shown in Figure 4-31) is covered by a polyethylene made dome with transmission characteristics to cover a wide range of wave length, consists of 250 compensating type thermocouples which detect radiation coming downward and upward. The dew on the surface of dome gives an appreciable impact on transmission characteristic of radiation in long wave length range and thus a provision was made to blow onto the outer surface of dome by a blower installed and also to supply a dry air stream inside the dome through a dehumidifier of thermoelectric cooling type. The net radiation measured by the instrument is again converted into both instantaneous value ($\text{cal}\cdot\text{cm}^{-2}\cdot\text{min}^{-1}$) and one hour cumulative value ($\text{cal}\cdot\text{cm}^{-2}\cdot\text{h}^{-1}$) and then is recorded together with pyranometer readings.

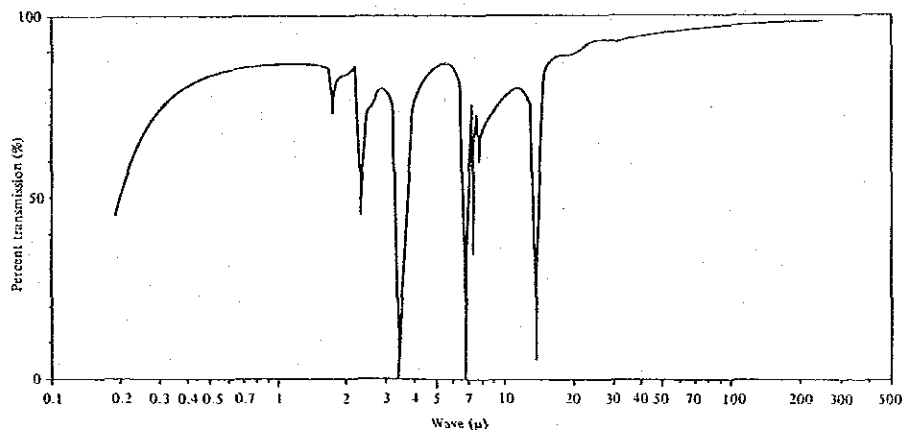


Figure 4-31 Transmission characteristics of polyethylene dome

(3) Measurement

Prior to the start of measurements, the recording part was set at one hour cumulative value by the cumulative recording selector and recording pens were set at the starting time. Thus both the radiation and radiation balance value were continuously and automatically monitored as instantaneous as well as one hour cumulative values.

(4) Calibration

The sensing parts of both pyranometer and net radiation meter had been calibrated at shop before they were delivered to the monitoring sites such that additional calibrations were not required. The instruments are thought serviceable so long as they don't show abnormal readings but it is thought desirable that they receive once a year inspection by the maker to assure the sensitivity.

(5) Inspections

Those listed in Table 4-43 are inspections practiced to maintain the reliable performances of pyranometer and net radiation meter for a longterm period.

Table 4-43 Inspections done on the pyranometer and net radiation meter

Items			Frequency			
	Objective	Contents	Daily	Weekly	Month	Whenever necessary
Pyranometer	1) pole	confirm vertical erection	x			
	2) glass dome	blur or damage	x			
	3) silicagel	supply or replacement				x
Net radiation meter	1) pole	confirm vertical erection	x			
	2) polyethylene dome	blur or damage tension of dome surface replacement of dome	x x			
	3) air pump	confirm flow rate replacement of silicagel	x		x	
Re-corder	1) recorder	confirm chart advance	x			
		confirm time slip of chart	x			
check ink shade		x				
replacement of chart					x	
	supply of ink					
	2) power supply & connection	confirm loose and disconnection	x	x		

(6) Measurement results

Table 4-44 summarizes the effective measuring hours of MS1 monitoring station with respect to both instruments, which shows the station satisfying a minimum required for an effective station in Japan.

Table 4-44 Effective measuring hours of the pyranometer and net radiation meter

Measurement	Effective measuring hrs	Availability
Radiation	8,654	98.5
Net radiation flux	8,558	97.4

Total hours for the period of Jan. 17, 1988 through Jan. 16, 1989 are 8,784.

The hourly means of radiation and net radiation observed are exemplified in Table 4-45 and Table 4-46 but complete set of data are enclosed in Appendix and discussions are included in the succeeding chapters.

Table 4-45 An example of measurements of solar radiation

Table with 40 columns: 1980YEAR, 2 MONTH, ITEM (3), SUN, ST. (1) (HS1) ONE STATION (W/H2), HOUR DAY, 1-24, MIN, MAX, AVE, HOUR TOTAL.

Table 4-46 An example of net radiation flux measurements

Table with 40 columns: 1980YEAR, 2 MONTH, ITEM (13), NET, ST. (1) (HS1) ONE STATION (W/H2), HOUR DAY, 1-24, MIN, MAX, AVE, HOUR TOTAL.

5. Short term field survey

The short term field survey addressed that of particle distribution of suspended particulate matter and was made in three times, firstly during January 6, 1988 through February 2, 1988, secondly during the period of March 3 1988 through March 27 1988 and thirdly (lastly) during the period of July 4, 1988 through July 28, 1988. During each period the atmospheric air was continuously aspirated by Andersen samplers for 13 days and the trapped dust samples were subject to size distribution analyses. In addition, the particulate sample trapped by filters was brought back in Japan and was subject to chemical, elemental and ion analyses after the sample was screened into two parts, fine part (<2.1 micron m) and coarse part (>2.1 micron m).

As for the chemical analysis, samples trapped by Low volume samplers during the same period were also subject to analysis together with other soil samples representative in Samut Prakarn, a road dust, two types of gasoline. Furthermore, the sulphur content of 10 fuels including gasoline and heavy oil in use in Thailand were measured by the chemical analysis.

5.1 Measurement of particle distribution about the dust sample collected by Andersen samplers

5.1.1 Outline of the survey

The Andersen samplers pre-calibrated and loaded with filters were installed at each monitoring station and were switched on at 11:00 AM of the starting day by members grouped in five teams. Then the atmospheric air was aspirated by each sampler at the flow rate of 28.3 liter per minute. After the instruments commissioned in this way, they were kept under inspection of patrols, twice a day in morning and in afternoon. Table 5-1 shows the format of a recording chart used and Table 5-2 the work schedule of each survey period.

Weighing of filters loaded with suspended particulate matter was practiced by precision chemical balances at Ishikawajima Inspection & Instrumentation Co., Ltd. after filters were desiccated in the thermohygrostat. The recording chart used here is shown Table 5-3. The atmospheric concentration was back-calculated by knowing the difference of weight between before and after measurement and air volume aspirated.

Table 5-1 Recording chart of Andersen sampler

Monitoring Station		Instrument No.		Sampling Time				Person in charge		
				Hours		minutes				
				(1) Total		minutes				
Monitoring Period		Front 1988		Morning Afternoon		hour min		(2) Average Flow Rate (l/min)		
		To 1988		Morning Afternoon		hour min		(3) (1)/(1000 Total Absorbed Volume (cc))		
Date	Flow Meter	Pressure	Date	Flow Meter	Pressure	Date	Flow Meter	Pressure	Classified	Filter
Month	Scale	(mmHg)	Month	Scale	(mmHg)	Month	Scale	(mmHg)	Stage	Number
Day			Day			Day			(µm)	
Start			/	a)		/	a)		>11	
/			/	b)		/	b)		11-7.0	
/	a)		/	a)		/	a)		7.0-6.7	
/	b)		/	b)		/	b)		6.7-3.3	
/	a)		/	a)		/	a)		3.3-2.1	
/	b)		/	b)		/	b)		2.1-1.1	
/	a)		/	a)		/	a)		1.1-0.65	
/	b)		/	b)		/	b)		0.65-0.43	
/	a)		/	a)		/	a)		<0.43	
/	b)		/	b)		/	b)		Remarks	
/	a)		/	a)		/	a)			
/	b)		/	b)		/	b)			
/	a)		/	a)		/	a)			
/	b)		/	b)		/	b)			
/	a)		/	a)		/	a)			
/	b)		/	b)		/	b)			
/	a)		/	a)		/	a)			
/	b)		/	b)		/	b)			
/	a)		/	a)		/	a)			
/	b)		/	b)		/	b)			

a) before adjustment
 b) after adjustment
 Flow Rate = B/min

Table 5-2 Work schedule of each field survey

1st field survey			2nd field survey			3rd field survey		
Date	Monitoring of TPM	Size distribution of TPM	Date	Monitoring of TPM	Size distribution of TPM	Date	Monitoring of TPM	Size distribution of TPM
1988 Jan. 9	Setting up	Setting up	1988 Mar. 8	Setting up	Setting up	1988 Jul. 12	Setting up	Setting up
10			9			13	started	started
11			10			14		
12			11	started	started	15		
13			12			16		
14			13			17		
15	Technician training	Technician training	14			18		
16			15			19		
17	started	started	16			20		
18			17			21		
19			18			22		
20			19			23		
21			20			24		
22			21			25		
23			22			26		
24			23					
25			24					
26								
27								
28								
29								
30								

- Monitoring of TPM
 - Flow rate arranged
 - Filter set
 - △ Flow rate check and adjustment
 - ▲ TPM monitoring completed
 - ◻ Filter replace, flow rate check and adjustment
 - Installation of Low Volume samplers
- Monitoring of size distribution of TPM
 - Flow rate arranged
 - Filter set
 - △ Flow rate check and adjustment
 - ▲ TPM monitoring completed, withdrawal of Andersen samplers
 - ◻ Installation of Andersen samplers

Table 5-3 Recording chart of Andersen samplers

Monitoring Station						Instrument No.			
Monitoring Period		From: 198							
		To: 198							
Incubating Time Before Sampling		From: 198							
		To: 198							
Incubating Time After Sampling		From: 198							
		To: 198							
Absorbing Time	(1)	min.	Incubating time before sampling	min.	Incubating time after sampling	min.			
Average Flow Rate	(2)	l/min.	Total Flow Rate (1)×(2)		(3)	m ³			
Classified Stage (μ)	Filter No.	Weight(mg) After sampling	Weight(mg) Before sampling	Sampled Volume (mg)	Particulate Conc. by Size(mg/m ³)	Remarks			
> 11				(4)					
11 - 7.0				(5)					
7.0 - 4.7				(6)					
4.7 - 3.3				(7)					
3.3 - 2.1				(8)					
2.1 - 1.1				(9)					
1.1 - 0.65				(10)					
0.65 - 0.43				(11)					
< 0.43				(12)					
Total Sampled Particulate(mg)				(13)	Temperature of laboratory		°c		
Total Particulate Conc. (mg/m ³)				(13)/(12)	Humidity of laboratory		%		
Remarks:									

5.1.2 Instrument and Handling Methods

(1) Andersen sampler

Andersen samplers employed in this study was a SIBATA Model AN-200 which was equipped with multi-layer jet nozzles and is designed to monitor size distribution of suspended particulate matter by impactor system. The samplers consist of size separating body, rotameter, pressure gage, pump and shelter.

The instrument is made of 8 layers stage corrosion resistant aluminum alloy and each stage has 800, 400 and 200 numbers of jet nozzles and, in the bottom of the stages, stainless steel made round collector plate is installed. The diameters of the jet nozzles are designed such that they get smaller from the top stage to the bottom one in descending order and so when the constant flow rate of air is aspirated from the upper inlet, the jet air velocity increases as it goes into the lower stages. As shown in Fig. 5-1, the size of particulates decreases as stage goes from top to bottom.

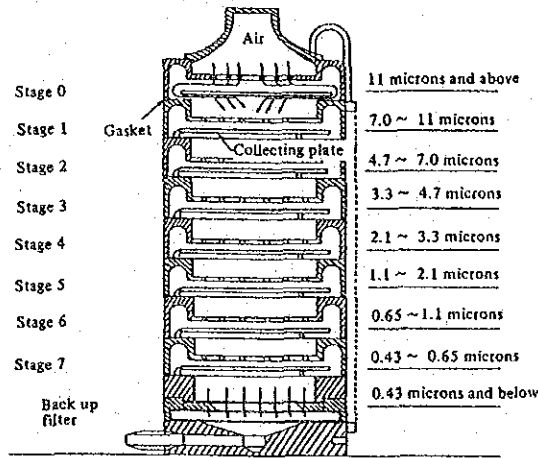


Fig. 5-1 Structure of Andersen sampler

Generally the inertial impaction parameter of impactor is defined by a functioning of the ratio of particulate size, flow velocity of particulate and section area of nozzle. According to Ranz and Wong, such relation between them can be expressed by the following equation.

$$\psi = \frac{C \cdot p \cdot V_c \cdot d_p^2}{18 \mu D_c} \dots\dots\dots \text{Equation (5-1)}$$

where,

C; Cunningham slip correction factor = $1.00 + \frac{0.16 \times 10^{-4}}{d_p}$

d_p ; size (cm) of particulate matter

μ ; air viscosity (1.84×10^{-4} g/cm. sec)

p; density of particulate matter (g/cm^3)

V_c ; air velocity passing through jet nozzles (cm/sec)

D_c ; diameter of jet nozzle (cm)

ψ ; non dimensional inertial impaction parameter

(when impaction efficiency 50%, $\psi_{50} = 0.14$)

When air sampling volume Q (cm^3/min), number of jet nozzles of the stage N, V_c is obtained by the following equation:

$$V_c = \frac{Q}{60 \pi (D_c/2)^2 N} \dots\dots\dots \text{Equation (5-2)}$$

When the Equation (5-2) is substituted by Equation (5-1), 50% aerodynamic particle size d_{p50} can be obtained from the following equation:

$$d_{p50} = \sqrt{\frac{18 \mu \psi_{50} N \pi \times 60 D_c^3}{4 C Q}} \dots\dots\dots \text{Equation (5-3)}$$

Where, $Q = 28,317 \text{ cm}^3/\text{min} = 28.3 \text{ l}/\text{min}$. Geometrical particle size is obtained as $\sqrt{d_p^2/p}$.

By the Equation (5-3), the particle sizes of particulate matter collected at the respective stages are obtained and the ranges of the particles size are shown in Table 5-4. The collection efficiency by the size is shown in Fig. 5-2.

Table 5-4 50% cut-off values of each stage

Stage	Nozzle diameter	Number of nozzle	Jet velocity	50% cut-off value	Catalogue value
0	1.18 mm	800	0.54 ms ⁻¹	10.0µm	11.0µm
1	1.18	400	1.07	7.0	7.0
2	0.91	400	1.85	4.7	4.7
3	0.71	400	2.98	3.3	3.3
4	0.53	400	5.34	2.1	2.1
5	0.34	400	13.0	1.03	1.1
6	0.25	400	24.0	0.62	0.65
7	0.25	200	48.0	0.42	0.43

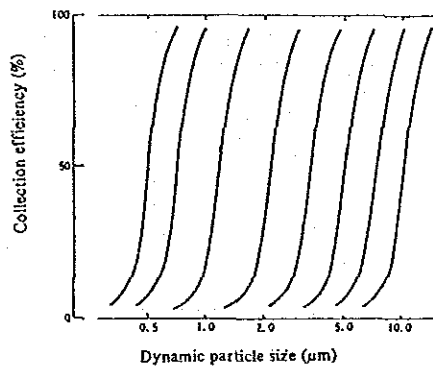


Fig. 5-2 Classification (sieving) characteristic of impactor

Table 5-5 shows the specifications of Andersen sampler and Fig. 5-3 shows external view of Andersen sampler.

Table 5-5 Specifications of Andersen sampler

Sampler main body:	8 layer stages, size classification sampler of suspended particulate matter
Pump:	Rotary compressor, HITACHI 200 W RC-20S type Max. pressure 0.5 kg/cm ² Operation pressure: 0.4 kg/cm ² Air supply: 55 NI/min (at operating) Output: 200 W Voltage: 100 V
Piping:	Flow meter (float-type area flow meter) Tokyo Keiki KK Scale: 4-40 l/min Elbow and Hitting: brass, nickel plated Connecting tube: Nylon 11 3/8" (inner diameter)

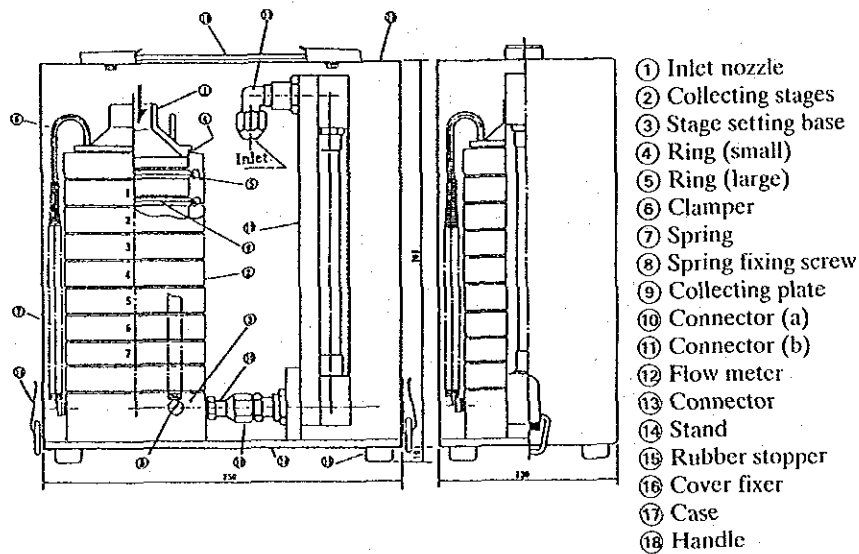


Fig. 5-3 Outside view of main body of Andersen sampler

The handling methods of Andersen sampler are as follows.

① Preparatory work

The collection plates of the respective stages are all completely cleaned and dried. (In this study, supersonic cleaning was employed as described later.)

Collection plates (Polyethylene sheets) and back-up filters are weighed prior to assembly.

② Procedure

(i) Remove the key of the bottom part of the case, and take out the main body from the case. Then the flow meter is connected to the pump by tube.

(ii) The back-up filters are placed on the back-up holder.

(iii) Install collection plates on the sieving stages.

- (iv) Remove the cover of air inlet located in the upper part of sampler, and then switch on the power. Adjust the flow rate by valve of the pump, and fix the rate at 28.3 ℓ/min by reading the previously calibrated rotameter and pressure meter.
- (v) Through patrols 2 or 3 times a day, confirm that the flow rate is kept exactly at 28.3 ℓ/min. If not kept right, adjust the rate by the valve of the pump.
- (vi) After the measurement is completed (in this study, for the period of about 13 days), transfer the collection plates and back-up filters into the air-conditioned room for de-siccation for about 24 hours. Then they are weighed by the precision chemical balance which has a sensitivity of weighing 0.01 mg.

③ Maintenance

After the monitoring is completed, all the stages are cleaned by a supersonic cleaner by using the neutral detergent, and are dried up. They are kept in the assembly case.

(2) Supersonic cleaner

A supersonic cleaner is used for cleansing of classified stages collection plates of Andersen sampler. In this study, a SHARP UTB-152 supersonic cleaner was employed.

The supersonic cleaner was designed to generate pressure waves in cleaning tank, produced countless number of fine bubbles, and removes all the dirt mechanically.

The Table 5-6 shows the specifications of the supersonic cleaner and Fig. 5-4 shows its outside view.

Table 5-6 Specifications of supersonic cleaner

Size of main body	350×425×360 mm
Size of cleaning bath	220×220×140 mm
Output	150 W
Bath capacity	6.0 liter
Weight	28 kg

Prior to starting the cleaner, pour detergent solution into the tub, and soak collecting plates of Andersen sampler using an attached service rack. It takes about 10 to 15 minutes to complete cleaning.

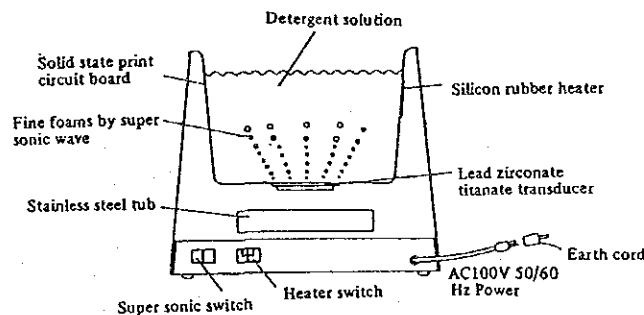


Fig. 5-4 Outside view of supersonic cleaner

(3) Filters

In this study, polyethylene sheet and polyfrone filter were used to analyze elements of particulate matter. The polyethylene sheets were placed on the 0~8 stage collecting plates of Andersen samplers while the polyfrone filter was used as back-up holder.

5.1.3 Calculations of TSP Size Distribution

(1) Calibration of Andersen sampler

The wet-type gas meter, bypass, pressure gage, rotameter, and suction pump were connected in series as shown in Fig. 5-5.

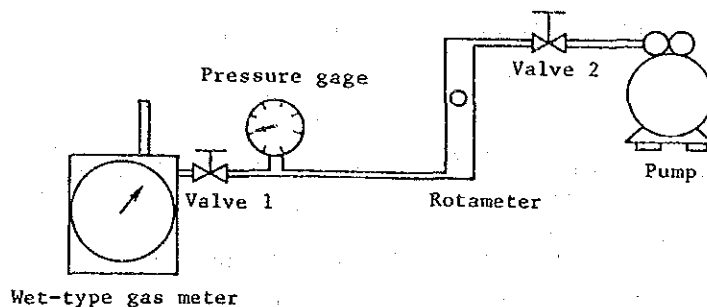


Fig. 5-5 Calibration of rotameter for Andersen sampler

- ① The flow rate reading indicated in rotameter was fixed at about 30 ℓ/min and also the pressure loss was adjusted at about 55 mmHg by controlling the valve of bypass 1.
- ② The pressure reading indicated in pressure gage were recorded when flow rate of rotameter were adjusted at 30, 25, 20 and 15 ℓ/min respectively, and the measurement time were recorded when the air volumes aspirated into the wet-type gas meter were 20 or 30 ℓ/min respectively. An example of the results is shown in Table 5-7, and all results are shown in the Appendix.

Table 5-7 An example of calculation results of rotameter for Andersen sampler

No200522 MS1

Pressure ΔP <mmHg>	Flow Meter Scale	Total Sampling Volume<ℓ>	Sampling Time <sec>	Wet Gas Meter Temp<°C>	Flow Val.Qg0 <ℓ/min>	Ave. Qg0	Flow Val.Qr0 <ℓ/min>
15	15	10	37.75	24.4	15.6589	15.67	14.74
15	15	10	37.75	24.4	15.6589		
15	15	10	37.65	24.4	15.7005		
25	20	20	57.55	24.6	20.5291	20.52	19.52
25	20	20	57.57	24.6	20.5220		
25	20	20	57.57	24.6	20.5220		
38	25	20	46.60	24.5	25.3616	25.39	24.18
38	25	20	46.46	24.5	25.4380		
38	25	20	46.80	24.5	25.3616		
55	30	20	39.30	24.4	30.0826	30.08	28.68
55	30	20	39.34	24.4	30.0520		
55	30	20	39.27	24.4	30.1056		

- ③ The flow rate calculated from the required time for aspirating the prescribed amount was corrected to that at the designed temperature (20°C) of rotameter by the Equation (5-4). An example of the results is shown in Table 5-7.

$$Q_{g_0} = \frac{273+T_0}{273+Temp.} \times V \times \frac{60}{t} \dots\dots\dots \text{Equation (5-4)}$$

where,

- Q_{g_0} ; flow rate of wet-type gas meter at 20°C (ℓ/min)
- Temp.; temperature of wet-type gas meter during calibration (°C)
- T_0 ; designed temperature of rotameter (20°C)
- V; measured air volume of wet-type gas meter (ℓ)
- t; necessary time for sucking the volume V (S)

- ④ Flow rate Q_{r_0} at the designed condition of rotameter was obtained by using the Equation (5-5) by correcting the reading value of rotameter (Q_r). An example of the results is shown in Table 5-7.

$$Q_{r_0} = Q_r \times \sqrt{\frac{273+T_0}{273+Temp.}} \times \sqrt{\frac{760-\Delta P}{P_0}} \dots\dots\dots \text{Equation (5-5)}$$

where,

- Q_{r_0} ; flow rate of rotameter at the designed condition (ℓ/min)
- Q_r ; reading value of rotameter (ℓ/min)
- P_0 ; designed pressure of rotameter (760 mmHg)
- ΔP ; reading value of pressure gage (mmHg)
- T_0 ; designed temperature of rotameter (20°C)
- Temp.; temperature at calibration (°C)

- ⑤ The relationship between Q_{g_0} [flow rate of wet-type gas meter calculated by the Equation (5-4)] and Q_{r_0} [flow rate of rotameter calculated by the Equation (5-5)] can be expressed by the Equation (5-6).

$$Q_{g_0} = a (Q_{r_0}) + b \dots\dots\dots \text{Equation (5-6)}$$

In above equation, a and b are regression coefficients. An example of calculation by the Equation (5-6) is shown in Fig. 5-6, and all other results are shown in the Appendix.

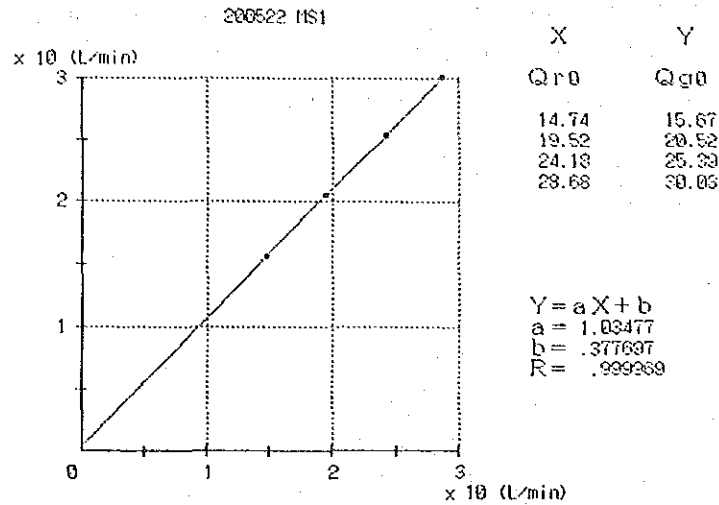


Fig. 5-6 An example of relation between flow rate of wet-type gas meter and rotameter

- ⑥ Flow rate of rotameter was calculated by Equation (5-6) when the Q_{g0} is 28.3 ℓ/min , and then Q_r values were estimated by the Equation (5-7) when the pressure losses were 40, 25 and 15 mmHg respectively. An example of the results is shown in Fig. 5-7, and all results are shown in the Appendix.

Those figures were posted on the inside-door of the shelter at each monitoring station.

$$Q_r = \frac{Q_{rs_0}}{\sqrt{\frac{273+T_0}{273+\text{Temp.}} \times \frac{760-\Delta P}{P_0}}} \dots\dots\dots \text{Equation (5-7)}$$

where,

- Q_r ; reading value of rotameter (ℓ/min)
- Q_{rs_0} ; flow rate of rotameter calculated by Equation (5-6) when the Q_{g0} is 10 ℓ/min (ℓ/min)
- P_0 ; designed pressure of rotameter (760 mmHg)
- ΔP ; reading value of pressure gage (mmHg)
- T_0 ; designed temperature of rotameter (20°C)
- Temp.; average estimation temperature (°C)
(average temperature which is estimated at actual-site survey)
- Jan. to Feb.: 27.0°C
- Mar. to Apr.: 29.8°C
- May to Jun.: 29.4°C
- Jul. to Aug.: 28.6°C
- Sept. to Oct.: 28.1°C
- Nov. to Dec.: 26.6°C

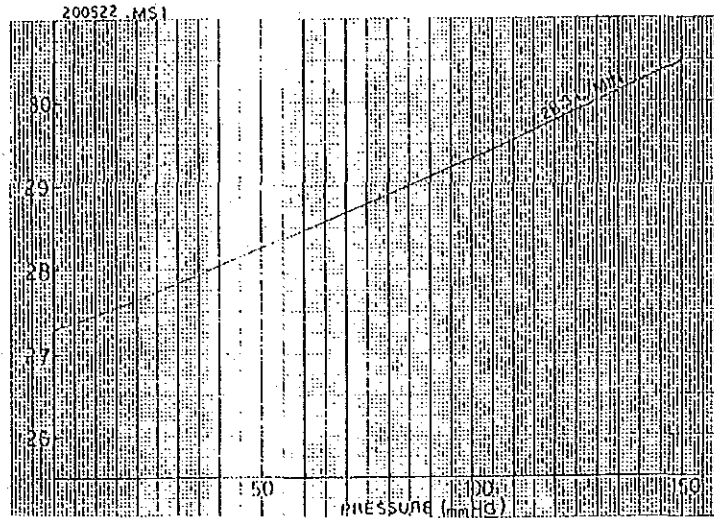


Fig. 5-7 The relation between reading value of rotameter and pressure value indicated in pressure gage when aspiration air volume is 28.3 ℓ/min

(2) Air aspiration volume of Andersen sampler

The total air aspiration volume of Andersen sampler was calculated by obtaining air sucking volume R_i between (i-1) patrol and (i) patrol, and by summing of them.

- ① Firstly, the flow rate of rotameter before and after the adjustment at patrols was corrected into the flow rate of rotameter at the designed condition (20°C, 760 mmHg) by using Equation (5-8) and (5-9).

$$Q_{ra_{0i-1}} = \sqrt{\frac{760 - \Delta P_{a_{i-1}}}{P_0}} \times \sqrt{\frac{273 + T_0}{273 + \text{Temp.}}} \times Q_{ra_{i-1}} \dots \dots \dots \text{Equation (5-8)}$$

$$Q_{rb_{0i}} = \sqrt{\frac{760 - \Delta P_{b_i}}{P_0}} \times \sqrt{\frac{273 + T_0}{273 + \text{Temp.}}} \times Q_{rb_i} \dots \dots \dots \text{Equation (5-9)}$$

where,

- $Q_{ra_{0i-1}}$; designed condition flow rate after adjustment at (i-1) patrol (ℓ/min)
- $Q_{rb_{0i}}$; designed condition flow rate before adjustment (i) patrol (ℓ/min)
- $Q_{ra_{i-1}}$; rotameter reading value after adjustment at (i-1) patrol (ℓ/min)
- Q_{rb_i} ; rotameter reading value before adjustment at (i) patrol (ℓ/min)
- T_0 ; designed condition temperature of rotameter (20°C)
- Temp.; average temperature which is estimated at monitoring (°C)
- P_0 ; designed pressure of rotameter (760 mmHg)
- $\Delta P_{a_{i-1}}$; reading value of pressure gage after adjustment at (i-1) patrol (mmHg)
- ΔP_{b_i} ; reading value of pressure gage before adjustment at (i) patrol (mmHg)

- ② Secondly, the flow rate Q_{r_0} at designed condition of rotameter was corrected into wet-type gas meter flow rate Q_{g_0} at 20°C by using Equation (5-10).

$$\left. \begin{aligned} Q_{g_{i-1}}^0 &= a(Q_{r_{i-1}}^0) + b \\ Q_{g_i}^0 &= a(Q_{r_i}^0) + b \end{aligned} \right\} \dots\dots\dots \text{Equation (5-10)}$$

where,

- $Q_{g_{i-1}}^0$; corrected flow rate at designed condition at (i-1) patrol (ℓ/min)
- $Q_{g_i}^0$; corrected flow rate at designed condition at (i) patrol (ℓ/min)

- ③ Air sucking volume R_i during (i-1) patrol and (i) patrol were obtained by multiplying lapse time t and the mean value of flow rate after adjustment at (i-1) patrol and that before adjustment at (i) patrol.

$$R_i = \frac{Q_{g_{i-1}}^0 + Q_{g_i}^0}{2} \times t \times \frac{1}{1000} \dots\dots\dots \text{Equation (5-11)}$$

where,

- R_i ; air sucking volume during (i-1) patrol and (i) patrol (m³)
- t ; lapse time during (i-1) patrol to (i) patrol (min)

- ④ The total air sucking volume at the designed temperature was obtained as the sum of air sucking volume during each patrolling time, and then the corrected total air sucking volume at field condition was estimated by the following Equation (5-12).

$$V_i = \sum_{i=1}^n R_i \frac{273 + \text{Temp}}{273 + T_0} \dots\dots\dots \text{Equation (5-12)}$$

where,

- V_i ; Total air sucking volume under the temperature at monitoring (m³)
- n ; number of patrols (excluding the time of commencement of monitoring, and including the time of completing of monitoring)
- T_0 ; designed temperature of rotameter (20°C)
- Temp.; average estimation temperature (°C)

An example of calculation results of sucking air volume by this method is shown in Table 5-8, and all results are shown in the Appendix.

In case accidental power failure occurs during monitoring, the estimated air sucking volume by this method becomes inaccurate. So, in this study, the power failure time was calculated by the charts of automatic and continuous instruments and the count values of integrated flow meter installed in Low-volume sampler. Power failure times are shown as follows.

Table 5-8 An example of calculation results of air sucking volume of Andersen sampler

MS1		ROTOR NO.200522			TEMP(°C) 27.0				
DATE	TIME	LAPSE TIME (MIN)	STOP TIME (MIN)	ROTOR METER (L/min)	PRESSURE DIFFERENCE (mmHg)	CORRECTED FLOW RATE (L/min)	CALIBRATED FLOW RATE (L/min)	FLOW VOL (m3)	
1/17	11:00	0	0	28.1	43.0	28.2	29.6		
1/17	15:44	B 284	0	28.0	43.0	28.1	29.5	8.4	
1/17	15:44	F 0	0	28.1	43.0	28.2	29.6		
1/18	9:50	B 1086	0	26.5	40.0	26.7	28.0	31.3	
1/18	9:50	F 0	0	28.2	45.0	28.3	29.6		
1/18	14:45	B 295	0	28.3	45.0	28.4	29.7	8.8	
1/18	14:45	F 0	0	28.3	45.0	28.4	29.7		
1/19	9:55	B 1150	0	29.0	48.0	29.0	30.4	34.6	
1/19	9:55	F 0	0	28.2	47.0	28.2	29.8		
1/19	15:21	B 326	0	28.0	45.0	28.1	29.4	9.6	
1/19	15:21	F 0	0	28.3	46.0	28.4	29.7		
1/20	10:54	B 1173	0	28.2	47.0	28.2	29.6	34.8	
1/20	10:54	F 0	0	28.2	47.0	28.2	29.6		
1/20	16:11	B 307	0	28.2	48.0	28.2	29.6	9.1	
1/20	16:11	F 0	0	28.2	48.0	28.2	29.6		
1/21	10:11	B 1090	0	28.3	55.0	28.2	29.5	32.2	
1/21	10:11	F 0	0	28.4	56.0	28.3	29.6		
1/22	10:00	B 1429	0	28.3	60.0	28.1	29.4	42.2	
1/22	10:00	F 0	0	28.6	61.0	28.4	29.7		
1/23	10:28	B 1468	0	28.4	67.0	28.0	29.4	43.4	
1/23	10:28	F 0	0	28.6	68.0	28.2	29.6		
1/24	8:57	B 1349	0	28.6	73.0	28.1	29.5	39.8	
1/24	8:57	F 0	0	28.7	74.0	28.2	29.6		
1/25	10:45	B 1548	0	28.2	76.0	27.7	29.0	45.3	
1/25	10:45	F 0	0	28.2	76.0	27.7	29.0		
1/26	10:40	B 1435	0	28.7	82.0	28.0	29.4	41.9	
1/26	10:40	F 0	0	28.7	82.0	28.0	29.4		
1/27	15:40	B 1740	0	28.5	84.0	27.8	29.1	50.9	
1/27	15:40	F 0	0	28.2	87.0	28.4	29.8		
1/28	14:13	B 1353	0	29.0	90.0	28.2	29.5	40.1	
1/28	14:13	F 0	0	29.0	90.0	28.2	29.5		
1/29	10:59	B 1246	0	28.0	86.0	27.3	28.6	36.2	
1/29	10:59	F 0	0	29.2	95.0	28.2	29.6		
1/30	11:00	B 1441	0	29.8	98.0	28.8	30.1	43.0	
TOTAL 18720 (min)							TOTAL 564.8 (m3)		

Regression coefficients; a = 1.035
b = 0.378

Table 5-9 Power failure time

Date	Monitoring station	Power failure time (minute)	Remarks
11:50 17/1, 1988 13:25 18/1, 1988	MS3	1535	Accident of suction pump
16:40-16:50 20/1, 1988	MS2	10	Power failure
12:45-13:05 21/1, 1988	MS5	20	Checking of suction pump
15:45-16:35 21/1, 1988	MS5	50	Checking of suction pump
9:10-11:10 18/7, 1988	MS5	120	Power failure

(3) Calculation of particulate matter on the each stage of Andersen sampler

The concentration of particulate matter on the each stage was calculated by weighing polyethylene sheets placed on the each plates before and after samplings and that of polyfluoro-carbon filter placed on the back-up holder. The ambient concentration of each stage was calculated by the Equation (5-13).

$$C_i = \frac{W_{c_i} - W_{s_i}}{V} \times 10^3 \dots\dots\dots \text{Equation (5-13)}$$

where,

- C_i; concentrations of particulate matter on the each stage (stage 0 to 7) and back-up holder ($\mu\text{g}/\text{m}^3$)
- W_{e_i}; weight of polyethylene sheets and polyfluorocarbon filter after sampling (mg)
- W_s; weight of polyethylene sheets and polyfluorocarbon filter before sampling (mg)
- V; sampling volume (m^3)

The list of particulate concentration classified by particle size is shown in Table 5-10.

Table 5-10 (1) Results of particulate concentration classified by particle size

THE FIRST FIELD SURVEY				STATION NO.1				STATION NO.4			
STAGE	DIAMETER (μm)	FILTER NO.	DUST WEIGHT (mg)	DUST CONC. (μg/m ³)	ACC.DUST CONC. (μg/m ³)	STAGE	DIAMETER (μm)	FILTER NO.	DUST WEIGHT (mg)	DUST CONC. (μg/m ³)	ACC.DUST CONC. (μg/m ³)
0	>11	MS1-S1-1	3.93	7.0	79.7	0	>11	MS4-S1-1	8.54	15.1	82.6
1	11-7.0	MS1-S2-1	3.36	5.9	72.7	1	11-7.0	MS4-S2-1	4.47	7.9	67.5
2	7.0-4.7	MS1-S3-1	5.99	10.6	66.7	2	7.0-4.7	MS4-S3-1	4.88	8.6	59.5
3	4.7-3.3	MS1-S4-1	5.64	10.0	56.1	3	4.7-3.3	MS4-S4-1	5.36	9.5	51.0
4	3.3-2.1	MS1-S5-1	4.19	7.4	46.2	4	3.3-2.1	MS4-S5-1	3.84	6.8	41.6
5	2.1-1.1	MS1-S6-1	3.95	7.0	38.7	5	2.1-1.1	MS4-S6-1	3.42	6.0	34.8
6	1.1-0.65	MS1-S7-1	4.36	7.7	31.7	6	1.1-0.65	MS4-S7-1	4.1	7.2	28.7
7	0.65-0.43	MS1-S8-1	4.22	7.5	24.0	7	0.65-0.43	MS4-S8-1	2.79	4.9	21.5
8	<0.43	MS1-BF-1	9.35	16.5	16.6	8	<0.43	MS1-BF-1	9.39	15.6	16.6
AIR VOLUME (m ³) = 564.8			TOTAL CONC.(μg/m ³) = 79.7			AIR VOLUME (m ³) = 566.5			TOTAL CONC.(μg/m ³) = 82.6		
STATION NO.2				STATION NO.5							
STAGE	DIAMETER (μm)	FILTER NO.	DUST WEIGHT (mg)	DUST CONC. (μg/m ³)	ACC.DUST CONC. (μg/m ³)	STAGE	DIAMETER (μm)	FILTER NO.	DUST WEIGHT (mg)	DUST CONC. (μg/m ³)	ACC.DUST CONC. (μg/m ³)
0	>11	MS2-S1-1	3.35	5.2	70.6	0	>11	MS5-S1-1	5.35	9.5	72.5
1	11-7.0	MS2-S2-1	2.85	5.0	64.3	1	11-7.0	MS5-S2-1	4.13	7.4	62.9
2	7.0-4.7	MS2-S3-1	4.7	8.2	59.3	2	7.0-4.7	MS5-S3-1	6.69	11.9	55.6
3	4.7-3.3	MS2-S4-1	4.68	8.2	51.1	3	4.7-3.3	MS5-S4-1	5.9	10.5	43.7
4	3.3-2.1	MS2-S5-1	3.78	6.6	42.8	4	3.3-2.1	MS5-S5-1	3.23	5.8	33.2
5	2.1-1.1	MS2-S6-1	3.72	6.5	36.2	5	2.1-1.1	MS5-S6-1	2.13	3.8	27.4
6	1.1-0.65	MS2-S7-1	4.6	8.1	29.7	6	1.1-0.65	MS5-S7-1	3.43	6.1	23.6
7	0.65-0.43	MS2-S8-1	3.43	6.0	21.6	7	0.65-0.43	MS5-S8-1	2.84	5.1	17.5
8	<0.43	MS2-BF-1	8.88	15.6	15.6	8	<0.43	MS5-BF-1	7	12.5	12.5
AIR VOLUME (m ³) = 569.8			TOTAL CONC.(μg/m ³) = 70.6			AIR VOLUME (m ³) = 561.6			TOTAL CONC.(μg/m ³) = 72.5		
STATION NO.3				STATION NO.6							
STAGE	DIAMETER (μm)	FILTER NO.	DUST WEIGHT (mg)	DUST CONC. (μg/m ³)	ACC.DUST CONC. (μg/m ³)	STAGE	DIAMETER (μm)	FILTER NO.	DUST WEIGHT (mg)	DUST CONC. (μg/m ³)	ACC.DUST CONC. (μg/m ³)
0	>11	MS3-S1-1	4.16	8.0	98.0	0	>11	MS3-S1-1	4.16	8.0	98.0
1	11-7.0	MS3-S2-1	3.74	3.3	90.0	1	11-7.0	MS3-S2-1	3.74	3.3	90.0
2	7.0-4.7	MS3-S3-1	3.59	6.9	86.7	2	7.0-4.7	MS3-S3-1	3.59	6.9	86.7
3	4.7-3.3	MS3-S4-1	6.57	12.6	79.8	3	4.7-3.3	MS3-S4-1	6.57	12.6	79.8
4	3.3-2.1	MS3-S5-1	4.62	8.8	67.2	4	3.3-2.1	MS3-S5-1	4.62	8.8	67.2
5	2.1-1.1	MS3-S6-1	4.8	9.2	50.4	5	2.1-1.1	MS3-S6-1	4.8	9.2	50.4
6	1.1-0.65	MS3-S7-1	7.95	13.5	49.2	6	1.1-0.65	MS3-S7-1	7.95	13.5	49.2
7	0.65-0.43	MS3-S8-1	9.32	17.8	35.7	7	0.65-0.43	MS3-S8-1	9.32	17.8	35.7
8	<0.43	MS3-BF-1	9.32	17.8	17.8	8	<0.43	MS3-BF-1	9.32	17.8	17.8
AIR VOLUME (m ³) = 522.0			TOTAL CONC.(μg/m ³) = 98.0			AIR VOLUME (m ³) = 522.0			TOTAL CONC.(μg/m ³) = 98.0		

Table 5-10 (2) Results of particulate concentration classified by particle size

STATION NO.1		200522		STATION NO.4		200526	
STAGE	DIAMETER (μm)	FILTER NO.	DUST WEIGHT (mg)	DUST CONC. ($\mu\text{g}/\text{m}^3$)	ACC.DUST CONC. ($\mu\text{g}/\text{m}^3$)	DUST WEIGHT (mg)	DUST CONC. ($\mu\text{g}/\text{m}^3$)
0	>11	MS1-S1-3	3.67	6.4	38.1	5.69	9.9
1	11-7.0	MS1-S2-3	2.19	3.8	31.7	2.81	4.9
2	7.0-4.7	MS1-S3-3	3.45	5.1	27.9	3.78	5.6
3	4.7-3.3	MS1-S4-3	2.9	5.1	21.9	3.06	5.3
4	3.3-2.1	MS1-S5-3	1.86	3.2	18.8	1.57	2.7
5	2.1-1.1	MS1-S6-3	0.85	1.5	13.6	0.73	1.3
6	1.1-0.65	MS1-S7-3	1.06	1.8	12.1	1.36	2.4
7	0.65-0.43	MS1-S8-3	2.11	3.7	10.2	1.75	3.1
8	<0.43	MS1-BF-3	3.76	6.6	5.6	4.44	7.8
AIR VOLUME (m ³) = 573.1		TOTAL CONC.($\mu\text{g}/\text{m}^3$) = 38.1		AIR VOLUME (m ³) = 573.0		TOTAL CONC.($\mu\text{g}/\text{m}^3$) = 44.0	
STATION NO.2		200523		STATION NO.5		200549	
STAGE	DIAMETER (μm)	FILTER NO.	DUST WEIGHT (mg)	DUST CONC. ($\mu\text{g}/\text{m}^3$)	ACC.DUST CONC. ($\mu\text{g}/\text{m}^3$)	DUST WEIGHT (mg)	DUST CONC. ($\mu\text{g}/\text{m}^3$)
0	>11	MS2-S1-3	1.78	3.1	41.3	2.23	3.9
1	11-7.0	MS2-S2-3	2.14	3.7	38.2	1.31	2.3
2	7.0-4.7	MS2-S3-3	3.24	5.6	34.6	2.41	4.2
3	4.7-3.3	MS2-S4-3	2.93	5.0	29.0	1.98	3.5
4	3.3-2.1	MS2-S5-3	1.9	3.3	24.0	1.29	2.3
5	2.1-1.1	MS2-S6-3	1.3	2.2	20.8	0.5	0.9
6	1.1-0.65	MS2-S7-3	1.97	3.4	18.5	0.78	1.4
7	0.65-0.43	MS2-S8-3	3.56	6.1	15.1	1.94	3.4
8	<0.43	MS2-BF-3	5.28	9.0	9.0	3.75	6.5
AIR VOLUME (m ³) = 583.6		TOTAL CONC.($\mu\text{g}/\text{m}^3$) = 41.3		AIR VOLUME (m ³) = 573.2		TOTAL CONC.($\mu\text{g}/\text{m}^3$) = 28.2	
STATION NO.3		200525		STATION NO.4		200526	
STAGE	DIAMETER (μm)	FILTER NO.	DUST WEIGHT (mg)	DUST CONC. ($\mu\text{g}/\text{m}^3$)	ACC.DUST CONC. ($\mu\text{g}/\text{m}^3$)	DUST WEIGHT (mg)	DUST CONC. ($\mu\text{g}/\text{m}^3$)
0	>11	MS3-S1-3	3.17	5.5	50.5	5.69	9.9
1	11-7.0	MS3-S2-3	2.06	3.6	45.0	2.81	4.9
2	7.0-4.7	MS3-S3-3	3.74	6.5	41.4	3.78	5.6
3	4.7-3.3	MS3-S4-3	3.58	6.2	34.9	3.06	5.3
4	3.3-2.1	MS3-S5-3	1.01	1.8	28.8	1.57	2.7
5	2.1-1.1	MS3-S6-3	2.53	4.4	26.9	0.73	1.3
6	1.1-0.65	MS3-S7-3	3.13	5.4	22.5	1.36	2.4
7	0.65-0.43	MS3-S8-3	2.97	5.2	17.0	1.75	3.1
8	<0.43	MS3-BF-3	6.81	11.9	11.9	4.44	7.8
AIR VOLUME (m ³) = 574.5		TOTAL CONC.($\mu\text{g}/\text{m}^3$) = 50.5		AIR VOLUME (m ³) = 573.0		TOTAL CONC.($\mu\text{g}/\text{m}^3$) = 44.0	

Table 5-10 (3) Results of particulate concentration classified by particle size

STATION NO. 1				STATION NO. 4				
ROTOR NO. 200522				ROTOR NO. 200526				
STAGE	DIAMETER (μm)	FILTER NO.	DUST WEIGHT (mg)	DUST CONC. ($\mu\text{g}/\text{m}^3$)	ACC. DUST CONC. ($\mu\text{g}/\text{m}^3$)	DUST WEIGHT (mg)	DUST CONC. ($\mu\text{g}/\text{m}^3$)	ACC. DUST CONC. ($\mu\text{g}/\text{m}^3$)
0	>11	MS1-S1-7	2.88	5.3	54.1	MS4-S1-3	5.32	53.8
1	11-7.0	MS1-S2-7	2.32	4.3	48.8	MS4-S2-3	2.89	44.0
2	7.0-4.7	MS1-S3-7	3.86	7.1	44.6	MS4-S3-3	4.00	39.0
3	4.7-3.3	MS1-S4-7	4.04	7.4	37.5	MS4-S4-3	3.64	31.6
4	3.3-2.1	MS1-S5-7	3.81	7.0	30.0	MS4-S5-3	2.91	24.9
5	2.1-1.1	MS1-S6-7	2.60	4.8	23.0	MS4-S6-3	1.94	19.5
6	1.1-0.65	MS1-S7-7	1.61	3.0	18.2	MS4-S7-3	1.70	15.9
7	0.65-0.43	MS1-S8-7	1.40	2.6	15.3	MS4-S8-3	1.22	12.7
8	<0.43	MS1-BF-7	6.89	12.7	12.7	MS1-BF-3	5.56	10.5
			AIR VOLUME (m ³) = 549.3				AIR VOLUME (m ³) = 540.2	
			TOTAL CONC. ($\mu\text{g}/\text{m}^3$) = 54.1				TOTAL CONC. ($\mu\text{g}/\text{m}^3$) = 53.8	
STATION NO. 2				STATION NO. 5				
ROTOR NO. 200523				ROTOR NO. 200549				
STAGE	DIAMETER (μm)	FILTER NO.	DUST WEIGHT (mg)	DUST CONC. ($\mu\text{g}/\text{m}^3$)	ACC. DUST CONC. ($\mu\text{g}/\text{m}^3$)	DUST WEIGHT (mg)	DUST CONC. ($\mu\text{g}/\text{m}^3$)	ACC. DUST CONC. ($\mu\text{g}/\text{m}^3$)
0	>11	MS2-S1-7	1.62	2.9	32.7	MS5-S1-3	4.07	33.9
1	11-7.0	MS2-S2-7	1.17	2.1	29.7	MS5-S2-3	1.83	26.4
2	7.0-4.7	MS2-S3-7	2.12	3.9	27.8	MS5-S3-3	3.11	23.1
3	4.7-3.3	MS2-S4-7	2.54	4.6	23.6	MS5-S4-3	2.96	17.4
4	3.3-2.1	MS2-S5-7	2.60	4.7	19.1	MS5-S5-3	2.18	11.9
5	2.1-1.1	MS2-S6-7	1.69	3.1	14.4	MS5-S6-3	1.02	7.9
6	1.1-0.65	MS2-S7-7	1.25	2.3	11.3	MS5-S7-3	0.49	5.1
7	0.65-0.43	MS2-S8-7	1.48	2.7	9.1	MS5-S8-3	0.64	5.2
8	<0.43	MS2-BF-7	3.51	6.4	6.4	MS5-BF-3	2.17	4.0
			AIR VOLUME (m ³) = 550.3				AIR VOLUME (m ³) = 544.5	
			TOTAL CONC. ($\mu\text{g}/\text{m}^3$) = 32.7				TOTAL CONC. ($\mu\text{g}/\text{m}^3$) = 33.9	
STATION NO. 3				STATION NO. 6				
ROTOR NO. 200525				ROTOR NO. 200525				
STAGE	DIAMETER (μm)	FILTER NO.	DUST WEIGHT (mg)	DUST CONC. ($\mu\text{g}/\text{m}^3$)	ACC. DUST CONC. ($\mu\text{g}/\text{m}^3$)	DUST WEIGHT (mg)	DUST CONC. ($\mu\text{g}/\text{m}^3$)	ACC. DUST CONC. ($\mu\text{g}/\text{m}^3$)
0	>11	MS3-S1-7	2.10	3.8	47.7	MS3-S1-7	2.10	47.7
1	11-7.0	MS3-S2-7	1.77	3.2	43.9	MS3-S2-7	3.00	40.7
2	7.0-4.7	MS3-S3-7	3.00	5.5	40.7	MS3-S3-7	3.14	35.2
3	4.7-3.3	MS3-S4-7	3.16	5.8	29.5	MS3-S4-7	2.48	23.7
4	3.3-2.1	MS3-S5-7	2.48	4.5	19.2	MS3-S5-7	2.52	14.6
5	2.1-1.1	MS3-S6-7	2.48	4.5	14.6	MS3-S6-7	2.08	10.8
6	1.1-0.65	MS3-S7-7	2.52	4.6	10.8	MS3-S7-7	5.89	10.8
7	0.65-0.43	MS3-S8-7	2.08	3.8	14.6	MS3-S8-7	5.89	10.8
8	<0.43	MS3-BF-7	5.89	10.8	10.8	MS3-BF-7	5.89	10.8
			AIR VOLUME (m ³) = 547.5				AIR VOLUME (m ³) = 547.5	
			TOTAL CONC. ($\mu\text{g}/\text{m}^3$) = 47.7				TOTAL CONC. ($\mu\text{g}/\text{m}^3$) = 47.7	

5.2 Analysis of chemical components contained in particulate matter

In order to analyze chemical components contained in the particulate matter, samples of particulate matter collected on filter papers by low-volume and Andersen samplers during the short term field survey from each station have been brought back to Japan for analysis of elements and anion & cation by instrumental neutron activation analyses (INAA), X-ray fluorescence (XRF), ion chromatography (IC), atomic absorption spectrometry (AAS), flame photometry (FP) and spectrophotometry (SP).

Samples on stage 0-7 and on a back up filter of Andersen sampler were divided into two groups and analyzed. One is coarse particle (over 2.1 μm ; stages 0-4 stages of Andersen sampler) and the other is fine particle (under 2.1 μm ; stages 5-7 and of back up filter of Andersen sampler).

Beside the above stated, additional analysis for the samples collected by Low-volume sampler with a quartz-fiber filter was conducted by pyrolysis of total carbon and non-volatile carbon (inorganic carbon).

Table 5-11 shows the chemical components analyzed in this study.

Table 5-11 Chemical components analyzed in this study

Analyzing method	Analyzed chemical components
INAA	Ag (Silver), Al (Aluminum), As (Arsenic), Ba (Barium), Br (Bromine), Ca (Calcium), Ce (Cerium), Cl (Chlorine), Co (Cobalt), Cr (Chromium), Cs (Cesium), Cu (Copper), Fe (Iron), Hf (Hafnium), K (Potassium), Mg (Magnesium), La (Lanthanum), Lu (Lutetium), Mn (Manganese), Na (Sodium), Ni (Nickel), Sb (Antimony), Sc (Scandium), Se (Selenium), Sm (Samarium), Th (Thorium), Ti (Titanium), V (Vanadium), W (Tungsten), Zn (Zinc)
XRF	Cd (Cadmium), Pb (Lead), S (Sulfur), Si (Silicon)
IC	Cl^- (Chloride), NO_3^- (Nitrate), SO_4^{2-} (Sulfate)
AAS	Mg^{2+} (Magnesium ion), Ca^{2+} (Calcium ion)
FP	Na^+ (Sodium ion), K^+ (Potassium ion)
SP	NH_4^+ (Ammonium ion)
Pyrolysis	Total carbon, Non-volatile carbon

5.2.1 Analysis of Elements by Instrumental Neutron Activation Analysis

(1) Principle of analysis

When the sample is placed in the reactor, the thermal neutron generated by fission of ^{235}U collides with atomic nucleus in the sample materials and causes neutron fission. As the result, the product nuclei is produced which is different from the original one. The product nuclei is radioactive and emits Beta ray and Gamma ray, and changes into daughter nuclide after a certain period. The energy of Gamma ray is particular to the type of atomic nucleus. Thus measurement of γ -ray energy enables us to identify elements contained in the original sample. Also the number of Gamma ray is proportional to the number of elements, and thus determination of amount of elements become possible.

In actual neutron activation analysis, various types of elements coexist in the sample and their half lives vary in the range of from second to day order or even to more than one month. So by selecting cooling period properly, nuclides with various half lives can be measured.

As described above, neutron activation method does not require a complex chemical pretreatment and makes it possible to analyze many types of elements simultaneously in non-destructive way even though the sample contains a very small amount of elements. For these reasons and others, this method is highlighted recently as one of the most advanced and sensitive analyses.

(2) Analyzing method

The samples are placed in the TRIGA II type reactor of Atomic Energy Research Laboratory, Musashi Institute of Technology, and are irradiated by thermal neutron beam. Then the various radioactive isotopes generated are measured by a semiconductor detector and multichannel analyzer coupled with a mini-computer. The irradiation of thermal neutron on the sample is conducted in two ways; for a short-term and for a long-term.

The irradiated sample for a short-term is measured in term of Gamma ray using a semiconductor detector. The irradiated sample for a long-term is cooled for varying time of several days to several weeks in the laboratory, and then Gamma ray is measured. Fig. 5-8 shows atomic furnace and its sectional view.

Thermal neutron flux is keep at $1.5 \times 10^{12} \text{ cm}^{-2} \cdot \text{s}^{-1}$.

The semiconductor detector is 8,100 type of Canberra Industries Inc. and has the capacity of detector efficiency, 10% and detector resolution, 2.0 KeV at 1333 KeV.

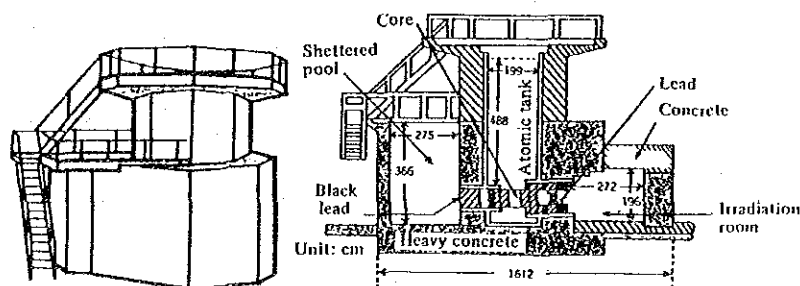


Fig. 5-8 External view and section of TRIGA II type reactor

① Analyzing conditions

- (i) Short lived nuclides—At thermal neutron flux of $(1.5 \times 10^{12} \text{ cm}^{-2} \cdot \text{s}^{-1})$, irradiation for 1 minute, and after cooling for about 3–4 minutes, measurement or detection for 300 seconds.
- (ii) Long lived nuclides (a)—At thermal neutron flux of $(1.5 \times 10^{12} \text{ cm}^{-2} \cdot \text{s}^{-1})$, irradiation for 5 hours, and after cooling for several days, measurement or detection for 1,000 seconds.
- (iii) Long lived nuclides (b)—After cooling long lived nuclides (a) for several weeks, measurement or detection for 3,000 seconds.

Table 5-12 shows analysis conditions of elements by nuclides.

Table 5-12 Elements by nuclides and analyzing conditions

Classification	Element	Target nuclear species	Isotope ratio (%)	Nuclides generated	Half life period	Gamma ray energy (KeV)	Analyzing conditions		
							Irradiation time	Cooling time	Measurement time
Short lived nuclides	Al	²⁷ Al	100	²⁸ Al	2.31 minutes	1778.9	1 minute	3-4 minutes	300 seconds
	Br	⁷⁹ Br	50.5	⁸⁰ Br	17.6 minutes	617.0	1 minute	3-4 minutes	300 seconds
	Ca	⁴⁸ Ca	0.185	⁴⁹ Ca	8.8 minutes	3083	1 minute	3-4 minutes	300 seconds
	Cl	³⁷ Cl	24.5	³⁸ Cl	37.3 minutes	1642.0	1 minute	3-4 minutes	300 seconds
	Cu	⁶⁵ Cu	30.9	⁶⁶ Cu	5.1 minutes	1039.0	1 minute	3-4 minutes	300 seconds
	Hn	⁵⁵ Hn	100	⁵⁶ Hn	2.58 hours	846.9, 1810	1 minute	3-4 minutes	300 seconds
	Ti	⁵⁰ Ti	5.34	⁵¹ Ti	5.79 minutes	320.0	1 minute	3-4 minutes	300 seconds
	V	⁵¹ V	99.8	⁵² V	3.76 minutes	1434.4	1 minute	3-4 minutes	300 seconds
Long lived nuclides (a)	As	⁷⁵ As	100	⁷⁶ As	26.3 hours	559.2	5 hours	Several days	1000 seconds
	K	⁴¹ K	6.88	⁴² K	12.5 hours	1524.7	5 hours	Several days	1000 seconds
	La	¹³⁹ La	99.9	¹⁴⁰ La	1.68 days	1595.4	5 hours	Several days	1000 seconds
	Na	²³ Na	100	²⁴ Na	15 hours	1368.4	5 hours	Several days	1000 seconds
	Sb	¹²¹ Sb	57.3	¹²² Sb	2.75 days	566.0	5 hours	Several days	1000 seconds
	Sm	¹⁵³ Sm	26.7	¹⁵³ Sm	1.96 days	103.2	5 hours	Several days	1000 seconds
	W	¹⁸⁶ W	28.4	¹⁸⁷ W	24.0 hours	685.7	5 hours	Several days	1000 seconds
Long lived nuclides (b)	Ag	¹⁰⁹ Ag	48.7	^{110m} Ag	253 days	657.8	5 hours	Several weeks	3000 seconds
	Ba	¹³⁰ Ba	0.101	¹³¹ Ba	11.5 days	496	5 hours	Several weeks	3000 seconds
	Ce	¹⁴⁰ Ce	88.5	¹⁴¹ Ce	32.5 days	165.4	5 hours	Several weeks	3000 seconds
	Co	⁵⁹ Co	100	⁶⁰ Co	5.26 years	1332.4	5 hours	Several weeks	3000 seconds
	Cr	⁵⁰ Cr	100	⁵¹ Cr	27.8 days	320.0	5 hours	Several weeks	3000 seconds
	Cs	¹³³ Cs	100	¹³⁴ Cs	2.07 years	795.8	5 hours	Several weeks	3000 seconds
	Fe	⁵⁸ Fe	0.33	⁵⁹ Fe	45.1 days	1098.6	5 hours	Several weeks	3000 seconds
	Hf	¹⁸⁰ Hf	35.2	¹⁸¹ Hf	64.6 days	482.2	5 hours	Several weeks	3000 seconds
	Lu	¹⁷⁶ Lu	2.59	¹⁷⁷ Lu	6.7 days	708.4	5 hours	Several weeks	3000 seconds
	Ni	⁵⁸ Ni	67.9	⁵⁸ Co	71.3 days	810.3	5 hours	Several weeks	3000 seconds
	Sc	⁴⁵ Sc	100	⁴⁶ Sc	83.9 days	889.4	5 hours	Several weeks	3000 seconds
	Se	⁷⁶ Se	0.87	⁷⁵ Se	121 days	264.6	5 hours	Several weeks	3000 seconds
	Th	²³² Th	100	²³³ Pa	27.0 days	311.8	5 hours	Several weeks	3000 seconds
	Zn	⁶⁴ Zn	48.9	⁶⁵ Zn	245 days	1115.4	5 hours	Several weeks	3000 seconds

② Preparation of sample and production of standard sample

As shown in Fig. 5-9, the filter from low-volume and Andersen sampler were cut in two parts, and 1/2 of the each filter were again cut into two parts and contained in the polyethylene bag of double layers which are then subject to short and long term irradiation. To prepare standard samples, the solution with appropriate reagent dissolved for each element is produced, and these standard solution is dropped on the filter, TOYO-ROSHI PF040, in constant quantity which is used in analysis as multi-element-standard.

Table 5-13 shows the reagent used for production of the standard sample for elements contained. In the table, Gamma ray counting rate of the standard samples is shown in terms of CPS (counts per sec.)/ μg . The standard samples have been used repeatedly and an example is shown in the table.

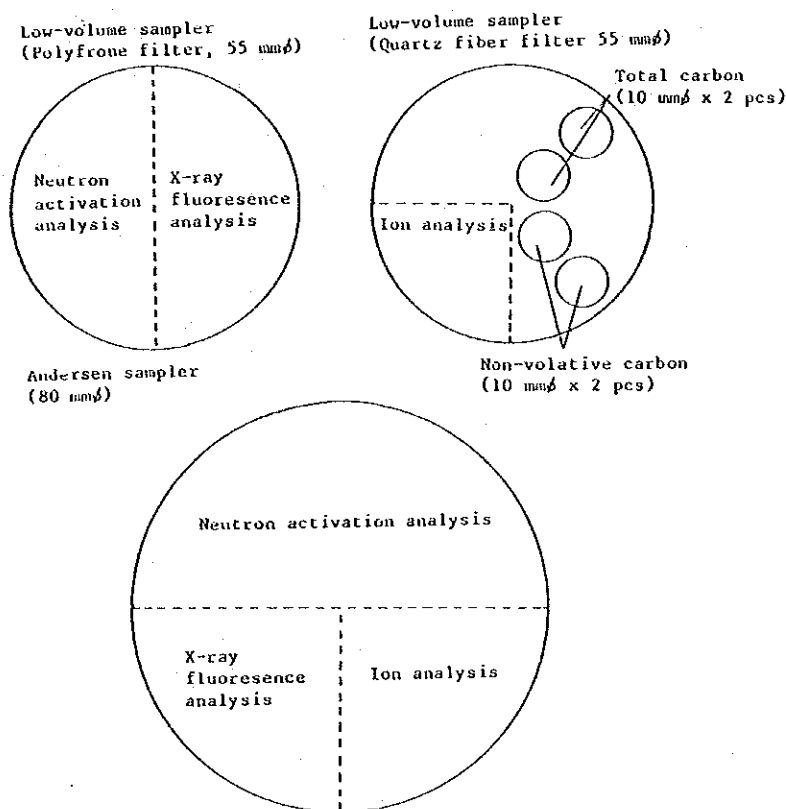


Fig. 5-9 Cutting of sampled filters for analysis

Table 5-13 An example of standard sample and Gamma ray counting rate

Classification	Element	Standard		Gamma ray counting rate (CPS/ μ g)	
		Reagent	Load of element (μ g)		
Short lived nuclides	Al	Al	199	6.80	
	Br	KBr	7.69	1.97	
	Ca	CaCO ₃	212	0.00609	
	Cl	KCl	179	0.0385	
	Cu	Cu	100	0.564	
	Mn	Mn	14.4	6.31	
	Ti	Ti	48.9	0.289	
	V	V	6.21	58.7	
	Long lived nuclides (a)	As	As ₂ O ₃	2.78	43.7
K		KCl	197	0.271	
La		La ₂ O ₃	0.734	11.2	
Na		Na ₂ CO ₃	201	11.6	
Sb		Sb	0.134	21.0	
Sm		Sm ₂ O ₃	0.0404	576	
W		W	0.704	30.7	
Long lived nuclides (b)	Ag	Ag ₂ SO ₄	0.695	0.307	
	Ba	BaCl ₂ ·2H ₂ O	37.7	0.0231	
	Ce	Ce(SO ₄) ₂ ·2(NH ₄) ₂ SO ₄ ·2H ₂ O	0.724	0.784	
		Co	CoCl ₂ ·6H ₂ O	1.01	0.356
		Cr	Cr	2.02	0.358
	Cs	Cs	0.394	1.34	
	Fe	Fe	301	0.00141	
	Hf	Hf	0.115	2.40	
	Lu	LuCl ₃ ·6H ₂ O	0.0241	103	
	Ni	Ni	100	0.0178	
	Sc	Sc ₂ O ₃	0.158	13.6	
	Se	H ₂ SeO ₃	1.39	0.353	
	Th	Th(NO ₃) ₄ ·4H ₂ O	0.0544	6.93	
	Zn	Zn	100	0.0185	

③ Sequence order of analysis

Pretreated sample and standard sample are placed in the irradiation capsule, and under the analyzing conditions shown in Table 5-12, irradiation of thermal neutron, cooling, and measurement of Gamma ray are conducted. The area of Gamma ray peak of each element is calculated and compared with the area of standard sample from which the amount of element contained in the samples is evaluated.

Following the above, and after subtracting blank value of the filter previously measured, the ambient element concentration is obtained, by dividing with air sucking flow rate. Analyzing sequence of neutron activation analyses are shown in Fig. 5-10.

(3) Analysis of ambient air standard sample

In order to evaluate the analyzing methods, standard sample AS-1 of known concentration of particulate matter was analyzed. The results of such analysis are shown in Table 5-14. The elements which showed a good agreement with analyzed values were Al, Ca, Cu, Mn, Ti, V, As, K, La, Na, Sm, Co, Fe, Ni, Sc, Se and Zn.

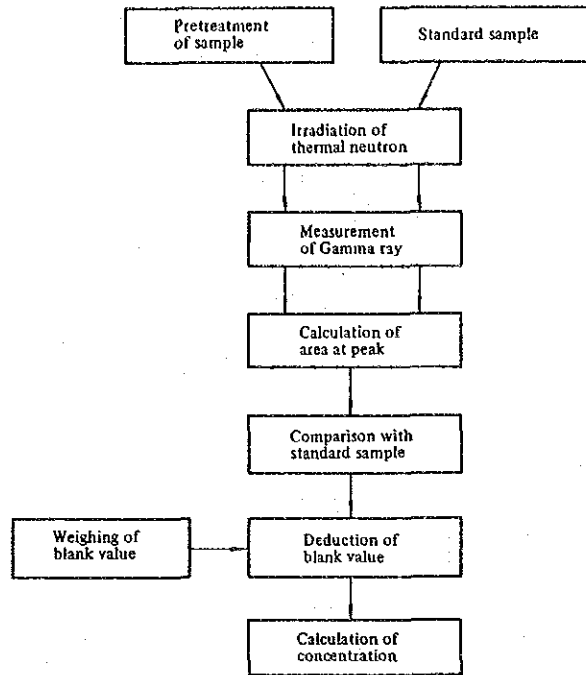


Fig. 5-10 Procedures of neutron activation analysis

Table 5-14 Analysis data of ambient air standard sample (AS-1)

Classification	Element	Standard sample (AS-1) of particulate matter	
		Analyzed value (ppm)	Literature value (ppm)*
Short lived nuclides	Al	48000 (2)	50000+7000
	Br	250 (5)	340+9
	Ca	53000 (2)	56000+5000
	Cl	37000 (1)	31000+4000
	Cu	430 (18)	400+140
	Mn	1200 (7)	1200+100
	Ti	4500 (5)	4200+1100
	V	240 (2)	230+70
Long lived nuclides (a)	As	40 (6)	43+13
	K	10000 (25)	9700**
	La	17 (13)	18+2
	Na	14000 (2)	14000+1000
	Sb	62 (2)	39+6
	Sm	3.5 (3)	3.4**
	W	30 (11)	21+13
Long lived nuclides (b)	Ag	9 (37)	3**
	Ba	970 (17)	410**
	Ce	40 (8)	30**
	Co	29 (7)	26+4
	Cr	350 (2)	240+30
	Cs	3.5 (20)	4.0+**
	Fe	48000 (3)	45000+3000
	Hf	3.9 (14)	3.4**
	Lu	0.06 (25)	0.3**
	Ni	200 (31)	200+30
	Sc	12 (2)	11+1
	Se	9 (44)	9+6
	Th	3.7 (9)	5.1**
	Zn	3200 (3)	3400+500

Table in bracket are counting error.

* T. Otoshi and J. Omi, Bulletin of JESC, No.3, 58 (1976).

** Noncertified values

(4) Limit of measurement and filter blank

Average limit of determination at analysis of particulate matter in the ambient and filter blank values are shown in Table 5-15.

Table 5-15 Average limit of measurement and filter blank value

Classification	Element	Limit of determination (µg)	Filter blank (ng/cm ²)		
			Poly-ethylene sheet	Poly-ethylene sheet + Back-up filter	Poly-frone filter
Short lived nuclides	Al	1	200	200	400
	Br	0.2	0	0	0
	Ca	20	0	0	0
	Cl	3	0	0	1000
	Cu	1	0	0	0
	Mn	0.02	0.4	0	4
	Ti	2	0	0	0
	V	0.02	1	0.3	3
	Long lived nuclides (a)	As	0.03	0	0
K		20	0	0	0
La		0.02	0	0	0
Na		0.1	100	100	800
Sb		0.005	0	0	0
Sm		0.002	0	0	0
W		0.05	0	0	0
Long lived nuclides (b)	Ag	0.04	0	0	0
	Ba	2	0	0	0
	Ce	0.02	0	0	0
	Co	0.005	0	0	0
	Cr	0.05	0	0.4	1
	Cs	0.005	0	0	0
	Fe	20	0	0	0
	HF	0.02	0	0	0
	Lu	0.005	0	0	0
	Ni	1	0	0	0
	Sc	0.002	0	0	0
	Se	0.05	0	0	0
	Th	0.01	0	0	0
	Zn	0.3	0	2	0

(5) Calculation method of elements and others

The weight of metal elements on the filter is calculated from the peak area of Gamma ray by the following Equation (5-14).

$$E_w = \left(\frac{St_w}{St_{ya}} \cdot S_{ya} \right) - F_{bw} \quad \text{Equation (5-14)}$$

where;

- E_w: Weight of element in analyzed sample (µg)
- St_w: Weight of element in standard sample (µg)
- St_{ya}: Peak area of Gamma ray in standard sample
- S_{ya}: Peak area of Gamma ray in analyzed sample
- F_{bw}: Filter blank value (µg)

The metal element concentration in the ambient air is obtained from the following Equation (5-15).

$$C_e = \frac{E_w}{V} \cdot \frac{F_a}{S_a} \times 1,000 \quad \text{Equation (5-15)}$$

where;

- Ce: Element concentration in the ambient (ng/m^3)
- Ew: Element weight in analyzed sample (μg)
- V: Air sucking flow rate (m^3)
- Fa: Total area of filter (cm^2)
- Sa: Filter area of analyzed sample (cm^2)

Peak area of Gamma ray is calculated as follows; the Gamma ray peak specific to the element is analyzed by multichannel analyser which has detector resolution of around 1 KeV and spectrum data shown as Fig. 5-11 are indicated by channel number of multichannel analyser and count number of Gamma ray corresponding to each channel is indicated. The spectrum data are the results of measuring number of dispersed Gamma ray in the channel box corresponding to energy.

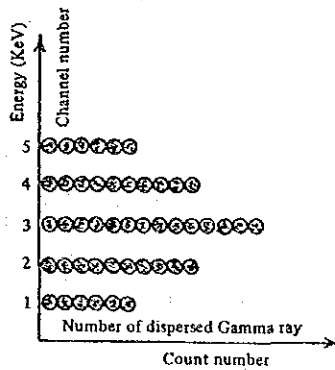


Fig. 5-11 Spectrum data (dispersion of Gamma particle)

The spectrum data indicate the dispersion curve as shown in Fig. 5-12, in which the noise portion so-called background portion and peak area of spectrum data are overlapped. When total count number around peak is T, background is B and net peak area is N, net peak area is obtained by the following Equation (5-16).

$$N = T - B \dots\dots\dots \text{Equation (5-16)}$$

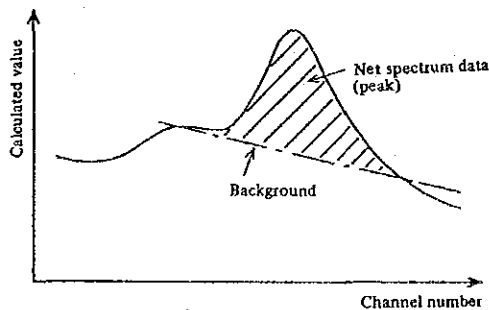


Fig. 5-12 Spectrum data and background

Furthermore, the measured value by detectors in certain time period has a statistical dispersion, and its dispersion behaviour conforms to poisson distribution. Calculated value C is significant value in the range of calculation error $\pm\sqrt{C}$. Net peak area N calculated by Equation III-5-3 has calculation error $\sigma_N(\%)$. σ_N is obtained by following equation.

$$\sigma_N = \frac{\sqrt{N + (n - \frac{1}{2}) \cdot B}}{N} \cdot B \times 100 \dots\dots\dots \text{Equation (5-17)}$$

where; n: number of channel

(in this study, of the neighboring makes 7 channels in total were used. So n = 3)

(6) Gamma ray Spectrum

Fig. 5-13 through 5-15 show some examples (3rd field survey at MS1 on coarse particle) of Gamma ray spectrum.

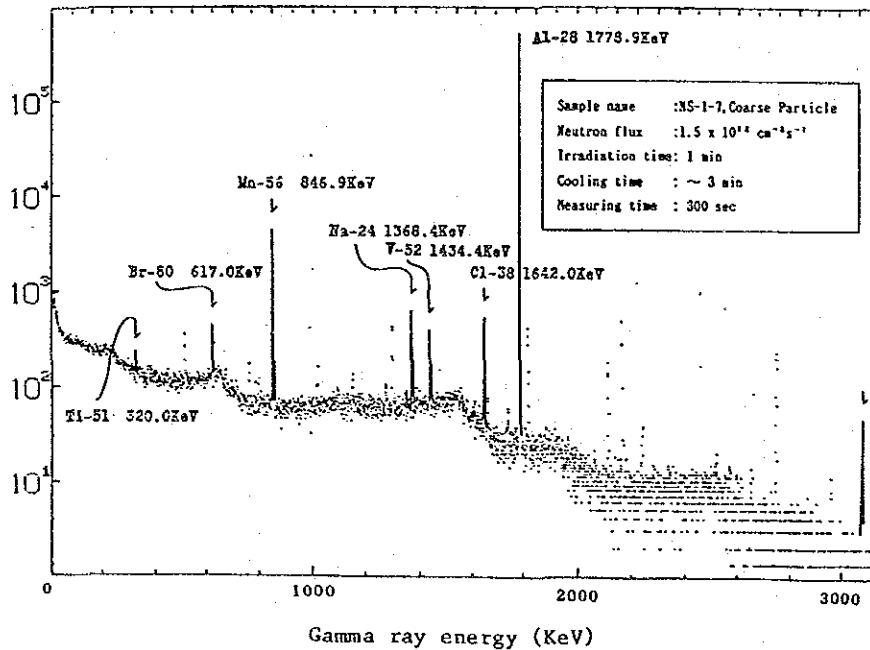


Fig. 5-13 An example of Gamma ray spectrum (short lived nuclides)

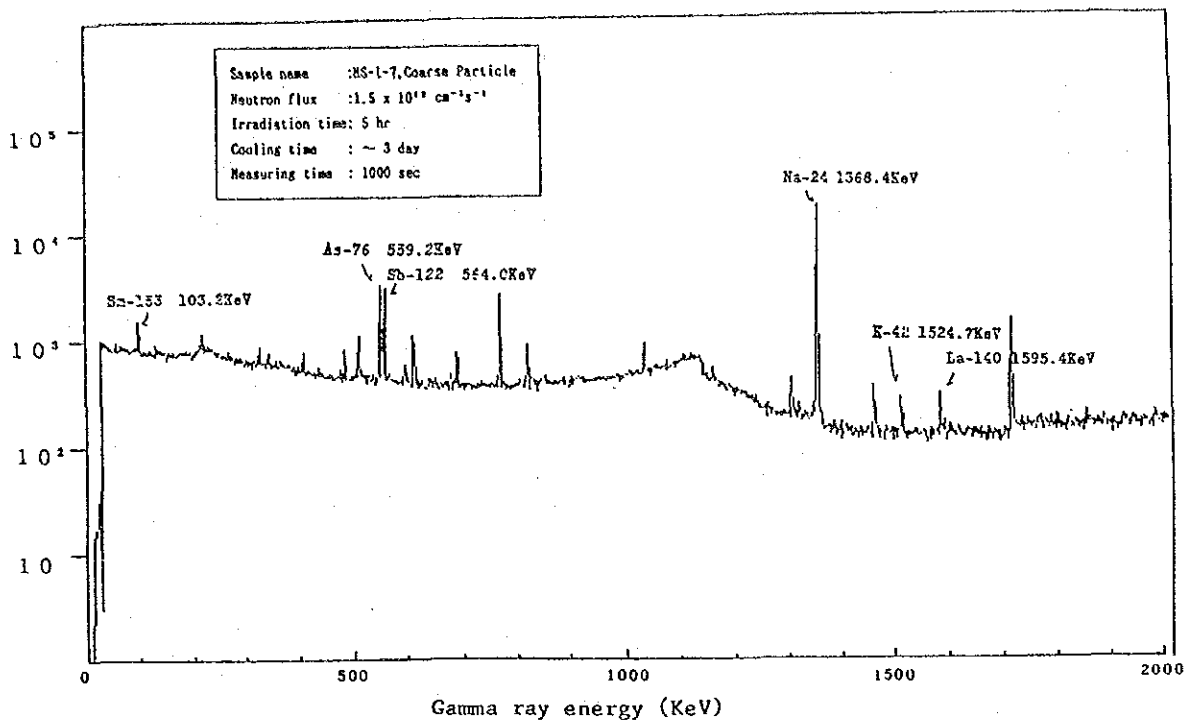


Fig. 5-14 An example of Gamma ray spectrum (long lived nuclides (a))

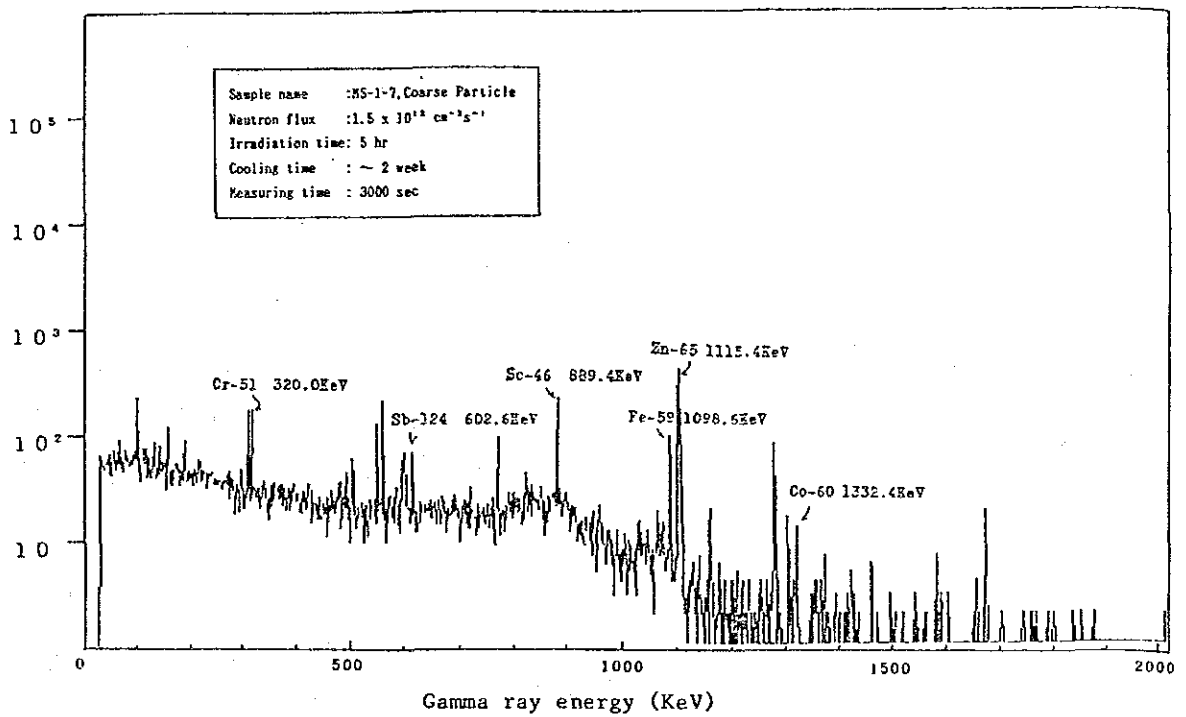


Fig. 5-15 An example of Gamma ray spectrum (long lived nuclides (b))

(7) Results of measurement

The results of analysis of elements by Instrumental Neutron Activation Analysis are shown in Table 5-16. In this table also shown are the results of measurement of Cd, Pb, S, and Si by X-ray fluorescence analysis, results of anion & cation by Ion chromatography, atomic absorption spectrometry, flame photometry and spectrophotometry, and results of total and non-volatile carbon by pyrolysis.

Table 5-16 (3) Results of element concentration contained in particulate matter by instrumental neutron activation analysis (Andersen sampler, coarse particle)

SURVEY	AG	AL	AS	SA	BR	CA	CE	CL	CO	CR	C2	CU	FE	MF	K	Zn
SURVEY1	M1	0.40	1.00	1.50	2.00	3.00	4.00	5.00	6.00	7.00	8.00	9.00	10.00	11.00	12.00	13.00
	M2	0.40	1.00	1.50	2.00	3.00	4.00	5.00	6.00	7.00	8.00	9.00	10.00	11.00	12.00	13.00
	M3	0.40	1.00	1.50	2.00	3.00	4.00	5.00	6.00	7.00	8.00	9.00	10.00	11.00	12.00	13.00
	M4	0.40	1.00	1.50	2.00	3.00	4.00	5.00	6.00	7.00	8.00	9.00	10.00	11.00	12.00	13.00
	M5	0.40	1.00	1.50	2.00	3.00	4.00	5.00	6.00	7.00	8.00	9.00	10.00	11.00	12.00	13.00
SURVEY2	M1	0.40	1.00	1.50	2.00	3.00	4.00	5.00	6.00	7.00	8.00	9.00	10.00	11.00	12.00	13.00
	M2	0.40	1.00	1.50	2.00	3.00	4.00	5.00	6.00	7.00	8.00	9.00	10.00	11.00	12.00	13.00
	M3	0.40	1.00	1.50	2.00	3.00	4.00	5.00	6.00	7.00	8.00	9.00	10.00	11.00	12.00	13.00
	M4	0.40	1.00	1.50	2.00	3.00	4.00	5.00	6.00	7.00	8.00	9.00	10.00	11.00	12.00	13.00
	M5	0.40	1.00	1.50	2.00	3.00	4.00	5.00	6.00	7.00	8.00	9.00	10.00	11.00	12.00	13.00

unit; ng/m³

Table 5-16 (4) Results of element concentration contained in particulate matter by instrumental neutron activation analysis (Andersen sampler, fine + coarse)

SURVEY	AG	AL	AS	SA	BR	CA	CE	CL	CO	CR	C2	CU	FE	MF	K	Zn
SURVEY1	M1	0.35	1.67	7.10	33	28.0	21.5	2.54	1420	7.08	0.230	24	1310	0.075	1200	
	M2	0.40	1.00	1.50	2.00	3.00	4.00	5.00	6.00	7.00	8.00	9.00	10.00	11.00	12.00	
	M3	0.40	1.00	1.50	2.00	3.00	4.00	5.00	6.00	7.00	8.00	9.00	10.00	11.00	12.00	
	M4	0.40	1.00	1.50	2.00	3.00	4.00	5.00	6.00	7.00	8.00	9.00	10.00	11.00	12.00	
	M5	0.40	1.00	1.50	2.00	3.00	4.00	5.00	6.00	7.00	8.00	9.00	10.00	11.00	12.00	
SURVEY2	M1	0.35	1.67	7.10	33	28.0	21.5	2.54	1420	7.08	0.230	24	1310	0.075	1200	
	M2	0.40	1.00	1.50	2.00	3.00	4.00	5.00	6.00	7.00	8.00	9.00	10.00	11.00	12.00	
	M3	0.40	1.00	1.50	2.00	3.00	4.00	5.00	6.00	7.00	8.00	9.00	10.00	11.00	12.00	
	M4	0.40	1.00	1.50	2.00	3.00	4.00	5.00	6.00	7.00	8.00	9.00	10.00	11.00	12.00	
	M5	0.40	1.00	1.50	2.00	3.00	4.00	5.00	6.00	7.00	8.00	9.00	10.00	11.00	12.00	

unit; ng/m³

Note: When concentration of elements are under the confidence, 1/2 of such the values are counted into calculation.

5.2.2 Analysis of Elements by X-ray Fluorescence

Elements (Pb, Si) which cannot be analyzed by neutron activation method and elements (Cd, S) in low sensitivity, were been analyzed by X-ray fluorescence method.

(1) Principle of measurement

When the sample is irradiated by primary X-ray produced from X-ray generator, secondary X-ray characteristic of elements in such sample generates from the sample. The fluorescence of X-ray has an intensity distribution corresponding to the element components, and so X-ray intensity corresponding to the elements is measured by spectro analysis of X-ray. The X-ray intensity corresponding to the standard sample was first measured and then it was compared with that of sample to be measured. Thus the amount of target element become known. Fig. 5-16 shows principle of X-ray fluorescence analyzing instrument.

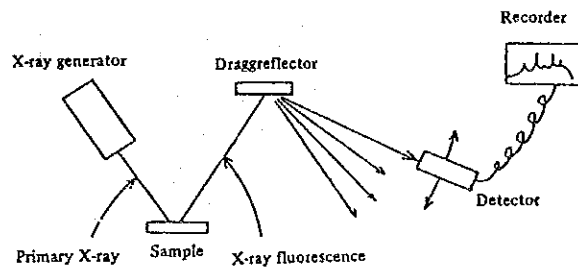


Fig. 5-16 Principle of X-ray fluorescence analyzing instrument

(2) Analyzing methods

As shown in Fig. 5-9, sampled filters for analysis are cut into a round shape of 47 mm ϕ , which is then placed on the X-ray fluorescence analyzing instrument, Gigerflex of RIGAKU DENKI KK. The instrument is set on sample stand as shown in Fig. 5-17.

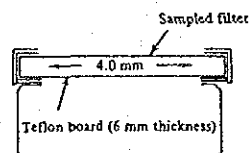


Fig. 5-17 Sample stand

① Analyzing conditions

Table 5-17 shows the type of X-ray tube, Bragy reflector, detector, analyzing line, measuring time applied to this study.

Table 5-17 Analyzing conditions of X-ray fluorescence analysis

Element	X-ray tube	Bragy reflector	Detector	Analytical line	Measuring time
Si	Chromium tube	EDDT*	Flow proportional counter	K α line (7.126 Å)	40 sec
S	Chromium tube	Ge	Flow proportional counter	K α line (5.373 Å)	40 sec
Cd	Chromium tube	Ge	Flow proportional counter	L α line (3.960 Å)	80 sec
Pb	Tungsten tube	LiF	Scintillation counter	L β line (0.982 Å)	40 sec

Notes: * EDDT: Ethylenediamine ditartrate
 ** Chromium tube: 40 KV - 35 mA
 Tungsten tube: 50 KV - 40 mA

Among X-ray tubes, Chromium tube was used for analysis of Si, S and Cd, while Tungsten tube was used for Pb. This is due to the fact that the relative intensity of Chromium tube at over 2.5 Å is superior and below 2.5 Å, it is the other way around as shown in Fig. 5-18.

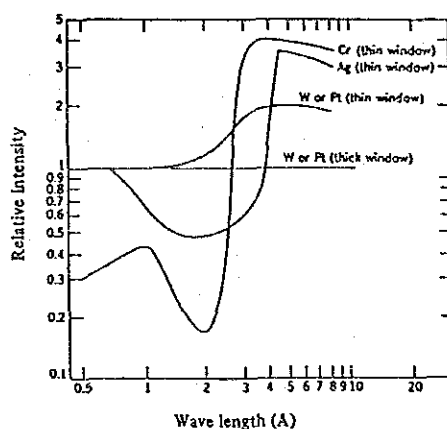


Fig. 5-18 Character of X-ray tubes

For Bragy reflector used for X-ray reflection, EDDT for Si and Cd, Ge for S, and LiF for Pb were employed. This is due to that applicable range of Bragy reflector corresponding to the analytical line of each element being limited as shown in Fig. 5-19. (Shaded line)

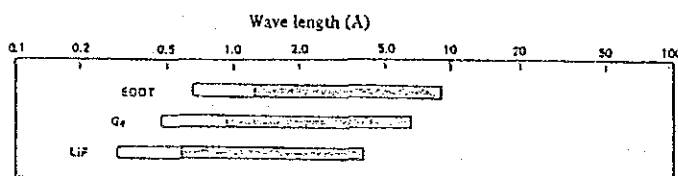


Fig. 5-19 Applicable range of Bragy reflectors

Furthermore Fig. 5-20 shows the relative intensity of flow proportional counter employed.

In this study, Argon has been employed.

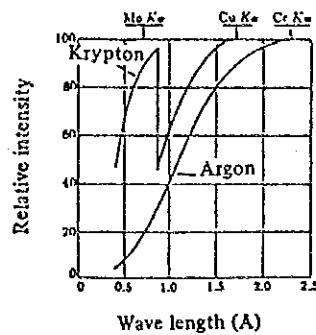


Fig. 5-20 Relative intensity of flow proportional counter

② Preparation of analytical line

(i) Pb, Cd (Filtration method of precipitate coprecipitated with iron)

A predetermined quantity of lead (Pb^{2+}) and cadmium (Cd^{2+}) are added into the solution containing 300 μg of iron (Fe^{3+}). Adjusting pH at 9.3 by sodium borate solution and 0.1N hydrogen chloride, precipitate is coagulated while heating, and was collected on a filter. The above procedures are repeated by changing quantity of lead and cadmium at each stage for production of standard samples to be used for developing the analytical line. Fig. 5-21 shows the analytical line.

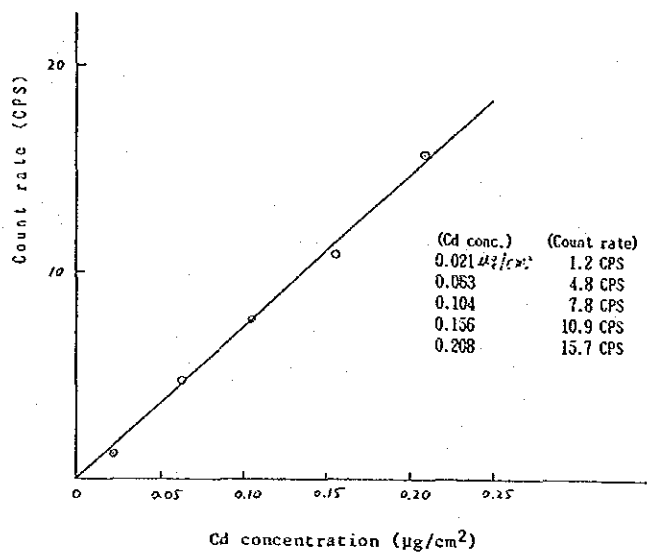
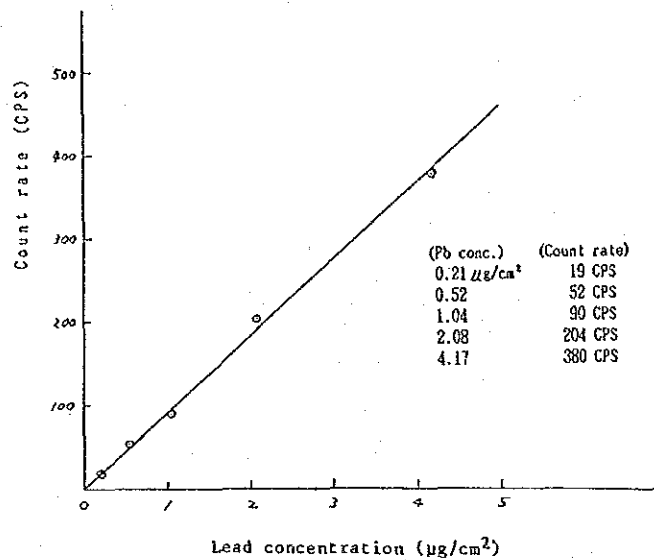


Fig. 5-21 Analytical line of lead and cadmium

(ii) Si, S (filtration method of powder)

Fly ash samples of known content of Si and S are fully ground in an agate mortar, and the powder is dispersed by air. The dispersed powder is collected on the filter after filtration under reduced pressure. From the weight of filter weighed before and after sampling, and concentration of silicon and sulphur, the contents of 2 elements are obtained. The filters having varying amounts of powder are produced as the standard samples for developing the analytical lines. Fig. 5-22 shows the analytical line.

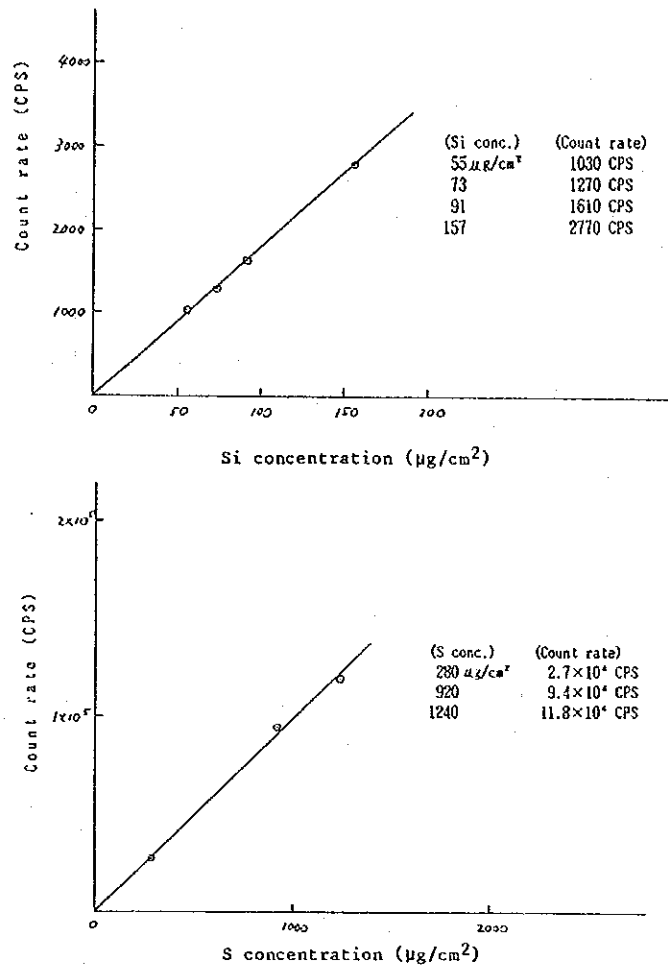


Fig. 5-22 Analytical line of silicon and sulphur

(3) Determination limit

The average detection limits of the elements in ambient particulate matter by X-ray fluorescence analysis are as follows. The blank values of filters are not usually obtainable.

Cd: $0.01 \mu\text{g}/\text{cm}^2$

Pb: $0.1 \mu\text{g}/\text{cm}^2$

Si: $1 \mu\text{g}/\text{cm}^2$

S: $1 \mu\text{g}/\text{cm}^2$

(4) Calculation method of elements concentration

The weight of elements on the filter were calculated from X-ray's peak (CPS) by the following equation.

$$E_w = \frac{St_w}{St_{CPS}} \cdot S_{CPS} \dots\dots\dots \text{Equation (5-18)}$$

where;

- E_w : Element weight contained in sample on unit area ($\mu\text{g}/\text{cm}^2$)
- St_w : Element concentration in standard sample ($\mu\text{g}/\text{cm}^2$)
- St_{CPS} : Count rate in standard sample (CPS)
- S_{CPS} : Count rate of analyzed sample (CPS)

Elements concentration in the ambient air are calculated by the following Equation (5-19).

$$C_c = \frac{E_w \cdot Fa}{V} \times 1,000 \dots\dots\dots \text{Equation (5-19)}$$

where;

- C_c : Element concentration in the ambient air (ng/m^3)
- E_w : Element weight in analyzed sample on unit area ($\mu\text{g}/\text{cm}^2$)
- Fa : Total area of filter (cm^2)
- V : Air flow rate (m^3)

(5) Spectrum of X-ray fluorescence

Fig. 5-23 shows an example spectrum of X-ray fluorescence about Road dust.

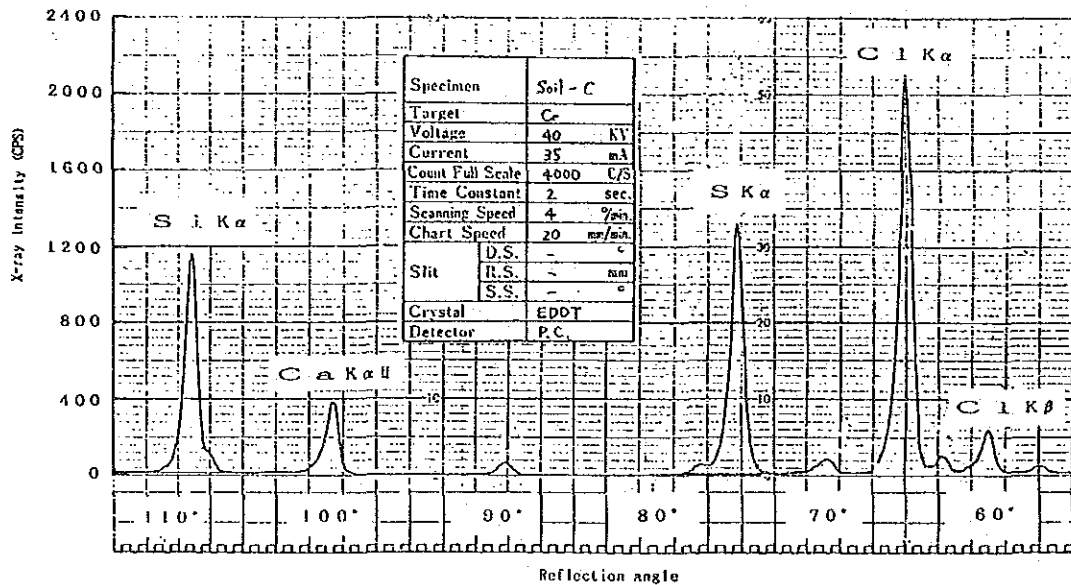


Fig. 5-23 An example of spectrum of X-ray fluorescence

(6) Results of measurement

Table 5-16 shows the results of element analysis done on particulate matter by X-ray fluorescence.

5.2.3 Analysis of Anion by Ion Chromatography

(1) Principle of analysis

Ion chromatography is a kind of column chromatography that uses an ion exchange resin as trapping phase.

A sample solution containing ions is introduced into a separation column together with an eluent, and ions are collected by ion exchange resin in the column. Due to eluent effect, each ion is separated selectively depending on its separation constant between ion and resin. Then they are led to a micro membrane suppressor where the eluent from separation column is removed or is neutralized. The target ions flows into an electric conductivity cell from the separation column one after another.

The instrument of ion chromatography consists of such components as eluent tank, solution transfer pump, sample injection valve, separation column, micro membrane suppressor and electric conductivity detector. Fig. 5-24 shows the outline of analysis by ion chromatography.

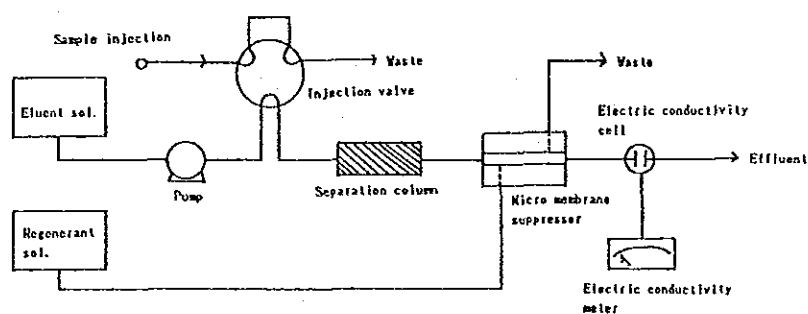


Fig. 5-24 Outline of ion chromatography

(2) Analyzing method

The filter was cut into 1/4 as shown in Fig. 5-9. A piece of the cut filter was dropped into the beaker containing 50 ml of deionized water and the solution was shaken about 90 minutes for extraction. The analysis was conducted by using Chromatography Model 10 of Dionex Co., Ltd.

① Analyzing conditions

The analysis has been carried out under the following conditions.

Separation column:	4 mm×50 mm + 4 mm×250 mm
Suppressor column:	Micro membrane suppressor
Sample volume:	100 μ l
Eluent:	0.0025M Na_2CO_3 /0.0022M NaHCO_3
Eluent flow rate:	138 ml/hr

② Development of analytical line

Standard stock solutions containing 1000 mg/l each of chloride ion, nitrate ion and sulfate ion were prepared. This standard stock solution was adequately diluted prior to application for the preparation of analytical line. These solutions were flown into the separation column under the same conditions as applied to the sample solution, and analytical line was developed. Fig. 5-25 shows analytical line of Cl^- , NO_3^- and SO_4^{2-} .

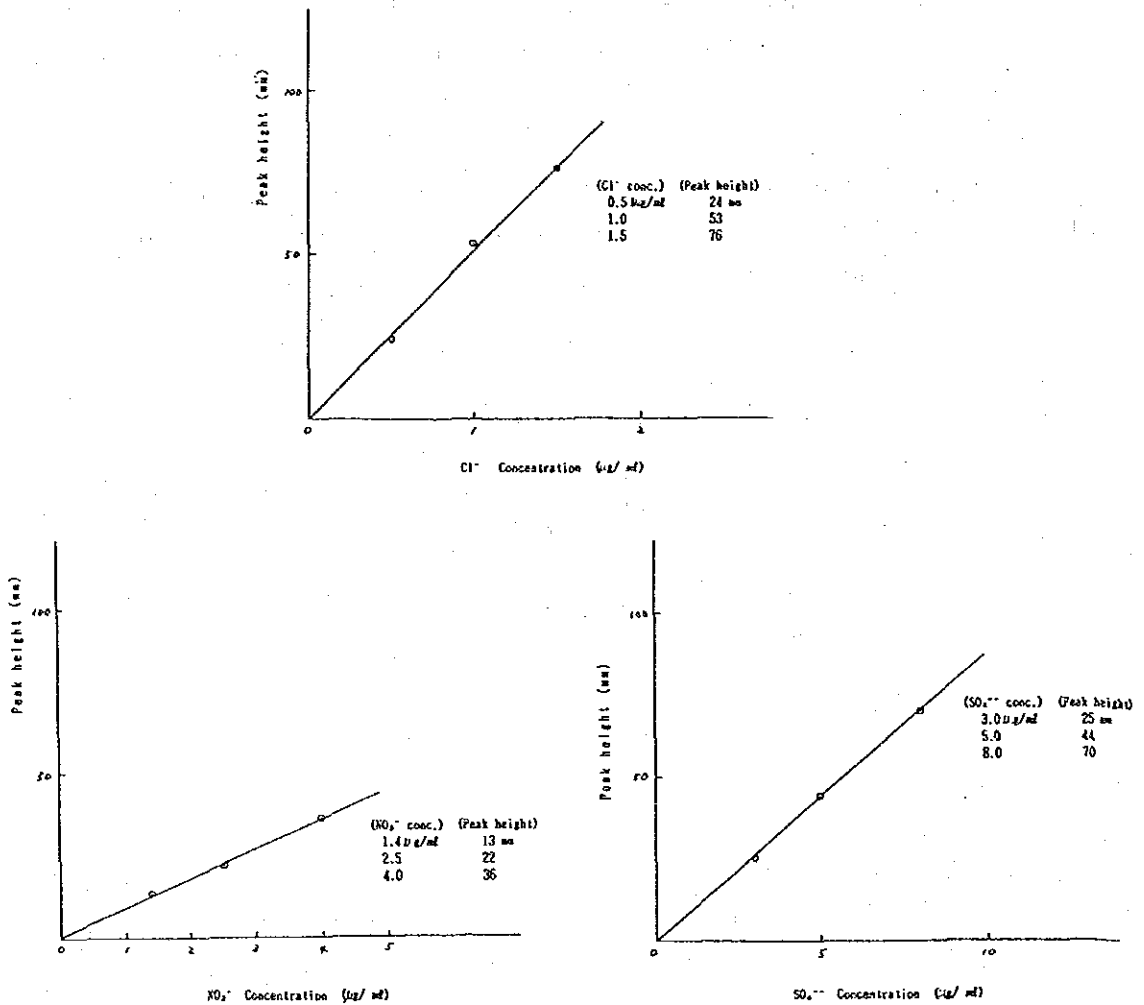


Fig. 5-25 Analytical lines of Cl^- , NO_3^- and SO_4^{2-}

(3) Determination limit and blank value of filter

The full scale of electric conductivity in this analysis is 30 $\mu\text{S}/\text{cm}$. The limits of determination and tare value of the filters are shown in Table 5-18.

Table 5-18 Determination limit and blank value of filter

Analyzed item	Determination limit ($\mu\text{g}/\text{m}^3$)	Tare value of filter (ng/cm^2)		
		Polyethylene sheet	Polyethylene sheet + back up filter	Polyfluorocarbon filter
Cl^-	0.1	100	40	1000
NO_3^-	0.1	0	0	0
SO_4^{2-}	0.1	300	0	0

(4) Calculation method of anion concentration

The anion concentration of sample is calculated as follows;

(a) Ion concentration of analyzed solution

$$C_{\text{sol}} = C_{\text{std}} \cdot \frac{H_{\text{sol}}}{H_{\text{std}}} \dots\dots\dots \text{Equation (5-20)}$$

where;

- C_{sol} : Ion concentration of analyzed solution ($\mu\text{g}/\text{m}^3$)
- C_{std} : Ion concentration of standard solution ($\mu\text{g}/\text{m}^3$)
- H_{sol} : Peak height of analyzed solution (mm)
- H_{std} : Peak height of standard solution (mm)

(b) Anion concentration in the ambient air

$$C_i = \frac{C_{\text{sol}} \cdot V_L \cdot S_a}{F_a \cdot V} \dots\dots\dots \text{Equation (5-21)}$$

where;

- C_i : Anion concentration in the ambient air ($\mu\text{g}/\text{m}^3$)
- C_{sol} : Ion concentration of analyzed solution ($\mu\text{g}/\text{m}^3$)
- V_L : Extracted solution volume (m^3)
- S_a : Total area of filter (cm^2)
- F_a : Filter area of analyzed sample (cm^2)
- V : Air aspiration flow rate (m^3)

(5) Ion Chromatogram

Fig. 5-26 shows the typical example of ion chromatogram (MS1, Coarse particle). Abscissa is the time after sample injection, and ordinate represents peak height. The peak height used for calculation of concentration is the height from the base-line connected flat part around the peak.

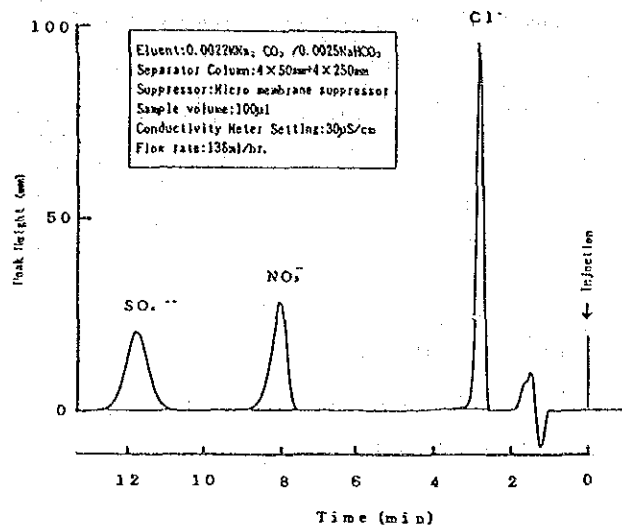


Fig. 5-26 An example of ion chromatogram

(6) Results of measurement

The anion concentration in the particulate matter measured by ion chromatography is shown in Table 5-16.

5.2.4 Analysis of Cation (Ca²⁺, Mg²⁺) by Atomic Absorption Spectrometry

(1) Principle of analysis

When a light beam of a specific wave length passes through the vapor of element, the atom in the ground state absorbs this light. Atomic absorption spectrophotometry is an analytical method based on this phenomenon. A sample solution containing a metal ion is introduced into flame, where the solution vaporizes and the metal atom contained in the solution changes into atomic state by heat of the flame. The light beam emitted from a hollow cathode lamp is made to pass this vapor and its absorbance is measured. The concentration of the metal element can be calculated from decrease of the absorbance.

(2) Analyzing method

The solution sample which is described in (2) of 5.2.3 is used for analysis. The analysis in this study was carried out by HITACHI 170-50A atomic absorption spectrometer.

① Analyzing conditions

The analyses were carried out under the following conditions

Analysis line: Ca²⁺, 422.7 nm

Mg²⁺, 285.2 nm

Flame: Acetylene-air

② Development of analytical line

Standard stock solutions containing each 1000 μg/ml of calcium ion and Magnesium ion were prepared. This standard stock solutions were properly diluted before it is used as

standard solutions for the preparation of analytical lines. The solution was poured into instrument of atomic absorption spectrometry under the same conditions as applied to sample solution. Fig. 5-27 shows analytical line of Ca^{2+} and Mg^{2+} .

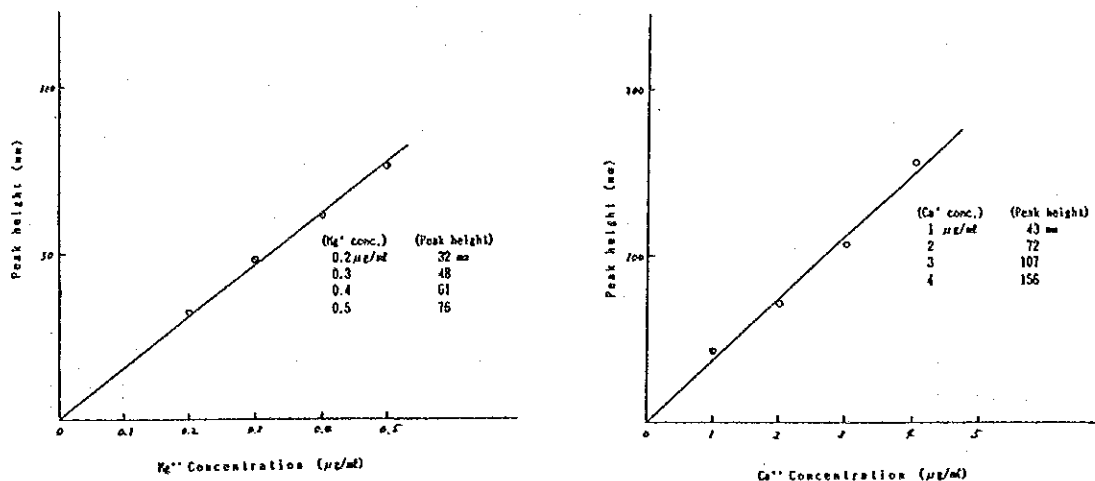


Fig. 5-27 Analytical line of Ca^{2+} and Mg^{2+}

(3) Determination limit and tare value of filter

The limit of determination and tare value of the filters are shown in Table 5-19.

Table 5-19 Determination limit and blanks value of filters

Analyzed item	Determination limit ($\mu\text{g}/\text{m}^l$)	Tare value of filter (ng/cm^2)		
		Polyethylene sheet	Polyethylene sheet + back up filter	Polyfluorocarbon filter
Ca^{2+}	0.03	900	500	6000
Mg^{2+}	0.01	300	100	800

(4) Calculation method of Ca^{2+} and Mg^{2+} concentration

The cation (Ca^{2+} , Mg^{2+}) concentration of sample is calculated as follow;

① Ion concentration of analyzed solution

$$C_{\text{sol}} = C_{\text{std}} \cdot \frac{H_{\text{sol}}}{H_{\text{std}}} \dots\dots\dots \text{Equation (5-22)}$$

where;

- C_{sol} : Ion concentration of analyzed solution ($\mu\text{g}/\text{m}^l$)
- C_{std} : Ion concentration of standard solution ($\mu\text{g}/\text{m}^l$)
- H_{sol} : Peak height of analyzed solution (mm)
- H_{std} : Peak height of standard solution (mm)

② Cation concentration in the ambient air

$$C_i = \frac{C_{sol} \cdot V_L \cdot S_a}{F_a \cdot V} \quad \text{Equation (5-23)}$$

where;

- C_i : Cation concentration in the ambient air ($\mu\text{g}/\text{m}^3$)
- C_{sol} : Cation concentration of analyzed solution ($\mu\text{g}/\text{m}\ell$)
- V_L : Extracted solution volume ($\text{m}\ell$)
- S_a : Total area of filter (cm^2)
- F_a : Filter area of analyzed sample (cm^2)
- V : Air sucking flow rate (m^3)

(5) Results of analysis

The cation (Ca^{2+} and Mg^{2+}) concentration in the particulate matter obtained by atomic absorption spectrometry is shown in Table 5-16.

5.2.5 Analysis of Cation (Na^+ and K^+) by Flame Photometry

(1) Principle of analysis

The concentration of an element is determined by spraying the sample solution into flame and by measuring the emission intensity of the element at specific wave length. This method is effective in case of the analysis of alkali and alkali earth elements.

(2) Analyzing method

The sample solution which is described in (2) of 5.2.3 is used for analysis. The analysis was carried out by using HITACHI 170-50A flame photometer.

① Analysis conditions

The analysis were carried out under the following condition

Analysis line: Na^+ , 589.3 nm

K^+ , 766.6 nm

Flame: Acetylene-air

② Development of analytical line

Standard stock solutions containing each 1000 $\mu\text{g}/\text{m}\ell$ of sodium ion and potassium ion were prepared. This standard stock solution was properly diluted before it is used for the preparation of analytical lines. The solution was poured into the flame photometer under the same conditions as applied to sample solution and analytical line is drawn. Fig. 5-28 shows analytical line of Na^+ and K^+ .

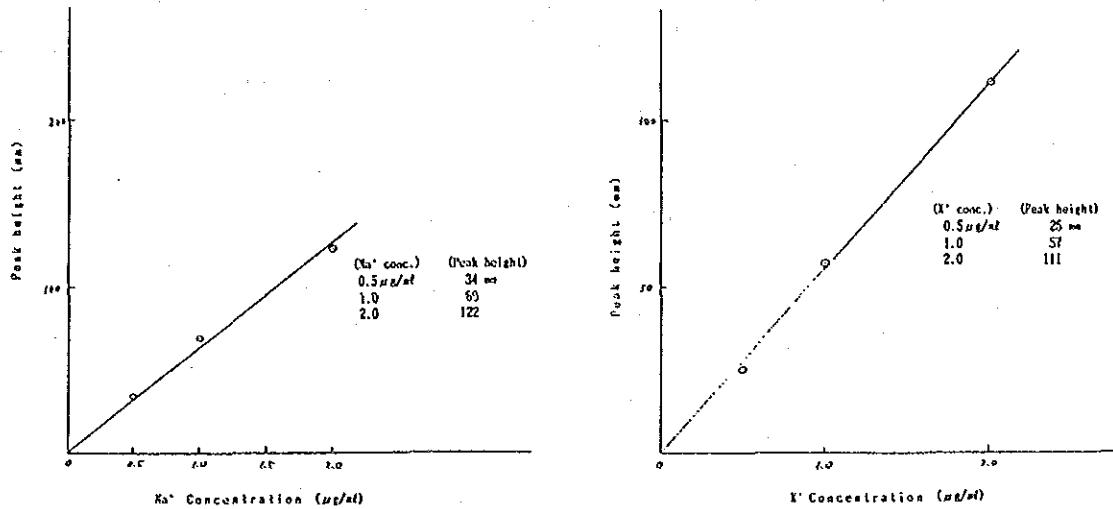


Fig. 5-28 Analytical line of Na⁺ and K⁺

(3) Determination limit and blank value of filter

The limit of determination and tare value of the filters are shown in Table 5-20.

Table 5-20 Determination limit and blank value of filter

Analyzed item	Determination limit (µg/m ³)	Tare value of filter (ng/cm ²)		
		Polyethylene sheet	Polyethylene sheet + back up filter	Polyfluorocarbon filter
Na ⁺	0.02	200	200	1500
K ⁺	0.02	100	80	300

(4) Calculation method of Na⁺ and K⁺ concentration

The calculation method for ion concentration of the analyzed solution and cation concentration in the ambient air are the same as those applied to cation by atomic absorption spectrometry.

(5) Results of analysis

The concentration of cation (Na⁺ and K⁺) in the particulate matter measured by flame photometry is shown in Table 5-16.

5.2.6 Analysis of Cation (NH₄⁺) by Spectrophotometry (Method of indephenol)

(1) Principle of analysis

Ammonium ion in a sample solution is made to react with phenol in the presence of sodium hypochlorite and the absorbance of developed color of indephenol is measured by spectrophotometry.

(2) Analyzing method

A 5-ml sample solution described in (2) of 4.3 was transferred into a stoppered test tube, and

25 ml of phenol-sodium nitroprusside solution was added. After shaking, 2.5 ml of sodium hypochlorite solution was added, and the solution was gently mixed. The solution was kept at 30°C for 2 hr to wait color development. This solution was used for analysis. The analysis was carried out by using SHIMAZU UV-240 spectrophotometer. Analysis line is 640 nm.

Preparation method for reagents is as follows:

① Phenol-sodium nitroprusside solution

Dissolve 5 g phenol and 25 mg sodium nitroprusside in distilled water and dilute up to 500 ml.

② Sodium hypochlorite solution

Dissolve 15 g NaOH in ammonia-free water, add 100 ml sodium hypochlorite solution containing 3 to 10% Cl⁻ and dilute up to 1000 ml.

Developed analytical line is as follows:

Standard stock solution containing 100 µg/ml of ammonium ion is prepared. This standard solution is properly diluted before it is used for the preparation of analytical line. Absorbance of the solution is measured with spectrophotometer under the same conditions as applied to those of sample solution. Fig. 5-29 shows analytical line of NH₄⁺.

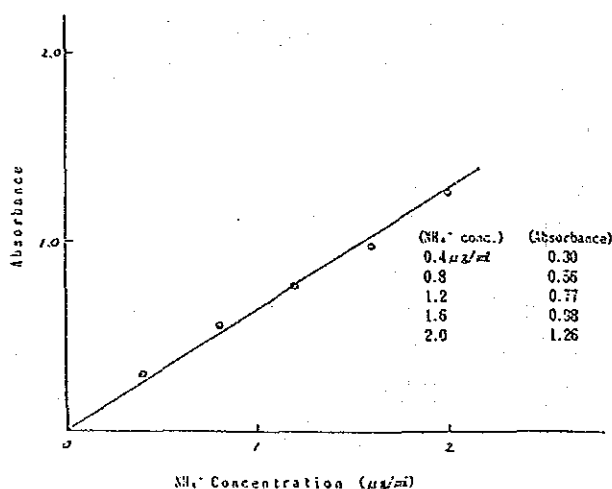


Fig. 5-29 Analytical line of NH₄⁺

(3) Determination limit and blank value of filters

The limit of determination and blank value of the filters are shown in Table 5-21.

Table 5-21 Determination limit and tare value of filters

Analyzed item	Determination limit (µg/ml)	Tare value of filter (ng/cm ²)		
		Polyethylene sheet	Polyethylene sheet + back up filter	Polyfluorocarbon filter
NH ₄ ⁺	0.02	0	0	0

(4) Calculation method of NH_4^+ concentration

Calculation method for NH_4^+ concentration in analyzed solutions and concentration of NH_4 in the ambient air are the same as those for analysis of cation by atomic absorption spectrometry.

(5) Results of analysis

The concentration of NH_4^+ in the particulate matter measured by spectrophotometry is shown in Table 5-16.

5.2.7 Analysis of total carbon and non-volatile carbon contained in particulate mater by differential thermal analysis

(1) Principle of analysis

Particulate matter sampled on the quartz-fiber filter is treated thermally and is classified into organic carbon and elemental carbon. After such carbons completely oxidized to CO_2 , they are introduced into differential thermal conductivity meter which has a CO_2 absorbing tube. The heat generated by absorption of CO_2 is detected as the output signal of a differential electronic signal.

In this study the sample was heat-treated in nitrogen stream at 400°C and the volatile carbon was driven off to determine non-volatile carbon, and the sample not thermally treated was used for analysis of the total carbon.

The schematic of the instrument is shown in Fig. 5-30. It consists of the decomposition furnace, a constant flow pump to intake the combustion gas sample, and a detector.

Through the inlet part of the combustion tube filled with He carrier gas, the sample is inserted on a platinum board. The sample is decomposed in the high temperature atmosphere and then completely oxidized in the presence of copper oxide catalyst. The gaseous components generated from the sample excluding CO_2 , H_2O , and N_2 are removed by the oxidation furnace and reduction furnace. The gas mix of CO_2 , H_2O , N_2 and He are then led to the differential thermal conductivity meter which has the H_2O and CO_2 absorbing tubes for. The concentrations of C, N, and H are evaluated in term of differential electric signal (count number).

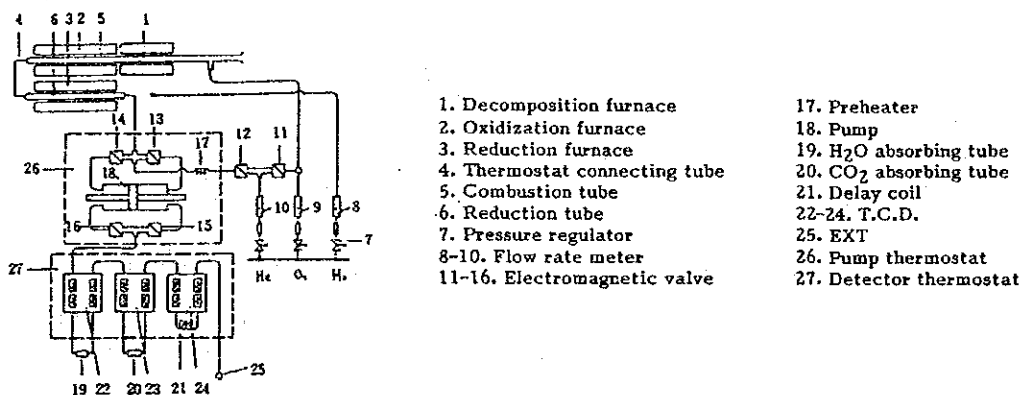


Fig. 5-30 Outline of carbon analyzing instrument

(2) Analyzing methods

As shown in Fig. 5-9, the quartz-fiber filter was cut into circle pieces in 1 cm diameter (2 pcs.) as samples for analysis. For the analysis of total carbon, no pretreatment was required, but for the analysis of non-volatile carbon, the sample pieces were pretreated (at 400°C in nitrogen stream) for 4 minutes as shown in Fig. 5-31, and the volatile carbon compounds were driven off prior to analysis.

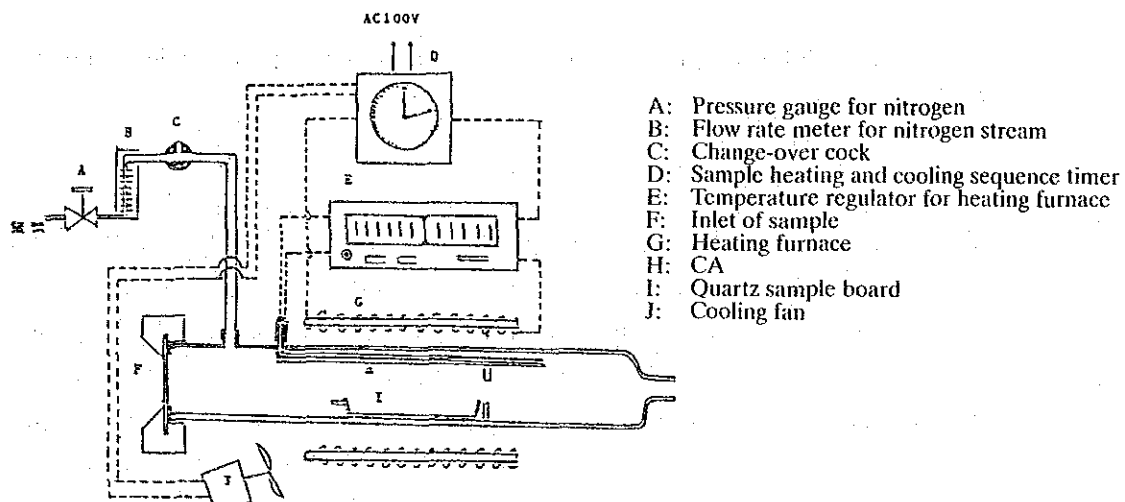


Fig. 5-31 Outline of pretreatment facility for analysis of elemental carbon

① Analyzing conditions

The analysis of carbon has been carried out under the following conditions.

Sample decomposition temperature:	950°C
Temperature of oxidization furnace:	850°C
Temperature of reduction furnace:	550°C
Temperature of pump thermostat:	55°C
Temperature of detector thermostat:	100°C
Flow rate of helium:	200 ml/min
Flow rate of oxygen gas:	20 ml/min
Bridge current:	65 mA

② Drawing of analytical line

o-Nitroaniline was employed as a standard substance and by a micro-balance 0.1 to 2.5 mg was weighed as sample. And the sample was also analyzed under the same conditions and analytical line was developed by measuring the volume of carbon contained. The analytical line is shown in Fig. 5-32.

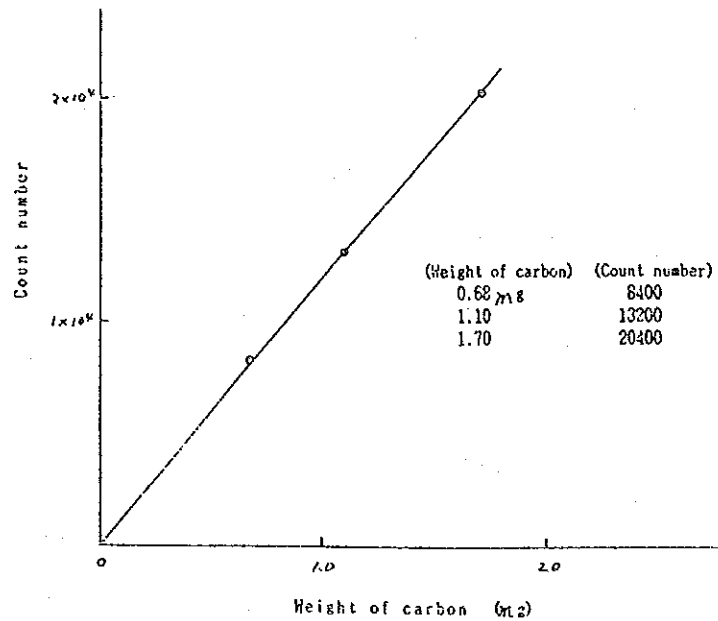


Fig. 5-32 Analytical line of carbon

(3) Limit of determination and tare value of filter

The limit of determination applied to analysis of ambient particulate matter by DTA is shown in Table 5-22, and the tare value of the filter is also shown in the same table.

Table 5-22 Limit of determination and blank value of filter

Item	Limit of determination	Filter blank value (quartz-fiber filter)
Total carbon	5 µg	38
Non-volatile carbon	5 µg	9

* Remarks: µg for 2 pieces filter of 1 cmφ

(4) Calculation methods of carbon concentration

Weight of carbon on the filter is calculated from count number of differential thermal conductivity meter by the following Equation 5-24.

$$C_w = \left(\frac{St_w}{St_{count}} \cdot S_{count} \right) - Fbw \quad \text{Equation (5-24)}$$

where;

- C_w: Weight of carbon in analyzed sample (mg)
- St_w: Weight of carbon in standard sample (mg)
- St_{count}: Count number of standard sample
- S_{count}: Count number of analyzed sample
- Fbw: Blank value of filter (mg)

Concentration of carbon in the ambient air is calculated by the following Equation 5-25.

$$C_c = \frac{C_w \cdot F_a}{V \cdot S_a} \dots\dots\dots \text{Equation (5-25)}$$

where;

- Cc: Concentration of carbon in the ambient air (mg/m³)
- Cw: Weight of carbon in analyzed sample (mg)
- V: Air flow rate (m³)
- Fa: Total area of filter (cm²)
- Sa: Filter area of analyzed sample (cm²)

(5) Results of analysis

The results of analysis of carbon concentration in the ambient air by DTA are shown in Table 5-16. In the table, the volatile carbon is represented by organic carbon, and non-volatile carbon is represented by elemental carbon.

5.3 Analysis of Chemical Components in Soil, Road Dust and Fuel Gasoline

Two typical types of ground soil and one type of road dust in Samut Praharn Industrial District have been sampled by ONEB and elements, anion, cation and carbon content of the samples have been analyzed by INAA, XRF, IC, AAS, FP, SP and DTA. The location of the sampling points are shown in Fig. 5-33.

As for gasoline, two types of fuel gasolines (Regular and Premium) commonly used in Thailand described in Chapter 5 were sampled and their elements were analyzed by INAA and XRF.

The method of analysis for soil, road dust and fuel gasoline are almost identical to one previously applied to particulate matter in a ambient air, but some steps of pretreatment are different.

5.3.1 Soil and road dust

The sample of soil and road dust were weather dried and impurities such as small stones were eliminated. After ground with a gate mortar, the sample were used as sample for analysis. The weighing of the samples was carried out after desiccation for several days with silicagel. The specified volume of the samples applied to the analysis are shown as follows.

(1) INAA

About 15 mg of the samples for short term irradiation and about 30 mg for long term irradiation were sealed in double layer polyethylene bags of 5×7 cm respectively.

(2) XRF

About 100 mg of the samples were equally distributed over membrane filters.

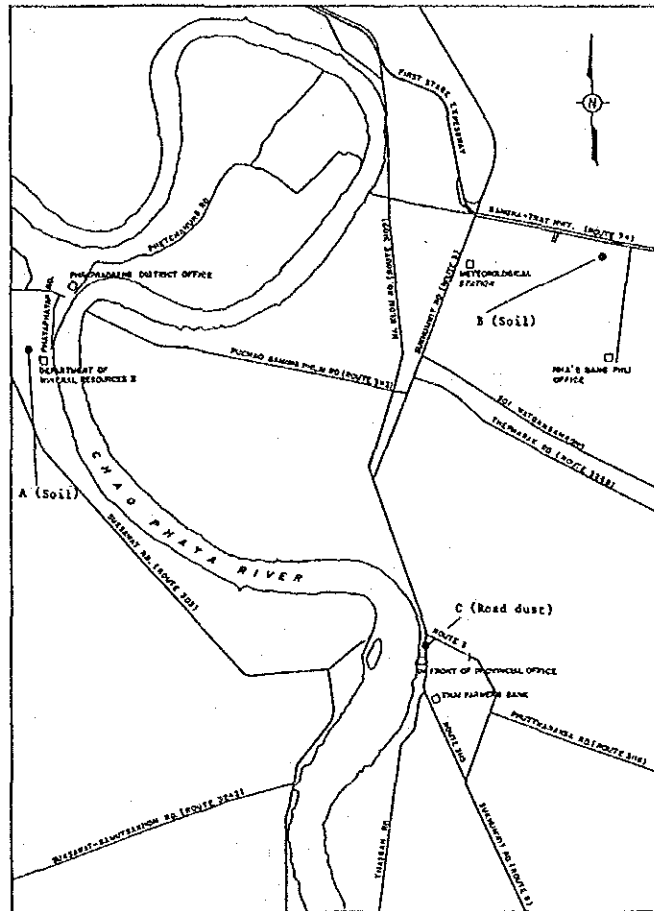


Fig. 5-33 Location of the sampling points for soil and road dust

(3) IC, AAS, FP and SP

Adding 100 ml of eluent in 1 g of the samples and shaking about 90 minutes for extraction, the sample solution are prepared after filtration of impurities.

(4) Differential Thermal Analysis

The samples (2~5 mg) were weighted on a platinum board and they were used for analysis of total carbon and non-volatile carbon.

5.3.2 Fuel gasoline

(1) INAA

About each 50 ml of sample for short term and long term irradiation was sealed in polyethylene beakers. The sample for short term irradiation was irradiated by thermal neutron beam for 5 minutes and the sample for long term irradiation was irradiated with thermal neutron for 5 hours. The thermal neutron flux was $5 \times 10^{11} \text{ cm}^{-2} \cdot \text{s}^{-1}$. After irradiation, the sample was transferred into a new polyethylene beaker, and then Gamma ray was measured.

(2) XRF

A 0.6-ml gasoline sample was titrated on a 47 mmφ membrane filter made by nitrocellulose, and was then dried up.

5.3.3 Results of analysis

The results of analysis of chemical components in soil, road dust and fuel gasoline are shown in Table 5-23.

Table 5-23 (I) Results of analysis of soil and road dust components

Unit: ppm

Name of sample Item	A	B	C
INAA			
Short lived nuclides			
Al	45000(1)	66000(1)	50000(2)
Br	<30	<40	150(5)
Ca	<2000	2500(22)	26000(5)
Cl	<1000	2000(16)	7300(6)
Cu	<200	<300	<300
Mg	<4000	7600(28)	1200(18)
Mn	270(12)	460(2)	610(2)
Ti	3000(7)	2400(10)	2300(5)
V	41(5)	30(5)	46(4)
Long lived nuclides (a)			
As	7.7(8)	19(5)	51(2)
K	21000(6)	42000(5)	21000(7)
La	22(5)	64(3)	22(5)
Na	4900(1)	8100(1)	7200(1)
Sb	2.8(10)	<0.7	3.4(9)
Sm	5.0(1)	14(1)	4.7(1)
W	8.6(15)	3.2(42)	4.1(24)
Long lived nuclides (b)			
Ag	<3	<3	<3
Ba	380(17)	410(19)	360(17)
Ce	54(4)	150(2)	47(3)
Co	6.9(13)	3.8(22)	6.3(12)
Cr	31(8)	24(13)	33(8)
Cs	3.6(12)	8.6(7)	3.8(10)
Fe	12000(5)	12000(5)	18000(4)
Hf	2.0(14)	14(3)	5.9(5)
Lu	0.21(20)	0.58(12)	0.69(7)
Ni	<60	<60	<50
Sc	4.5(2)	4.4(2)	4.5(2)
Se	6.4(24)	12(20)	6.1(26)
Th	12(2)	55(1)	11(2)
Zn	<30	<40	130(15)
XRF			
Cd	1.2	1.8	1.8
Pb	60	80	130
S	180	480	4700
Si	390000	320000	310000
IC, AAS, FP and SP			
Na ⁺	600	780	1500
K ⁺	410	790	360
Ca ²⁺	33	190	460
Mg ²⁺	55	98	160
NH ₄ ⁺	400	990	3400
NO ₃ ⁻	4	26	30
SO ₄ ²⁻	58	240	2000
Pyrolysis			
T - C	1900	6600	17500
E - C	1400	5100	16900
O - C	500	1500	600

Remarks: Figures in parenthesis are analytical error (%)

Table 5-23 (2) Results of analysis of fuel gasoline

Unit: ppb

Item	Premium	Regular	Geometrical average *
Al	<200	<200	<200
Br	86000(7)	82000(7)	84000(7)
Cs	<4000	<3000	<4000
Cl	190000(4)	190000(4)	190000(4)
Cu	<1000	<700	<800
Mg	<10000	<10000	<10000
Mn	<5	<5	<5
Ti	<5000	<5000	<5000
V	<10	<10	<10
As	<40	<40	<40
K	<10000	<10000	<10000
La	<20	<20	<20
Na	<200	<200	<200
Sb	<20	<20	<20
Sm	<2	<2	<2
W	<50	<50	<50
Ag	<0.4	<0.2	<0.3
Be	<40	<40	<40
Ce	<0.8	<0.9	<0.8
Co	<0.2	<0.2	<0.2
Cr	<1	<1	<1
Cs	<0.06	<0.05	<0.05
Fe	<50	<40	<50
Hf	<0.09	<0.09	<0.09
Lu	<0.08	<0.09	<0.08
Ni	<10	<7	<8
Sc	<0.01	<0.01	<0.01
Se	<0.7	<0.7	<0.7
Th	<0.06	<0.06	<0.06
Zn	39(20)	8.0(47)	22(34)
Cd	<200	<200	<200
Pb	15000	7000	11000
S	12000	4000	7600
Si	<20	<20	<20

Remarks: Figures in parenthesis are analytical error (%)

* Premium: Regular = 45.6 : 54.4 (%)

5.4 Analysis of sulfur content in fuels for normal uses in Thailand

Ten samples of fuels as shown in Table 5-24 were brought back to Japan and were subject to analysis to determine sulfur content in fuels. Those fuels are commercially available and sold in Thailand for normal commercial applications. The Japanese Industrial Standard, JIS K2541, was applied to the analysis of sulfur content in the fuels. Results are shown in Table 5-24.

Details of analytical procedure are shown in the Appendix.

Table 5-24 Results of sulfur content in fuels

Sample No.	Kind of fuels	Sulfur content (%)	Testing method
1	Fuel oil No. 1 (Shell)	1.98	1
2	Fuel oil No. 4 (Shell)	2.58	1
3	Fuel oil No. 5 (PTT)	3.04	1
4	Fuel oil No. 6 (Shell)	1.88	1
5	Diesel oil (Shell)	0.65	1
6	Diesel oil (Esso)	0.46	1
7	Gasoline Regular (Shell)	47 ppm	2
8	Gasoline Regular (Esso)	<1 ppm	3
9	Gasoline Premium (Shell)	316 ppm	2
10	Gasoline Premium (Esso)	<1 ppm	3

1: Bomb-combustion, gravimetry

2: Micro-coulometry

3: H₂-O₂ flame combustion, dimethylsulfonazo III - Volumetry

**PART III ANALYTICAL STUDY ON CURRENT ATMOSPHERIC POLLUTANT
CONCENTRATIONS AND METEOROLOGICAL VARIABLES**

The pollutant concentration and meteorological data monitored were subject to analytical study such that the reporter can develop a better picture about the pollution status of the Samut Prakarn industrial district. The obtained data were grouped into two parts depending on the survey period (short term and long term). The former field survey was carried out during the periods of January, March and July in 1988 to measure the distribution and concentration of total particulate matter, while the latter continued for one year throughout 1988 to monitor ambient pollutant concentrations and meteorological variables.

1. Analysis of Long-Term Field Survey Data

In the long-term field survey, the hourly values of wind direction, wind velocity, atmospheric turbulence, solar radiation, net radiation, SO₂, NO₂, NO_x and SPM by β -ray dust meter were measured for a period of one year. These hourly data were used to make meteorological analysis, environmental concentration analysis, and analysis of the correlation between meteorological factors and the environmental concentrations. The measurement period was from January 17, 1988 to January 16, 1989, and the monthly average value for January was calculated as the mean of the same month in both 1988 and 1989.

1.1 Meteorological Analysis

Pollutants emitted from factories are transported and dispersed by wind. Accordingly, meteorological conditions, such as wind direction, wind velocity and atmospheric turbulence will have large effects on the environmental concentration, together with the emitted volume of pollutants. Therefore, analysis of meteorological data in the addressed area is essential not only for simply determining meteorological conditions but also for predicting the future environmental concentration. Accordingly, in this survey, analysis of meteorological factors was made by using the measured data of wind direction, wind velocity, atmospheric turbulence, solar radiation and net radiation, which were obtained in the survey of the target area.

1.1.1 Seasonal and Hourly Classification

The predictive simulation applied to this survey was the "yearly average concentration prediction model", where predictions were made based on calculated hourly concentration values corresponding to each meteorological condition (combination of wind direction, wind velocity and atmospheric stability). Then, the yearly average concentrations calculated by taking the weight-averaging of such hourly values while the occurrence frequency of meteorological conditions were taken into consideration. The approach thus cannot avoid some difficulty of reproducing the pollutant concentrations accurately for each meteorological condition because of restrictions existing in the diffusion model itself and the available volume of sourcing and meteorological data. To overcome such ambiguity, the reporter first made the statistical analyses on daily and seasonal changes of source activities, meteorological conditions and ambient concentrations (as shown in Fig. 1-1 and Fig. 1-2)

and then two time scales, hourly and seasonal, were selected to test the conformity of calculated concentrations with measured ones as shown in Table 1-1. In accordance, the study on meteorological variables has to be made with respect to same time scales.

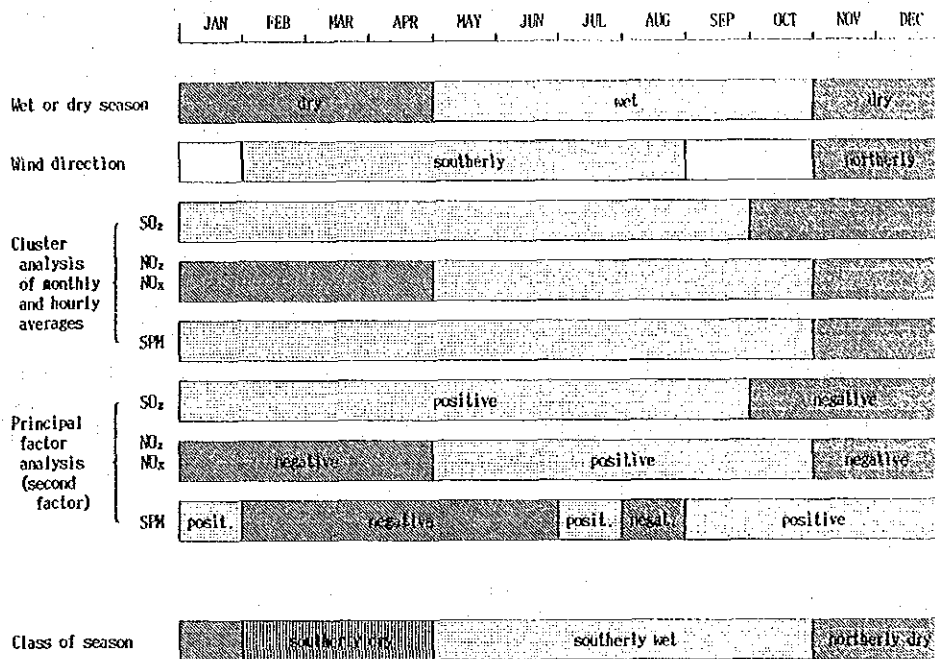


Fig. 1-1 Monthly Variations of Meteorological Conditions and Ambient Pollutant Concentration

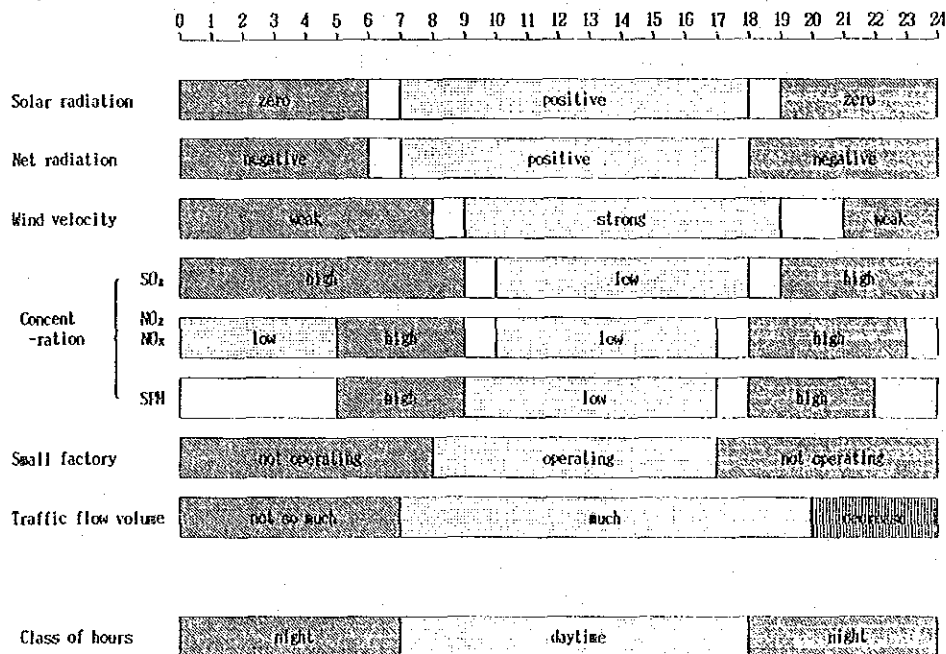


Fig. 1-2 Hourly Variations of Meteorological Conditions and Ambient Pollutant Concentration

Table 1-1 Seasonal and Hourly Classification

Season	Rainy May to Oct.	Dry Nov. to Jan.	Mid-term Feb. to Apr.
Daytime	7:00~17:59	7:00~17:59	7:00~17:59
Nighttime	18:00~ 6:59	18:00~ 6:59	18:00~ 6:59

1.1.2 Monthly and Hourly Average Wind Velocity

The monthly average and hourly average of wind velocity are shown in Fig. 1-3 and Fig. 1-4, respectively. Table 1-2 shows the daytime and nighttime averages of wind velocity for each observation site for three seasons.

When monitoring stations are compared, wind velocity changes in the descending order of MS1, MS2 and MS5, for both the monthly and hourly basis. With respect to monthly variations, although large differences are not seen throughout the year, the relatively strong wind in March is noteworthy. As for hourly variations, winds are strong in daytime and weak in nighttime. The trend is true for every monitoring station.

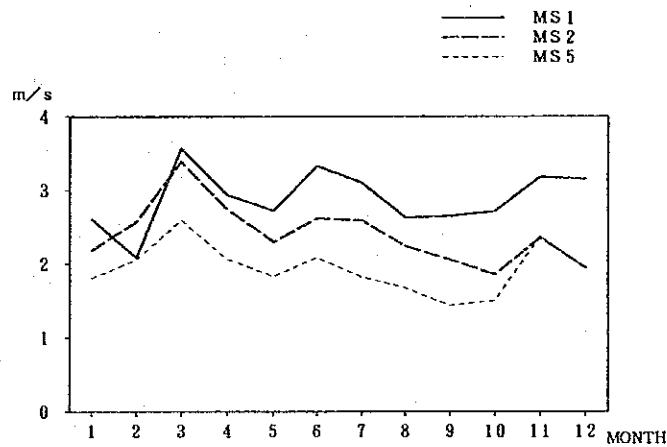


Fig. 1-3 Monthly Variations of Wind Velocity

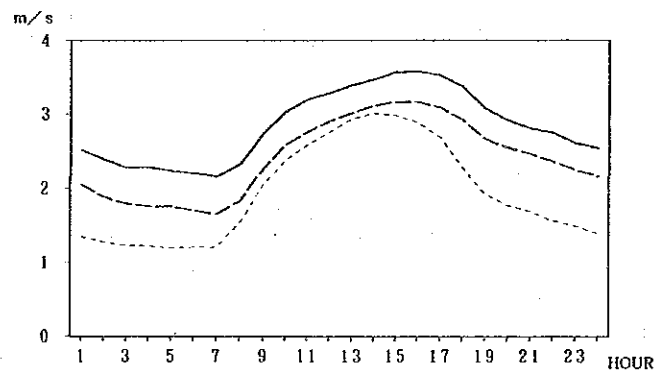


Fig. 1-4 Hourly Variations of Wind Velocity

Table 1-2 Average Wind Velocity for Each Season and Day and Night

Unit: m/s

Season	Rainy May to Oct.			Dry Nov. to Jan.			Mid-term Feb. to Apr.			Annual		
	MS1	MS2	MS5	MS1	MS2	MS5	MS1	MS2	MS5	MS1	MS2	MS5
Daytime	3.2	2.8	2.3	3.4	2.5	2.8	3.0	3.2	2.9	3.2	2.8	2.5
Nighttime	2.3	1.9	1.3	2.6	1.8	1.4	2.7	2.7	1.7	2.5	2.1	1.4
All day	2.7	2.3	1.7	3.0	2.2	2.0	2.9	2.9	2.2	2.8	2.4	1.9

1.1.3 Occurance Frequency of Wind by Velocity Rank

The frequency distribution of wind velocity for a one year period is shown in Fig. 1-5, which shows that MS1 and MS2 have a gentle peak in the neighborhood of a 2 m/s wind velocity range while MS5 has a peak around 1 m/s, and the frequency is the highest between 1 to 5 m/s.

In formulating a model for meteorological analysis, wind velocity is classified into several wind velocity ranks. In doing so, it is thought necessary to take account of the appearance frequency distribution of wind velocity as well as the sensitivity of the diffusion calculating equation with respect to wind velocity. In this survey wind velocity has been classified into 6 ranks of 1) 0-0.4 m/s, 2) 0.5-0.9 m/s, 3) 1.0-1.9 m/s, 4) 2.0-2.9 m/s, 5) 3.0-4.9 m/s and 6) 5.0 m/s or more. The occurrence frequency of wind by velocity rank, as classified above, is shown in Table 1-3.

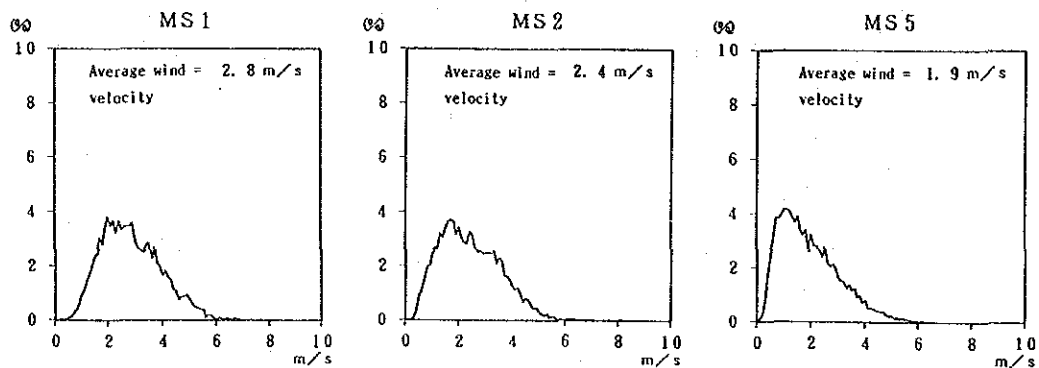


Fig. 1-5 Frequency Distribution of Wind Velocity

Table 1-3 Appearance Frequency of Wind by Velocity Rank

Wind Velocity Rank (m/s)	Appearance Frequency of Wind Velocity (%)		
	(MS1) ONEB STATION	(MS2) POWER PLANT	(MS5) H. & I. ESTATE
0-0.4	0.07	0.41	2.92
0.5-0.9	1.49	7.53	17.38
1.0-1.9	21.39	31.74	36.56
2.0-2.9	35.19	29.00	25.05
3.0-4.9	37.56	29.73	16.75
5.0-	4.31	1.60	1.34

1.1.4 Wind Rose

Annual wind rose and monthly wind rose at each monitoring station are shown in Fig. 1-6 and Fig. 1-7, respectively. Fig. 1-8 shows the wind rose of daytime and nighttime for each season.

With respect to annual wind rose, the most frequent wind directions are the S and SSE directions at MS1, the S direction at MS2 and the SSW direction at MS5, respectively, thereby indicating that winds of the S direction are dominant at every station. Furthermore, a difference in average wind velocity by wind direction can be hardly seen.

With respect to monthly wind rose, winds of the S direction are frequent during a period from January to August, and winds of the N to NE direction increase in velocity in November through December. These trends are seen at every station.

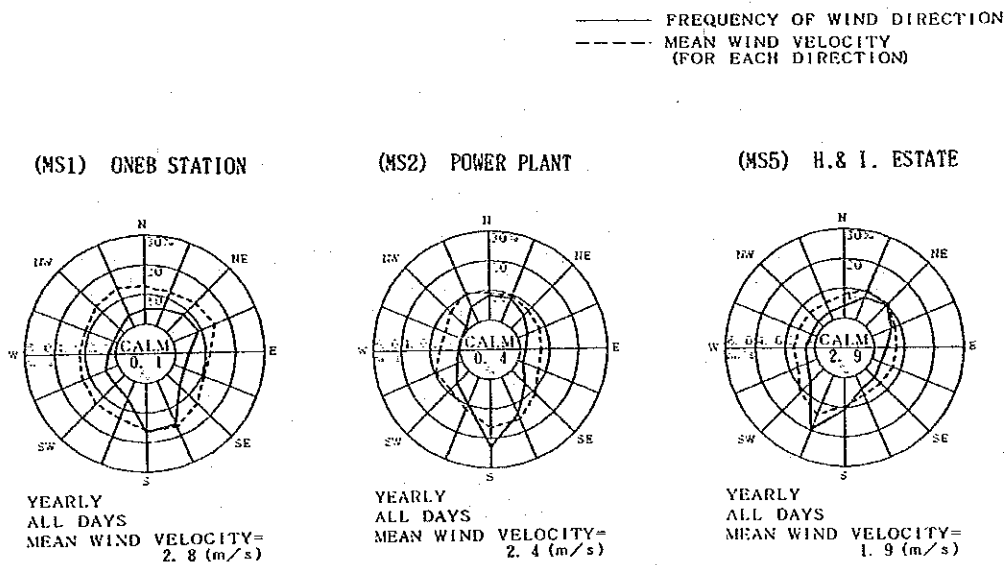


Fig. 1-6 Wind Rose at Each Monitoring Station (Annual)

(MS1) ONEB STATION

----- FREQUENCY OF WIND DIRECTION
 - - - - - MEAN WIND VELOCITY
 (FOR EACH DIRECTION)

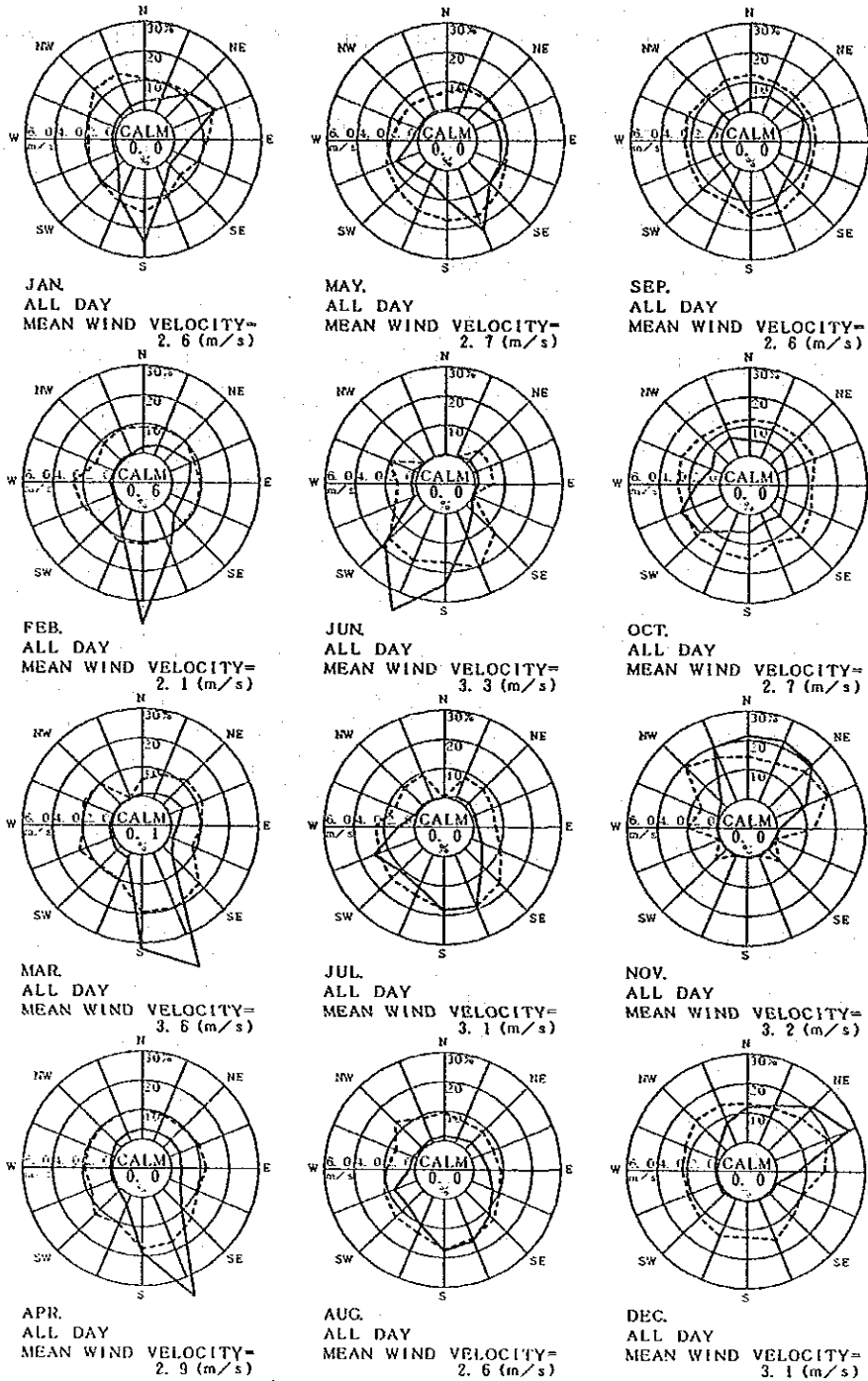


Fig. 1-7 (1) Monthly Wind Rose at Each Monitoring Station

(MS2) POWER PLANT

———— FREQUENCY OF WIND DIRECTION
 - - - - - MEAN WIND VELOCITY
 (FOR EACH DIRECTION)

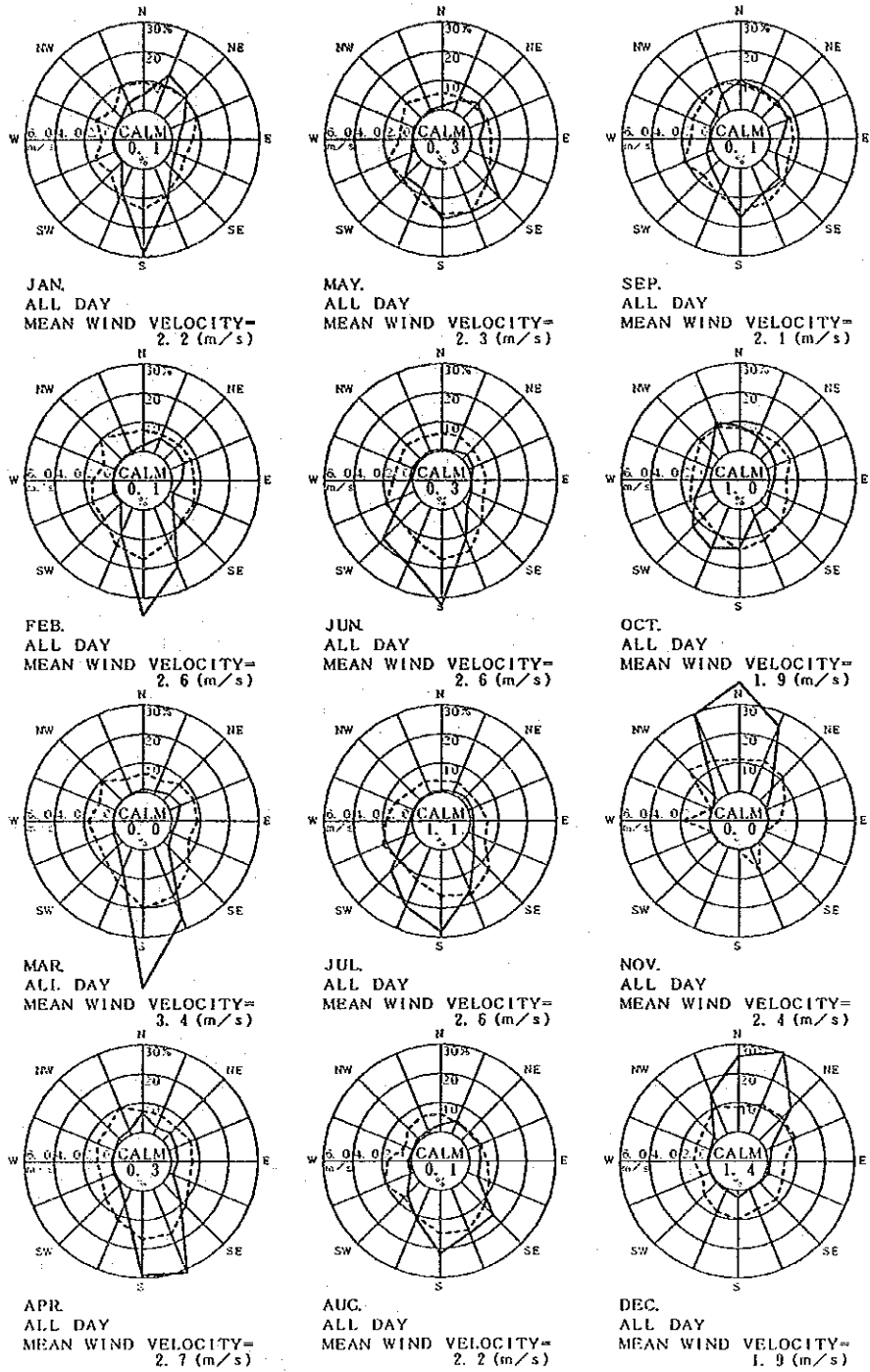


Fig. 1-7 (2) Monthly Wind Rose at Each Monitoring Station

(MS5) H. & I. ESTATE

—— FREQUENCY OF WIND DIRECTION
 - - - - MEAN WIND VELOCITY
 (FOR EACH DIRECTION)

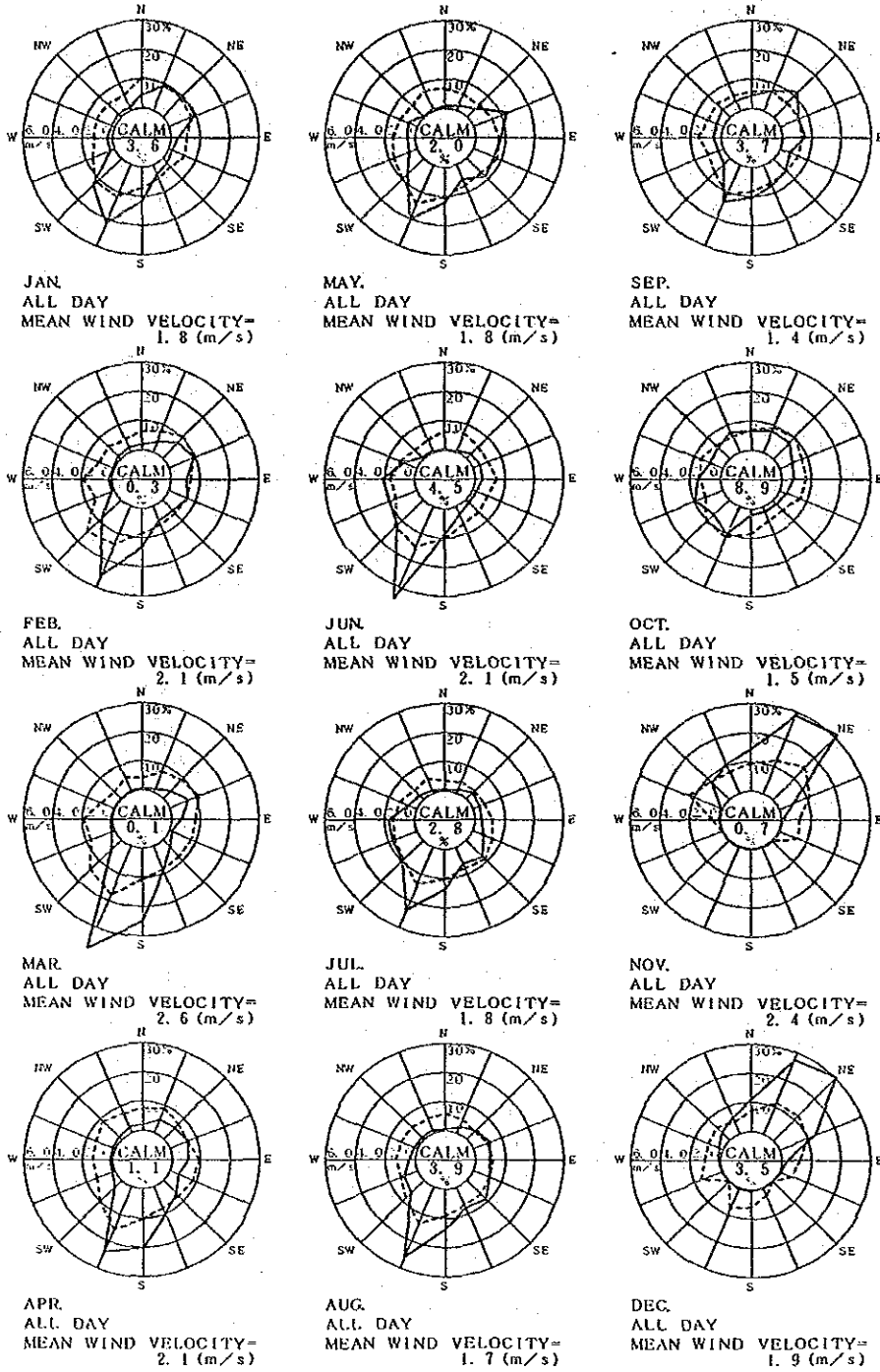


Fig. 1-7 (3) Monthly Wind Rose at Each Monitoring Station

(MS1) ONEB STATION

———— FREQUENCY OF WIND DIRECTION
 - - - - - MEAN WIND VELOCITY
 (FOR EACH DIRECTION)

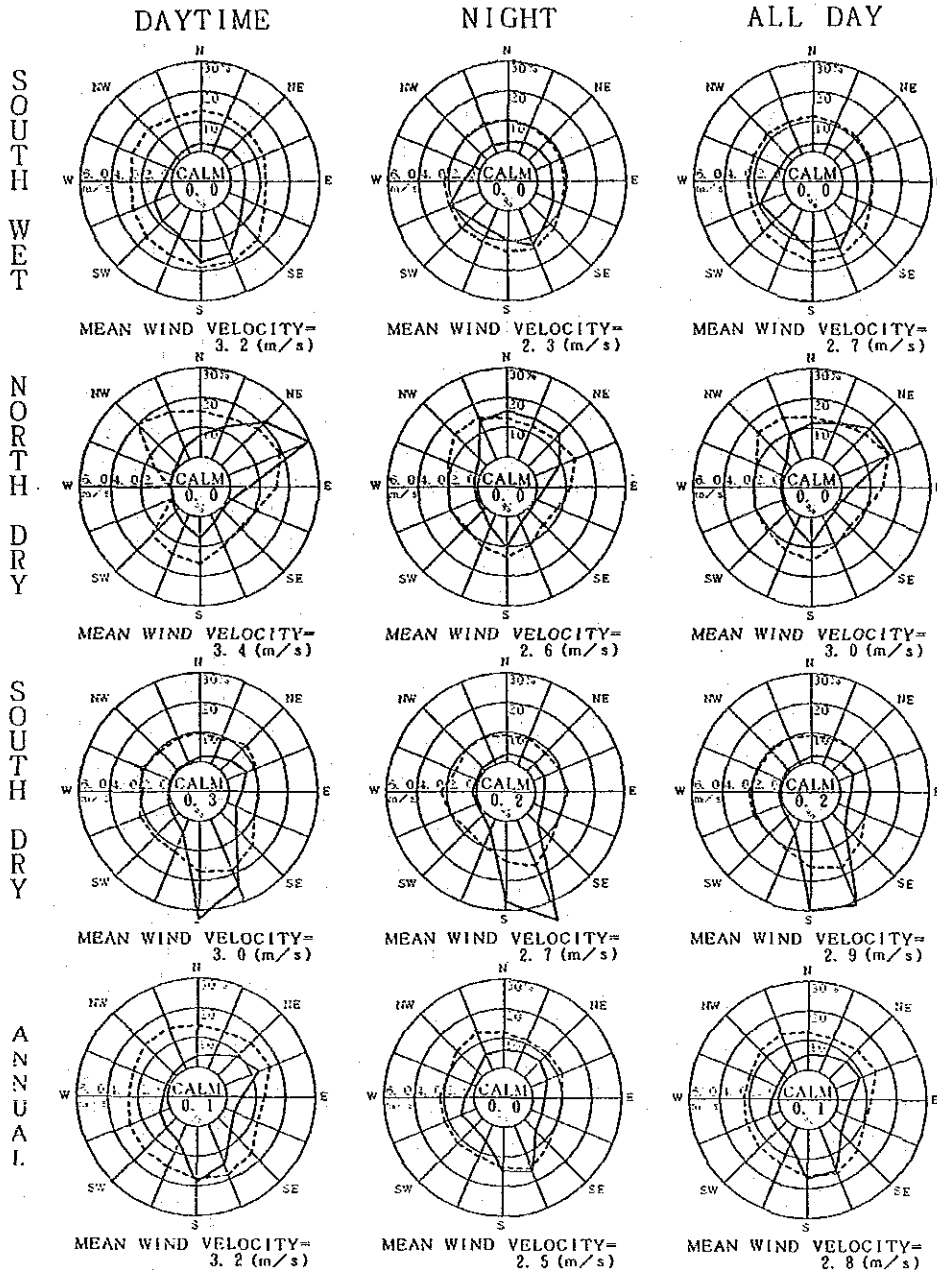


Fig. 1-8 (1) Wind Rose of Daytime and Nighttime for Each Season

(MS2) POWER PLANT

----- FREQUENCY OF WIND DIRECTION
 - - - - - MEAN WIND VELOCITY
 (FOR EACH DIRECTION)

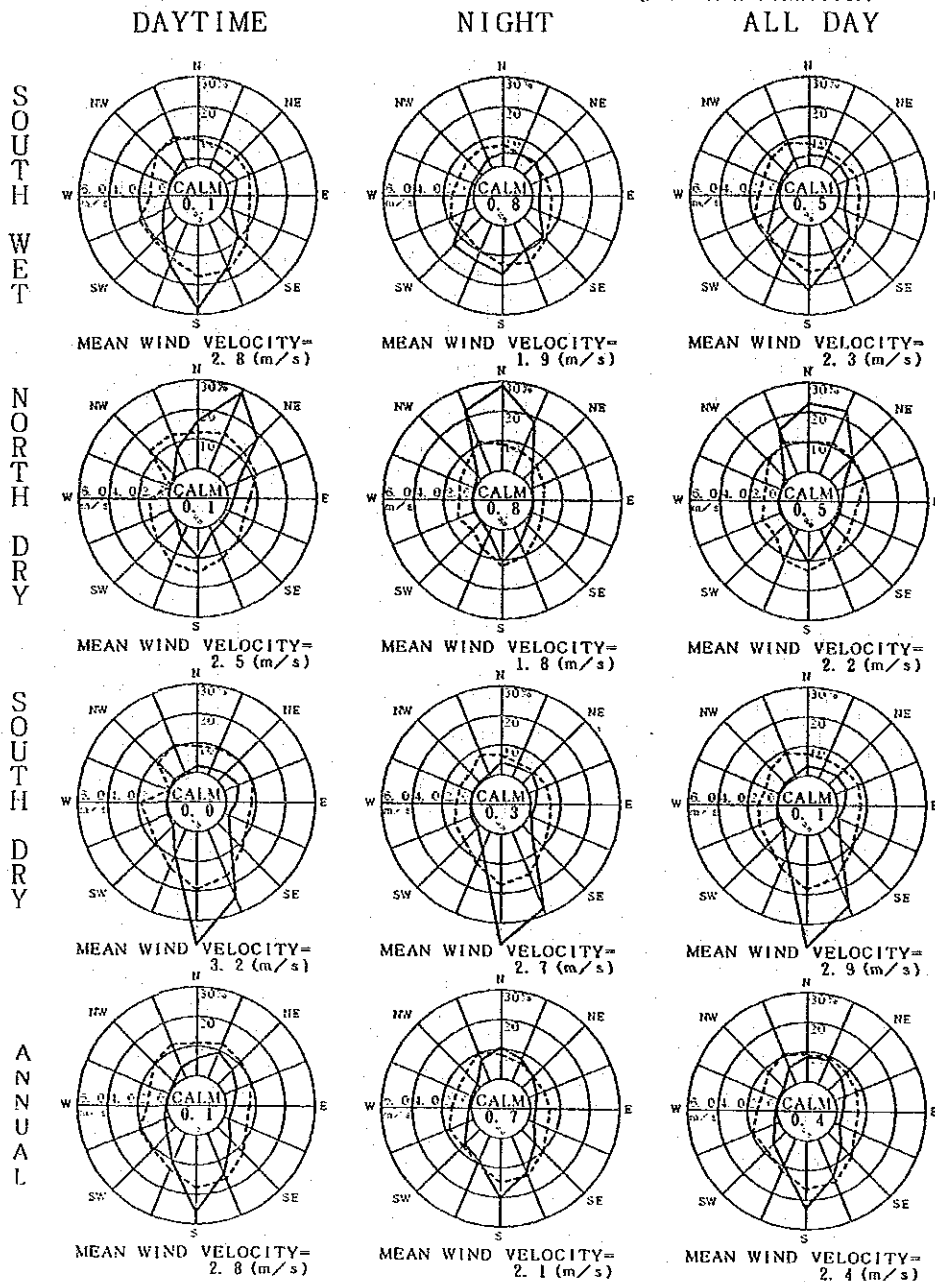


Fig. 1-8 (2) Wind Rose of Daytime and Nighttime for Each Season

(MS5) H & I. ESTATE

—— FREQUENCY OF WIND DIRECTION
 - - - - MEAN WIND VELOCITY
 (FOR EACH DIRECTION)

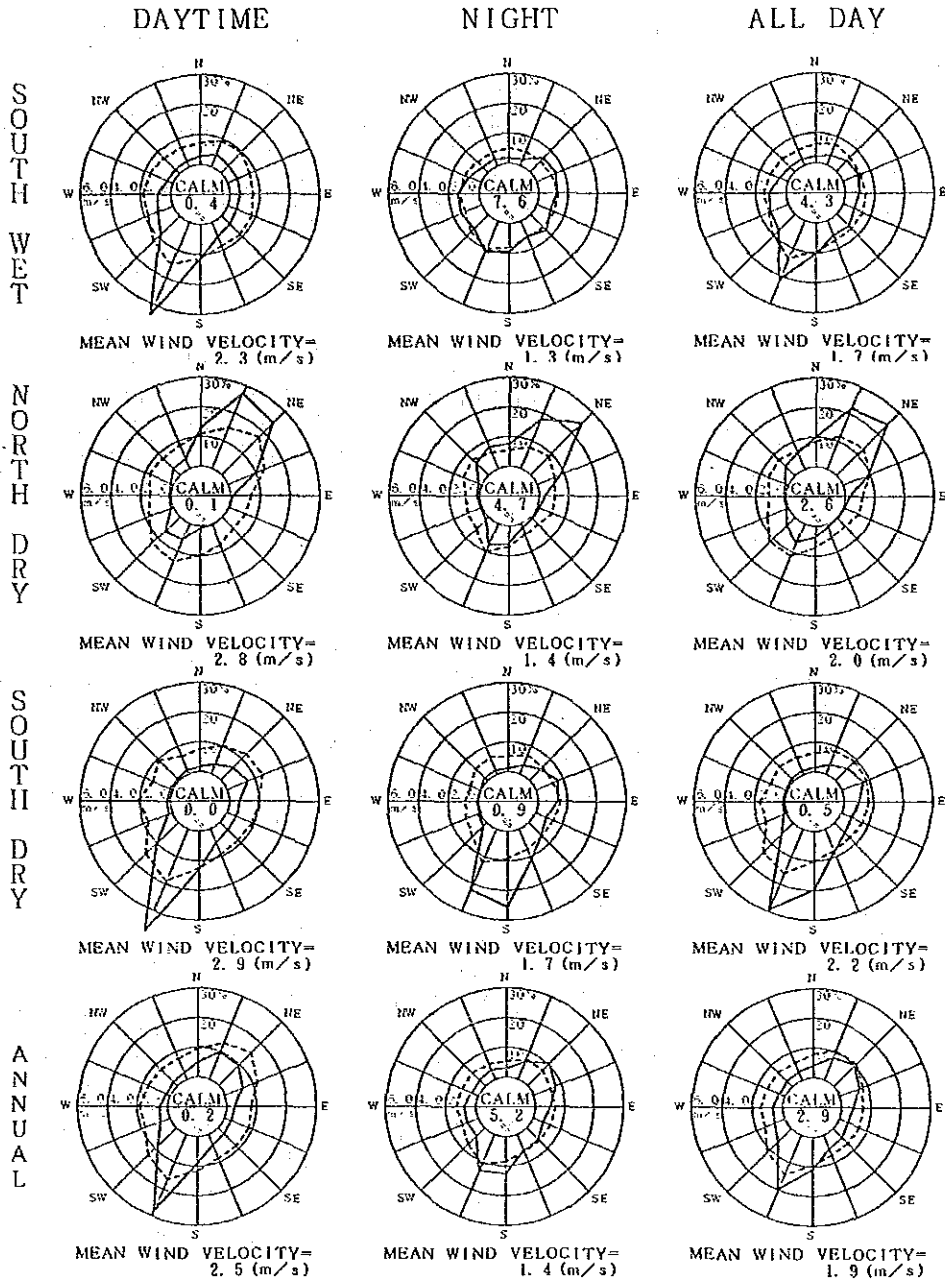


Fig. 1-8 (3) Wind Rose of Daytime and Nighttime for Each Season

1.1.5 Correlation Coefficient of Wind Direction and Wind Velocity Vectors

Based on the measurement data of hourly wind direction and velocity at each monitoring station, the degree of resemblance of wind among measurement points was examined.

As an index for the degree of resemblance of wind direction and velocity among measurement points, an approximate correlation coefficient, which is calculated by the following method, is frequently used.

The θ_i , which is the angle between V_{Ai} and V_{Bi} , at time i ($i = 1, 2 \dots N$) is obtained from the observed values $V_{A1}, V_{A2}, \dots, V_{AN}$ of the wind vector at measurement point A and the wind vectors $V_{B1}, V_{B2}, \dots, V_{BN}$ simultaneously measured at point B. From these, the correlation coefficients of the wind between measurement point A and B can be obtained by the following equation.

$$r(A, B) = \frac{\sum_i V_{Ai} V_{Bi} \cos \theta_i}{\sum_i V_{Ai} V_{Bi}} \dots\dots\dots (1-1)$$

Where, V_{Ai} and V_{Bi} are the wind velocity at time i at measurement point A and B, respectively.

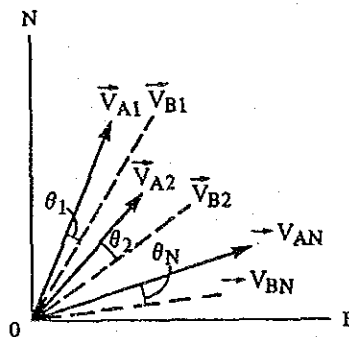


Fig. 1-9 Wind Vectors between Point A and B

Correlation coefficients of wind direction and wind velocity vectors between each measurement point obtained in the above manner are as shown in Table 1-4. In reviewing the table, correlation coefficients of yearly wind direction and wind velocity vectors are 0.909 between MS1 and MS2, 0.838 between MS2 and MS5, and 0.853 between MS1 and MS5, thereby indicating a significant correlation. Also, when correlation coefficients of monthly wind direction and wind velocity vectors are reviewed, most of the values found are 0.8 or more. Therefore, it is understood that meteorological conditions in the target area are nearly uniform. This may be due to a nearly flat configuration of the ground in the area.

Table 1-4 Correlation Coefficients of Wind Direction and Wind Velocity Vectors

	MS1 -MS2	MS2 -MS5	MS5 -MS1
Jan.	0.899	0.824	0.828
Feb.	0.925	0.826	0.848
Mar.	0.960	0.880	0.843
Apr.	0.950	0.826	0.846
May.	0.924	0.804	0.836
Jun.	0.953	0.855	0.924
Jul.	0.929	0.861	0.909
Aug.	0.904	0.814	0.849
Sep.	0.831	0.747	0.755
Oct.	0.856	0.756	0.812
Nov.	0.923	0.884	0.929
Dec.	0.818	0.850	0.865
Yearly	0.909	0.838	0.853

1.1.6 Monthly and Hourly Solar Radiation and Net Radiation

Monthly solar radiation and net radiation flux are shown in Fig. 1-10, and hourly solar radiation and net radiation flux in Fig. 1-11. When hourly variations are reviewed, it is found that both solar radiation and net radiation flux increase from around 07:00 hour, reach the peak value at around 13:00, and thereafter decline until around 19:00. Furthermore, monthly solar radiation and net radiation flux do not show any significant variation throughout the year.

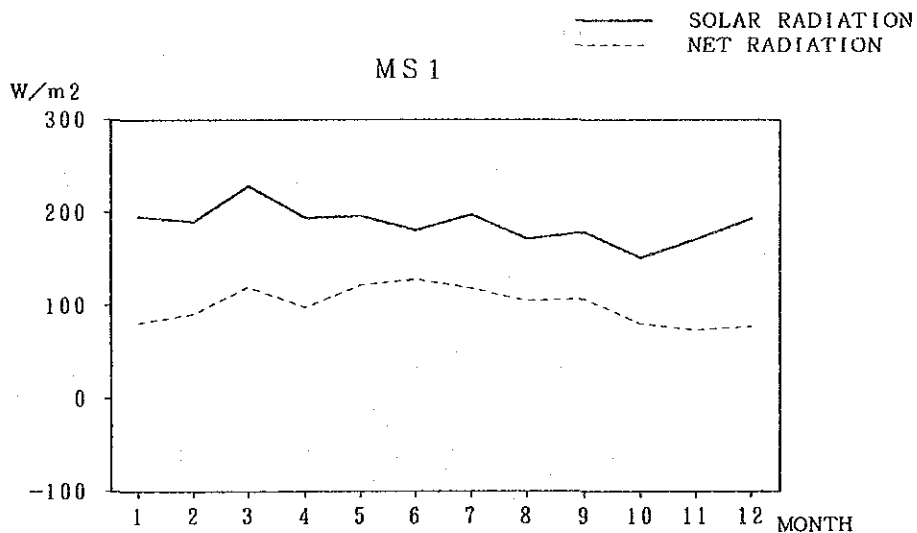
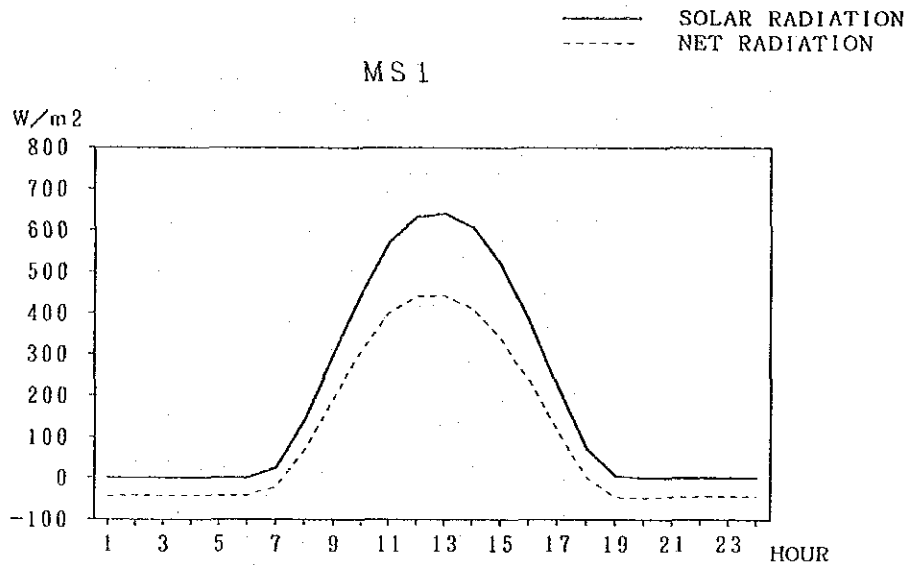


Fig. 1-10 Monthly Variations of Solar Radiation and Net Radiation Flux



MS 1

Fig. 1-11 Hourly Variations of Solar Radiation and Net Radiation Flux

1.1.7 Atmospheric Stability

Atmospheric stability is an index to show stability of the atmosphere, and is closely related to the vertical distribution of the air temperature. Under an unstable condition, air temperature in the upper level is lower than that approximated by the dry adiabatic decreasing rate ($0.98^{\circ}\text{C}/100\text{ m}$), thereby generating a convection current due to the difference of the density of air between the upper and lower layers and thus resulting in large air turbulence. On the other hand, under a stable condition, the temperature increases with increasing level, thereby resulting in a state where turbulence is suppressed. These phenomena are indicated in a graph as shown in Fig. 1-12.

Characteristics of plume diffusion corresponding to each of the above atmospheric stabilities are as shown in Fig. 1-13. Atmospheric stability also serves as an index for determining smoke plume diffusion width.

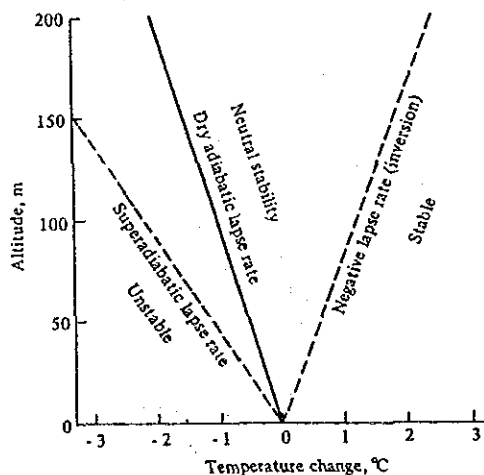


Fig. 1-12 Atmospheric Temperature Lapse Rates

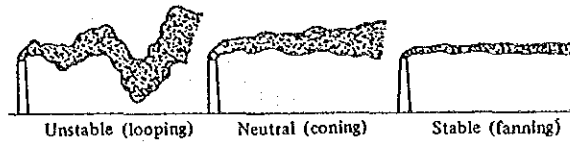


Fig. 1-13 Smoke Plume Diffusion Conditions by Atmospheric Stability

Atmospheric stability is classified by the vertical profile of atmospheric temperature as described above. However, it is difficult to make continuous measurements (up to an altitude of 1000 m above the ground) of the vertical distribution of atmospheric temperature. Also, smoke plume diffusion is greatly influenced not only by the vertical distribution of atmospheric temperature but also by wind velocity, and is related to other factors as well. Therefore, Pasquill¹⁾ proposed a method of classifying the atmospheric stability into A through F, from simple meteorological observations, with respect to wind velocity, solar radiation and cloud amount, and this method had been adopted by the Meteorological Agency of England. Pasquill's stability classification is shown in Table 1-5.

Table 1-5 Pasquill's Stability Classification

Surface wind speed (m/sec)	Key to stability categories				
	Insolation			Night	
	Strong	Moderate	Slight	Thinly overcast or $\geq 4/8$ low cloud	$\leq 3/8$ cloud
< 2	A	A-B	B	-	-
2-3	A-B	B	C	E	F
3-5	B	B-C	C	D	E
5-6	C	C-D	D	D	D
> 6	C	D	D	D	D

(for A-B take average of values for A and B etc.)

Strong insolation corresponds to sunny midday in midsummer in England, slight insolation to similar conditions in midwinter. Night refers to the period from 1 hr before sunset to 1 hr after dawn. The neutral category D should also be used, regardless of wind speed, for overcast conditions during day or night, and for any sky conditions during the hour preceding or following night as defined above.

In Pasquill's stability classifications, solar radiation was not given quantitatively and nighttime classifications were dependent on the cloud volume. But recently due to the rapid progress made in measuring instruments, solar radiation and net radiation flux are easily obtainable, and Pasquill's stability classification was thereby greatly improved.

In this survey, based on Pasquill's classification of atmospheric stability, the reporter calculated the appearance frequency of atmospheric stability, where hourly atmospheric stability was obtained in compliance with the atmospheric stability classification (Table 1-6) of the Ministry of International Trade and Industry (MITI) which uses net radiation in place of cloud amount. The results are shown in Table 1-7 and Table 1-8.

Table 1-6 Classification of Atmospheric Stability (MITI's Method)

Wind Velocity (m/s) (About 10 meters above ground)		Solar Radiation				Net Radiation	
Range of Wind Velocity	Representative Wind Velocity	Upper: (cal/cm ² ·hr), Lower: (W/m ²)				0~-2.9	-3.0~
		~50	49~25	24~13	12~0		
		~580	579~290	289~151	150~0	0~-34	--35~
0.0~0.3	0.0	CA	CB	CC	CC	CC	CD
0.4~0.9	0.6	A	B	B	D	E	F
1.0~2.9	2.0	B	B	C	D	E	F
3.0~4.9	4.0	B	C	C	D	D	E
5.0~7.9	6.5	C	D	D	D	D	D
8.0~	10.0	D	D	D	D	D	D

From the Manual for Predicting Environmental Concentration in Atmosphere in the comprehensive preliminary investigation of industrial pollution.

Table 1-7 Appearance Frequency of Atmospheric Stability

(Unit : %)

Monitoring stations	Calm				Windy					
	CA	CB	CC	CD	A	B	C	D	E	F
(MS1) ONEB STATION	0.03	0.01	0.00	0.03	0.09	18.21	16.42	15.11	23.62	26.48
(MS2) POWER PLANT	0.00	0.00	0.04	0.33	0.04	22.13	13.65	12.57	22.60	28.60
(MS5) H. & I. ESTATE	0.00	0.01	1.04	1.88	0.13	23.36	12.74	10.45	16.26	34.13

Table 1-8 Appearance Time of Atmospheric Stability by Wind Velocity Rank and Solar Radiation and Net Radiation Flux Rank

(MS1) ONEB STATION

Wind velocity (m/s)	Solar radiation (W/m ²)				Net radiation (W/m ²)		Total
	T ≥ 580	580 > T ≥ 290	290 > T ≥ 151	151 > T ≥ 0	Q ≥ -34	-34 > Q	
0.0 - 0.4	CA: 2	CB: 1	CC: 0	CC: 0	CC: 0	CD: 2	5
0.5 - 0.9	A: 7	B: 13	B: 10	D: 10	E: 16	F: 56	112
1.0 - 1.9	B: 71	B: 157	C: 113	D: 145	E: 413	F: 713	1612
2.0 - 2.9	B: 193	B: 305	C: 184	D: 244	E: 501	F: 1218	2645
3.0 - 4.9	B: 617	C: 591	C: 232	D: 285	D: 242	E: 842	2809
5.0 -	C: 112	D: 94	D: 28	D: 30	D: 19	D: 37	320
Total	1002	1161	567	714	1191	2868	7503

(MS2) POWER PLANT

Wind velocity (m/s)	Solar radiation (W/m ²)				Net radiation (W/m ²)		Total
	T ≥ 580	580 > T ≥ 290	290 > T ≥ 151	151 > T ≥ 0	Q ≥ -34	-34 > Q	
0.0 - 0.4	CA: 0	CB: 0	CC: 1	CC: 2	CC: 3	CD: 28	34
0.5 - 0.9	A: 3	B: 19	B: 37	D: 46	E: 201	F: 336	642
1.0 - 1.9	B: 93	B: 265	C: 187	D: 268	E: 626	F: 1243	2632
2.0 - 2.9	B: 398	B: 449	C: 205	D: 219	E: 328	F: 826	2425
3.0 - 4.9	B: 600	C: 515	C: 203	D: 211	D: 216	E: 745	2490
5.0 -	C: 38	D: 49	D: 11	D: 15	D: 7	D: 15	135
Total	1132	1297	644	761	1381	3193	8408

(MS5) H. & I. ESTATE

Wind velocity (m/s)	Solar radiation (W/m ²)				Net radiation (W/m ²)		Total
	T ≥ 580	580 > T ≥ 290	290 > T ≥ 151	151 > T ≥ 0	Q ≥ -34	-34 > Q	
0.0 - 0.4	CA: 0	CB: 1	CC: 1	CC: 7	CC: 78	CD: 156	243
0.5 - 0.9	A: 11	B: 56	B: 51	D: 84	E: 391	F: 858	1451
1.0 - 1.9	B: 171	B: 306	C: 242	D: 335	E: 604	F: 1379	3037
2.0 - 2.9	B: 385	B: 468	C: 226	D: 200	E: 207	F: 593	2079
3.0 - 4.9	B: 500	C: 418	C: 110	D: 122	D: 72	E: 146	1368
5.0 -	C: 60	D: 39	D: 2	D: 7	D: 2	D: 3	113
Total	1127	1288	632	765	1354	3135	8291

1.1.8 Analysis of Horizontal Wind Fluctuation σ_A and Vertical Wind Fluctuation σ_E

(1) The relationship between air turbulence and diffusion width

The dispersion of emission substances in the atmosphere is closely associated with the random movement of ambient air and air turbulence as the driver. Countless numbers of eddy currents existing in the air are grouped into two, one mechanically driven by buildings and trees and the other caused by the temperature difference in air layers along the vertical direction. The degree of air turbulence is called "atmospheric stability." Parameters used to express such atmospheric stability include the Richardson number, Stability-length by Monin-Obukhov, and Barad's stability ratio, in which a factor commonly required for their approximation is the measurement of wind and temperature profiles in air layers of high level above ground. In other words, it is thought not appropriate to introduce these parameters in any practical method to be applied for estimation of diffusion width.

1) Horizontal diffusion width σ_y

The estimation of horizontal diffusion width σ_y is subject to either of the following two methods.

- (i) Empirical equation or diagram developed by using experimental data
- (ii) Modeling equation obtainable based on Taylor's statistical theory with parameters to be empirically set

According to Taylor's statistical theory,²⁾ the horizontal diffusion width σ_y can be estimated by knowing the wind velocity fluctuation σ_v when diffusion time is small (being close to the emission source) and air turbulence is kept consistent and thus in the vicinity of the emission source, σ_y increases in proportion to diffusion time T.

$$\sigma_y(T)^2 = \sigma_v^2 \cdot T^2 \dots\dots\dots (1-2)$$

In Figure 1-14, the horizontal diffusion width σ_y divided by the wind velocity fluctuation σ_v (horizontal wind velocity standard deviation), σ_y/σ_v , is plotted against diffusion period T in the Log-Log scale diagram. From the graph, it is known that the diffusion width increases for up to 2-3 hours proportionally to the 1st order of the time lapse. Accordingly, by applying wind fluctuation σ_A in place of σ_v ($\sigma_v/u = \tan \sigma_A$) and the downflow distance x ($x=u \cdot T$) instead of diffusion time T, the horizontal diffusion width σ_y can be expressed as Equation (1-3). According to Yokoyama-Yamamoto³⁾ the constant which is $\sigma_y/\sigma_A \cdot x$ was estimated to be 0.018 whereas Draxler⁴⁾ gave the value as a function of diffusion time T and Lagrangian time scale T_1 , and Pasquill⁵⁾ as a function of downflow distance x.

$$\sigma_y = \text{const} \cdot \sigma_A \cdot x \dots\dots\dots (1-3)$$

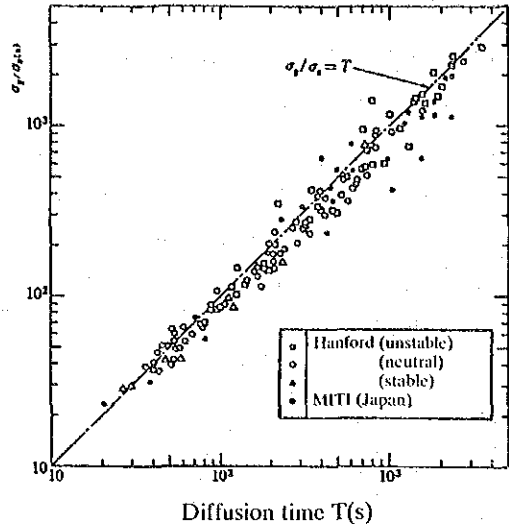


Fig. 1-14 The Relationship Between Horizontal Diffusion Width and Diffusion Time

2) Diffusion width in the vertical direction

There are a few methods for estimation of the vertical diffusion width as shown below.

- (i) a method to estimate σ_z by using wind velocity fluctuation σ_w which is closely associated with the former or vertical fluctuation of wind direction $\sigma_E \cong (\sigma_w/u)$ through field observation
- (ii) a method to estimate from meteorological data such as the temperature profile of the high altitude level
- (iii) a method which uses ground level observation data such as wind velocity, solar radiation, cloud volume, etc.

Among methods shown above, the method (i) was found most reliable and has options such as one proposed by Yamamoto-Yokoyama³⁾ and the other by Draxler⁴⁾. The method (ii) has TVA diagram⁶⁾ and the method (iii) has such options as the P-G diagram⁷⁾ and Turner diagram⁸⁾.

The relation between σ_z and σ_E can be expressed as Equation (1-4), where the constant k varies according to the degree of atmospheric stability as such treated by Yamamoto-Yokoyama or Draxler gave the value, k, as a function of diffusion time T and Lagrangian time scale T_L .

$$\sigma_z = k\sigma_E \cdot x \dots\dots\dots (1-4)$$

(2) Calculation of σ_A , σ_E

Based on the hourly measurement data of air turbulence by means of the three dimensional ultrasonic anemometer, hourly average of fluctuation of horizontal wind direction σ_A and vertical fluctuation of wind direction σ_E were calculated by the following equations.

$$\sigma_A = \sqrt{\frac{1}{6} \sum_{i=1}^6 SA_{i(10)}^2 + \frac{1}{6} \sum_{i=1}^6 (WD_{i(10)} - WD)^2} \dots\dots\dots (1-5)$$

where

$SA_{i(10)}$; Reading value of $\sigma\theta$ at an interval of 10 minutes (degree)
 $\sigma\theta$; 10 minutes running average value of standard deviation of horizontal wind direction

$\frac{1}{6} \sum_{i=1}^6 SA_{i(10)}$; 1 hour value of standard deviation of horizontal wind direction (degree)

$WD_{i(10)}$; Reading value of $\bar{\theta}$ at an interval of 10 minutes (degree)
 $\bar{\theta}$; 10 minutes running average value of horizontal wind direction

WD ; 1 hour average value of horizontal wind direction (degree)

$$WD = \frac{1}{6} \sum_{i=1}^6 WD_{i(10)}$$

$$\sigma_E = \frac{180}{\pi} \sqrt{\frac{1}{6} \sum_{i=1}^6 \left\{ \tan^{-1} \frac{SW_{i(10)}}{U_{i(10)}} \right\}^2 + \frac{1}{6} \sum_{i=1}^6 \left\{ \tan^{-1} \frac{W_{i(10)} - W}{U} \right\}^2} \dots\dots\dots (1-6)$$

where

$SW_{i(10)}$; Reading value of σ_w at an interval of 10 minutes (m/s)
 σ_w ; 10 minutes running average value of standard deviation of vertical wind velocity (m/s)

$U_{i(10)}$; Reading value of \bar{U} at an interval of 10 minutes (m/s)
 \bar{U} ; 10 minutes running average value of horizontal wind velocity

$W_{i(10)}$; Reading value of \bar{W} at an interval of 10 minutes (m/s)
 \bar{W} ; 10 minutes running average value of vertical wind velocity

W ; 1 hour average value of vertical wind velocity (m/s)

$$W = \frac{1}{6} \sum_{i=1}^6 W_{i(10)}$$

U ; 1 hour average value of horizontal wind velocity (m/s)

$$U = \frac{1}{6} \sum_{i=1}^6 U_{i(10)}$$

The calculated hourly values of σ_A and σ_E are exemplified in Table 1-9 and the complete set of data is enclosed in the Data File.

Table 1-9 (1) Example of Air Turbulence Measurement Result (σ_A)

MONTHLY REPORT table with columns: 1988YEAR, 2 MONTH, ITEM (9), SIGA/10, ST. (1) (MS1) ONEB STATION, MIN, MAX, AVE, HOUR TOTAL. Rows include hourly data from 1 to 29 and summary statistics.

Table 1-9 (2) Example of Air Turbulence Measurement Result (σ_B)

MONTHLY REPORT table with columns: 1988YEAR, 2 MONTH, ITEM (10), SIG E, ST. (1) (MS1) ONEB STATION, MIN, MAX, AVE, HOUR TOTAL. Rows include hourly data from 1 to 29 and summary statistics.

(3) Study result of σ_A and σ_E

Table 1-10 shows values of σ_A and σ_E investigated with respect to such parameters as wind velocity range, solar radiation and net radiation flux. It is seen from the graph that both σ_A and σ_E decrease with increasing wind velocity or increase proportionally to solar radiation intensity when the wind velocity maintains constant. On the other hand, Table 1-11 shows values of σ_A and σ_E consolidated in accordance with the same categories of air stability as mentioned in Table 1-6. From Table 1-11, one can notice that both σ_A and σ_E increase as the atmosphere becomes unstable or decrease as stability of the atmosphere improves.

Table 1-10 (1) Average Standard Deviation of Horizontal Wind Direction (σ_A) at Each Wind Velocity Rank, Solar Radiation Rank and Net Radiation Flux Rank

South Wet (deg)

Wind velocity (m/s)	Solar radiation (W/m ²)				Net radiation (W/m ²)		Average
	T ≥ 580	580 > T ≥ 290	290 > T ≥ 151	151 > T ≥ 0	Q ≥ -34	-34 > Q	
0.0 - 0.4	— (0)	— (0)	— (0)	— (0)	— (0)	— (0)	— (0)
0.5 - 0.9	— (0)	42.6 (1)	— (0)	76.0 (2)	46.6 (5)	49.8 (5)	52.1 (13)
1.0 - 1.9	44.2 (5)	40.5 (30)	32.5 (44)	34.1 (56)	31.2 (312)	28.2 (290)	30.8 (737)
2.0 - 2.9	31.2 (74)	31.1 (130)	22.5 (89)	25.4 (101)	21.7 (359)	16.1 (423)	21.7 (1176)
3.0 - 4.9	22.5 (259)	22.4 (288)	20.8 (129)	20.4 (142)	22.8 (180)	15.9 (152)	21.2 (1150)
5.0 -	17.3 (17)	16.5 (32)	15.0 (18)	16.7 (15)	18.1 (11)	23.6 (1)	16.6 (94)
Average	24.4 (355)	25.5 (481)	22.8 (280)	24.6 (316)	25.4 (867)	20.3 (871)	23.6 (3170)

North Dry (deg)

Wind velocity (m/s)	Solar radiation (W/m ²)				Net radiation (W/m ²)		Average
	T ≥ 580	580 > T ≥ 290	290 > T ≥ 151	151 > T ≥ 0	Q ≥ -34	-34 > Q	
0.0 - 0.4	— (0)	— (0)	— (0)	— (0)	— (0)	— (0)	— (0)
0.5 - 0.9	— (0)	— (0)	47.6 (1)	21.8 (2)	26.8 (6)	43.5 (9)	35.7 (18)
1.0 - 1.9	57.3 (8)	34.4 (12)	24.7 (12)	26.6 (24)	34.0 (19)	22.8 (143)	26.5 (223)
2.0 - 2.9	32.3 (49)	29.2 (89)	25.4 (54)	21.0 (89)	17.1 (68)	14.9 (570)	18.6 (919)
3.0 - 4.9	24.6 (169)	21.4 (181)	19.3 (57)	18.8 (85)	15.6 (27)	14.1 (263)	19.0 (782)
5.0 -	18.5 (53)	17.7 (34)	15.5 (7)	15.5 (4)	16.0 (7)	15.0 (10)	17.5 (115)
Average	26.0 (279)	23.7 (316)	22.3 (131)	20.6 (204)	19.7 (127)	16.1 (1000)	19.7 (2057)

South Dry (deg)

Wind velocity (m/s)	Solar radiation (W/m ²)				Net radiation (W/m ²)		Average
	T ≥ 580	580 > T ≥ 290	290 > T ≥ 151	151 > T ≥ 0	Q ≥ -34	-34 > Q	
0.0 - 0.4	30.6 (2)	31.4 (1)	— (0)	— (0)	— (0)	50.5 (2)	38.7 (5)
0.5 - 0.9	23.2 (6)	20.6 (8)	27.9 (5)	16.7 (4)	13.3 (2)	26.1 (37)	24.2 (62)
1.0 - 1.9	22.3 (43)	27.3 (76)	27.9 (38)	23.2 (48)	23.9 (44)	21.0 (259)	23.0 (508)
2.0 - 2.9	27.1 (49)	24.0 (65)	27.4 (37)	19.7 (45)	22.6 (58)	14.5 (218)	19.6 (472)
3.0 - 4.9	19.2 (182)	17.8 (116)	16.0 (44)	14.6 (54)	19.5 (29)	14.1 (425)	16.0 (850)
5.0 -	15.6 (40)	15.0 (27)	14.8 (3)	13.8 (11)	13.6 (1)	13.5 (26)	14.7 (108)
Average	20.5 (322)	21.5 (233)	23.3 (127)	18.6 (162)	22.1 (134)	16.5 (957)	18.9 (2005)

Annual (deg)

Wind velocity (m/s)	Solar radiation (W/m ²)				Net radiation (W/m ²)		Average
	T ≥ 580	580 > T ≥ 290	290 > T ≥ 151	151 > T ≥ 0	Q ≥ -34	-34 > Q	
0.0 - 0.4	30.6 (2)	31.4 (1)	— (0)	— (0)	— (0)	50.5 (2)	38.7 (5)
0.5 - 0.9	23.2 (6)	23.1 (9)	31.2 (6)	33.2 (8)	32.3 (13)	31.5 (51)	30.3 (93)
1.0 - 1.9	30.7 (56)	31.4 (118)	29.6 (94)	28.6 (128)	30.5 (375)	24.4 (697)	27.4 (1468)
2.0 - 2.9	30.3 (172)	28.9 (284)	24.4 (180)	22.6 (235)	21.2 (485)	15.2 (1211)	20.2 (2567)
3.0 - 4.9	22.1 (610)	21.2 (585)	19.5 (230)	18.8 (281)	21.6 (236)	14.4 (840)	19.0 (2782)
5.0 -	17.3 (110)	16.5 (93)	15.1 (28)	15.5 (30)	17.1 (19)	14.2 (37)	16.3 (317)
Average	23.6 (956)	23.9 (1090)	22.8 (538)	22.0 (682)	21.4 (1120)	17.5 (2838)	21.2 (7232)

Table I-10 (2) Average Standard Deviation of Vertical Wind Direction (σ_v) at Each Wind Velocity Rank, Solar Radiation Rank and Net Radiation Flux Rank

South Wet (deg)

Wind velocity (m/s)	Solar radiation (W/m ²)				Net radiation (W/m ²)		Average
	T ≥ 580	580 > T ≥ 290	290 > T ≥ 151	151 > T ≥ 0	Q ≥ -34	-34 > Q	
0.0 - 0.4	— (0)	— (0)	— (0)	— (0)	— (0)	— (0)	— (0)
0.5 - 0.9	— (0)	19.2 (1)	19.2 (3)	11.6 (3)	8.1 (7)	7.9 (7)	10.6 (21)
1.0 - 1.9	16.5 (12)	14.1 (52)	10.5 (67)	8.3 (69)	5.9 (348)	5.5 (237)	6.9 (835)
2.0 - 2.9	12.0 (80)	10.4 (142)	8.6 (92)	7.5 (107)	6.8 (372)	6.3 (422)	7.6 (1215)
3.0 - 4.9	9.4 (257)	8.6 (288)	8.0 (130)	7.4 (144)	7.6 (184)	7.1 (152)	8.2 (1155)
5.0 -	8.3 (18)	7.8 (32)	7.5 (18)	7.6 (15)	7.8 (11)	8.3 (1)	7.8 (95)
Average	10.2 (367)	9.6 (515)	8.8 (300)	7.7 (338)	6.6 (922)	6.2 (879)	7.7 (3321)

North Dry (deg)

Wind velocity (m/s)	Solar radiation (W/m ²)				Net radiation (W/m ²)		Average
	T ≥ 580	580 > T ≥ 290	290 > T ≥ 151	151 > T ≥ 0	Q ≥ -34	-34 > Q	
0.0 - 0.4	— (0)	— (0)	— (0)	— (0)	— (0)	— (0)	— (0)
0.5 - 0.9	35.2 (1)	35.7 (2)	28.4 (2)	15.9 (3)	5.6 (6)	6.2 (12)	12.3 (26)
1.0 - 1.9	20.0 (11)	15.7 (15)	11.2 (14)	7.2 (25)	6.1 (19)	4.9 (147)	7.1 (231)
2.0 - 2.9	12.9 (55)	11.1 (94)	9.4 (53)	7.7 (85)	7.0 (64)	6.0 (559)	7.4 (910)
3.0 - 4.9	9.8 (163)	9.1 (177)	8.3 (66)	7.7 (84)	7.8 (27)	7.1 (262)	8.3 (769)
5.0 -	8.1 (49)	7.9 (32)	7.6 (7)	7.7 (4)	8.0 (7)	7.5 (10)	7.9 (109)
Average	10.6 (279)	10.0 (320)	9.3 (132)	7.8 (201)	7.0 (123)	6.2 (930)	7.8 (2045)

South Dry (deg)

Wind velocity (m/s)	Solar radiation (W/m ²)				Net radiation (W/m ²)		Average
	T ≥ 580	580 > T ≥ 290	290 > T ≥ 151	151 > T ≥ 0	Q ≥ -34	-34 > Q	
0.0 - 0.4	50.3 (2)	39.7 (1)	— (0)	— (0)	— (0)	13.4 (2)	33.4 (5)
0.5 - 0.9	32.2 (6)	29.8 (10)	24.0 (5)	23.7 (4)	10.6 (3)	12.1 (37)	18.2 (65)
1.0 - 1.9	18.4 (47)	16.3 (89)	12.7 (39)	9.2 (49)	6.9 (46)	7.1 (262)	10.2 (532)
2.0 - 2.9	12.3 (51)	10.2 (66)	8.9 (37)	7.9 (47)	7.0 (60)	6.0 (220)	7.8 (481)
3.0 - 4.9	9.1 (184)	8.3 (117)	7.9 (45)	7.3 (54)	5.8 (30)	6.9 (425)	7.6 (855)
5.0 -	8.0 (40)	7.6 (27)	7.5 (3)	7.4 (11)	4.4 (1)	7.8 (26)	7.7 (108)
Average	11.5 (330)	11.7 (310)	10.2 (129)	8.4 (165)	6.8 (140)	7.0 (972)	8.7 (2045)

Annual (deg)

Wind velocity (m/s)	Solar radiation (W/m ²)				Net radiation (W/m ²)		Average
	T ≥ 580	580 > T ≥ 290	290 > T ≥ 151	151 > T ≥ 0	Q ≥ -34	-34 > Q	
0.0 - 0.4	50.3 (2)	39.7 (1)	— (0)	— (0)	— (0)	13.4 (2)	33.4 (5)
0.5 - 0.9	32.6 (7)	29.9 (13)	23.4 (10)	17.7 (10)	7.6 (16)	10.3 (56)	15.4 (112)
1.0 - 1.9	18.3 (70)	15.5 (156)	11.4 (110)	8.4 (143)	6.0 (413)	6.0 (706)	8.0 (1598)
2.0 - 2.9	12.4 (186)	10.6 (302)	8.9 (182)	7.6 (239)	6.8 (496)	6.1 (1201)	7.6 (2606)
3.0 - 4.9	9.4 (604)	8.7 (582)	8.1 (231)	7.5 (232)	7.4 (241)	7.0 (839)	8.1 (2779)
5.0 -	8.1 (107)	7.8 (91)	7.5 (28)	7.5 (30)	7.7 (19)	7.7 (37)	7.8 (312)
Average	10.7 (976)	10.3 (1145)	9.2 (551)	7.9 (704)	6.7 (1185)	6.4 (2841)	8.0 (7412)

Table I-11 (1) Average Standard Deviation of Horizontal Wind Direction (σ_h) by Atmospheric Stability

(deg)

Stability		South Wet	North Dry	South Dry	AVE
Calm	CA	— (0)	— (0)	30.6 (2)	30.6 (2)
	CB	— (0)	— (0)	31.4 (1)	31.4 (1)
	CC (Day)	— (0)	— (0)	— (0)	— (0)
	CC (Night)	— (0)	— (0)	— (0)	— (0)
	CD	— (0)	— (0)	50.5 (2)	50.5 (2)
Windy	A	— (0)	— (0)	23.2 (6)	23.2 (6)
	B	27.4 (499)	28.5 (328)	22.7 (428)	26.1 (1255)
	C	22.7 (567)	21.4 (357)	19.9 (275)	21.6 (1199)
	D (Day)	23.4 (366)	20.1 (245)	18.0 (192)	21.1 (803)
	D (Night)	22.5 (192)	15.5 (44)	16.6 (56)	20.3 (292)
	E	24.4 (828)	16.0 (356)	15.8 (529)	20.0 (1713)
	F	21.2 (718)	16.8 (727)	18.6 (514)	18.9 (1959)
AVE	23.6 (3170)	19.7 (2057)	18.9 (2005)	21.2 (7232)	

Note) Standard deviation (number of hours)

Table 1-11 (2) Average Standard Deviation of Vertical Wind Direction (σ_E)
by Atmospheric Stability

(deg)

Stability		South Wet	North Dry	South Dry	AVE
Calm	CA	-- (0)	-- (0)	50.3 (2)	50.3 (2)
	CB	-- (0)	-- (0)	39.7 (1)	39.7 (1)
	CC (Day)	-- (0)	-- (0)	-- (0)	-- (0)
	CC (Night)	-- (0)	-- (0)	-- (0)	-- (0)
	CD	-- (0)	-- (0)	13.4 (2)	13.4 (2)
Windy	A	-- (0)	35.2 (1)	32.2 (6)	32.6 (7)
	B	10.7 (547)	11.5 (342)	12.6 (452)	11.6(1341)
	C	8.6 (585)	8.9 (349)	8.9 (278)	8.8(1212)
	D (Day)	7.7 (388)	7.8 (240)	8.3 (195)	7.9 (823)
	D (Night)	7.6 (196)	7.7 (44)	6.7 (57)	7.5 (297)
	E	6.5 (879)	7.0 (351)	6.9 (534)	6.7(1764)
	F	6.0 (726)	5.8 (718)	7.0 (519)	6.2(1963)
AVE		7.7(3321)	7.8(2045)	8.7(2046)	8.0(7412)

Note) Standard deviation (number of hours)

1.2 Analysis of Ambient Pollutant Concentration (SO₂, NO₂, NO_x and SPM)

1.2.1 Monthly and Diurnal Variations of Concentration

Variations of SO₂ concentration are shown in Fig. 1-15, variations of NO₂ concentration in Fig. 1-16, variations of NO_x in Fig. 1-17 and variations of SPM in Fig. 1-18, respectively.

With respect to SO₂, high concentrations are seen in both monthly and hourly variations at MS2 and MS3. High concentrations are particularly seen in January through April at MS3, and in November through December at MS2. When hourly SO₂ concentration is reviewed, high values are seen from night through morning (around 19:00 to 09:00 hours) at every monitoring station, and peaks are at around 08:00 hour and 21:00 to 22:00 hours, and low concentrations are recorded in daytime.

As for monthly radiations of NO₂ and NO_x concentrations, high concentrations are seen at MS1 and MS4 along the trunk highways. Especially, high concentrations were recorded in August through October at MS1 and in November through December at MS4. No significant trends are seen in monthly variations of NO₂ and NO_x concentration at other monitoring stations. When diurnal variations of NO₂ and NO_x are reviewed, there are 2 peaks at every station, one in 07:00–08:00 and the other in 19:00–21:00.

With respect to SPM, significant differences in concentration cannot be seen between stations. As for monthly variations, high concentrations are recorded in October through March, which correspond to the dry season, and SPM concentrations are low at every station in May through August, which correspond to the wet season. In reviewing hourly variations, there can be seen a trend for 2 peaks, in the same manner as the cases of SO₂, NO₂ and NO_x. Seasonal, daytime and nighttime ambient pollutant concentration are shown in Table 1-12.

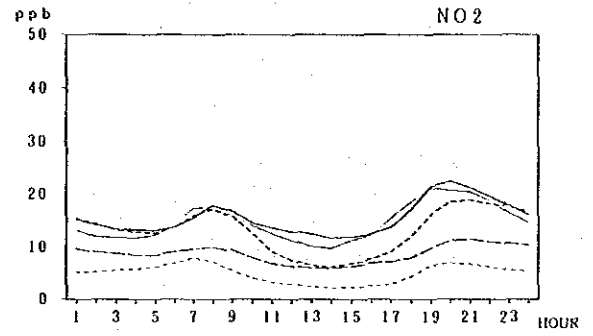
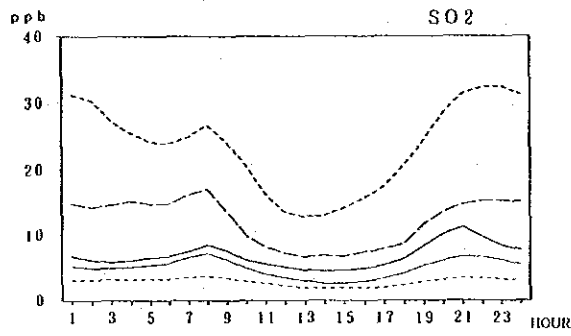
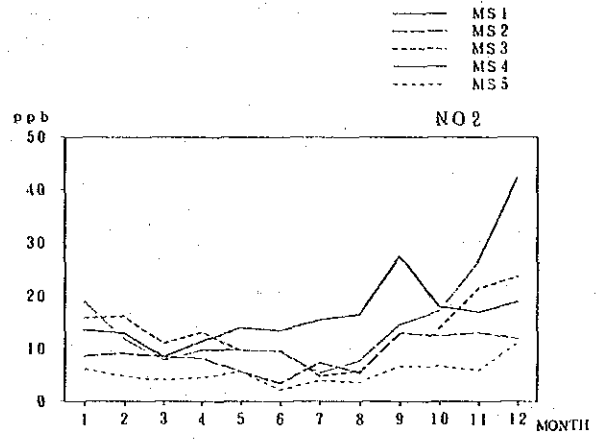
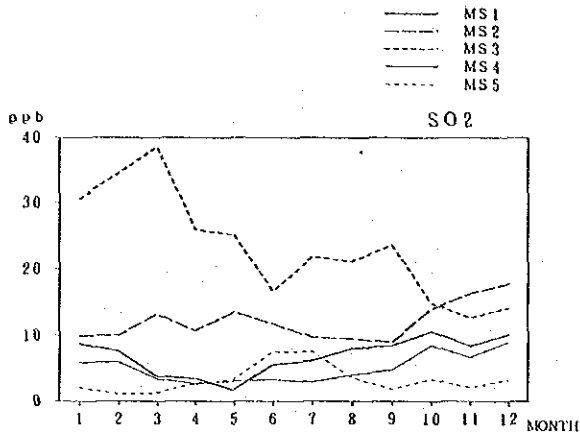


Fig. 1-15 Monthly and Diurnal Variations of SO₂ Concentration

Fig. 1-16 Monthly and Diurnal Variations of NO₂ Concentration

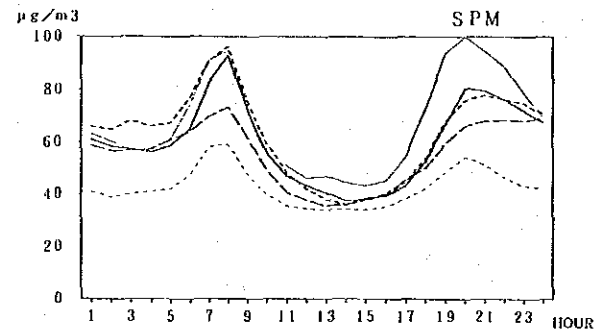
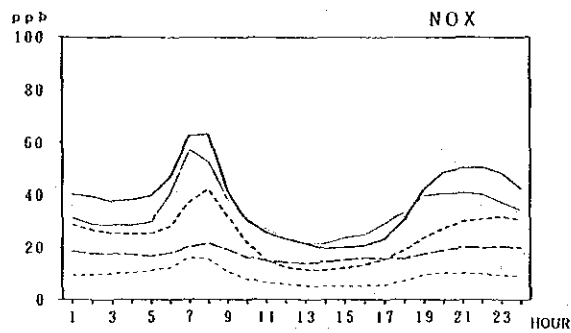
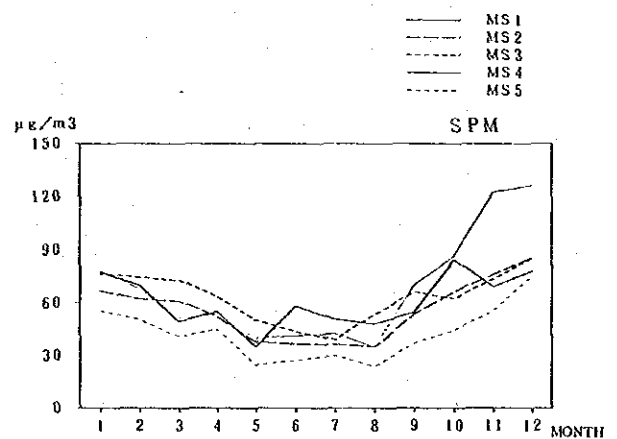
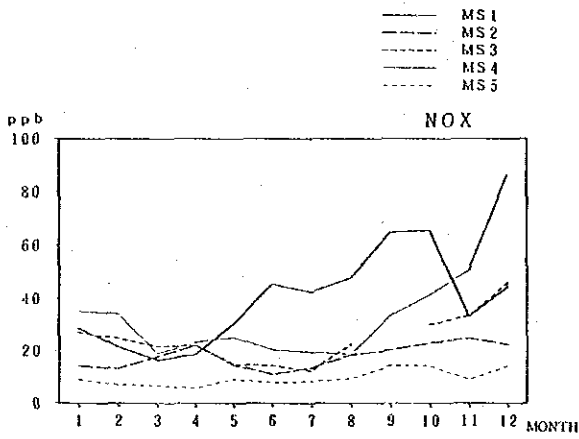


Fig. 1-17 Monthly and Diurnal Variations of NO_x Concentration

Fig. 1-18 Monthly and Diurnal Variations of SPM Concentration

Table 1-12 Average Concentration of Air Pollutants Classified Seasonal and Day/Night

Item	Station	Southerly Wet			Northerly Dry			Southerly Dry			Annual		
		Day	Night	Ave.	Day	Night	Ave.	Day	Night	Ave.	Day	Night	Ave.
SO ₂ (ppb)	MS 1	6.4	7.1	6.8	5.9	11.8	9.1	4.6	5.3	4.9	5.8	7.8	6.9
	MS 2	9.3	12.9	11.3	8.5	19.7	14.7	9.7	12.8	11.4	9.2	14.6	12.2
	MS 3	17.1	23.5	20.6	15.9	22.6	19.6	20.9	43.3	33.1	17.7	20.3	23.5
	MS 4	3.6	5.1	4.4	5.3	8.7	7.1	3.8	4.1	4.0	4.0	5.7	5.0
	MS 5	3.5	4.4	4.0	1.8	3.0	2.5	1.6	1.7	1.7	2.4	3.2	2.9
NO ₂ (ppb)	MS 1	17.8	17.0	17.4	10.9	21.1	16.5	10.0	11.7	11.0	14.1	16.7	15.6
	MS 2	7.3	8.1	7.7	7.2	14.3	11.1	7.6	9.5	8.6	7.3	9.8	8.7
	MS 3	6.9	9.7	8.4	14.6	24.8	20.2	10.4	16.1	13.5	10.1	15.7	13.2
	MS 4	10.3	11.1	10.7	27.1	34.7	31.2	9.2	10.0	9.7	13.5	15.7	14.7
	MS 5	3.4	5.7	4.7	4.1	8.3	6.4	3.5	5.2	4.4	3.6	6.1	5.0
NO _x (ppb)	MS 1	39.7	56.4	48.8	20.3	47.7	35.3	17.2	19.9	18.7	29.2	45.1	37.9
	MS 2	16.2	16.7	16.5	15.0	24.4	20.1	17.0	18.0	17.6	16.2	18.7	17.6
	MS 3	14.3	20.0	17.4	25.5	44.4	35.8	19.1	26.0	22.8	18.8	28.5	24.1
	MS 4	24.4	28.6	26.7	49.8	71.7	61.7	25.5	25.1	25.3	29.9	36.7	33.6
	MS 5	8.3	12.0	10.3	6.8	11.5	9.4	5.5	7.1	6.3	7.2	10.5	9.0
SPM (µg/m ³)	MS 1	48.0	59.7	54.3	54.1	92.9	75.3	55.0	60.5	58.0	51.2	67.9	60.3
	MS 2	40.3	46.8	43.8	51.0	96.7	76.0	54.5	62.5	58.9	46.4	63.3	55.6
	MS 3	44.9	58.3	52.2	60.0	93.8	78.4	58.5	60.0	70.2	52.1	72.6	63.3
	MS 4	45.2	58.8	52.6	63.3	129.2	108.1	55.6	59.3	57.6	57.3	76.2	67.6
	MS 5	30.1	32.5	31.4	54.3	68.7	62.2	42.4	47.8	45.3	39.5	45.8	42.9

1.2.2 Resemblance among Monitoring Stations by Cluster Analysis and Principal Component Analysis

(1) Cluster analysis

This analysis is applied to a number of measurements that represent a plural number of group units and classifies such units based on mutual resemblance. The method is often called as Numerical Classification or Numerical Taxonomy and in this study measurement data and group unit correspond to pollutant concentrations and station respectively. The analytical method has been developed as advancement of computer technology and has versatile application fields such as medical science, biology and economics. The method was found effective for sorting of diseases based on diagnostic and medical data or in biological study for classification of bacteria by knowing their geometrical and behavioral data. The economics addresses its application to characterization of enterprises based on financial data.

Among many proposed options of cluster analysis, application to this study is one that depends on correlation coefficients of atmospheric pollutant concentrations as measure to represent similarity between monitoring stations. The clustering distance is calculated by group average method.

The clustering of group units (stations) starts such that the clustering distance first calculated directs which group units to be combined first (between near-most two) and then distance calculation is repeated for a new cluster system and second stage clustering takes place again about two units having the shortest distance. The repetitive calculations and clusterings proceed until the all

group units are combined in one.

The correlation coefficients among stations were calculated with respect to monthly average concentrations of SO₂, NO_x and SPM and are shown in Table 1-13. Those coefficient data were used for cluster analysis, the result of which is as shown by a hierarchical structure or dendrogram in Fig. 1-19.

Fig. 1-19 shows the clustering of MS1 and MS4 about SO₂, that of MS4 and MS5 about NO₂, and that of MS1 and MS5 about NO_x as indicated by similarity value being larger than 0.8 in each case. Other clustering was not observed among stations but as for SPM the similarity value exceeded 0.8 about all combinations among stations. This may be probably due to the fact that the secondary particulate borne by the air and broadly existing across the area deprived stations of regional characteristics.

Table 1-13 Correlation Coefficients among Stations with respect to Atmospheric Pollutant Concentrations

(SO₂)

	MS 1	MS 2	MS 3	MS 4	MS 5
MS1) ONEB STATION					
MS2) POWER PLANT	-0.82				
MS3) MIN.DEP.OFFICE	0.37	0.01			
MS4) S.P.PRO.OFFICE	0.95	-0.68	0.39		
MS5) H.& I.ESTATE	0.60	0.31	-0.94	0.59	

(NO_x)

	MS 1	MS 2	MS 3	MS 4	MS 5
MS1) ONEB STATION					
MS2) POWER PLANT	-0.62				
MS3) MIN.DEP.OFFICE	-0.22	-0.11			
MS4) S.P.PRO.OFFICE	0.52	-0.68	0.60		
MS5) H.& I.ESTATE	0.93	-0.72	-0.18	0.43	

(NO₂)

	MS 1	MS 2	MS 3	MS 4	MS 5
MS1) ONEB STATION					
MS2) POWER PLANT	-0.00				
MS3) MIN.DEP.OFFICE	-0.44	0.80			
MS4) S.P.PRO.OFFICE	-0.34	0.30	0.70		
MS5) H.& I.ESTATE	-0.38	-0.30	0.24	0.82	

(SPM)

	MS 1	MS 2	MS 3	MS 4	MS 5
MS1) ONEB STATION					
MS2) POWER PLANT	0.87				
MS3) MIN.DEP.OFFICE	0.86	1.00			
MS4) S.P.PRO.OFFICE	0.99	0.86	0.84		
MS5) H.& I.ESTATE	0.97	0.92	0.91	0.94	